The Dissertation Committee for Michael Andrew Cantrell Certifies that this is the approved version of the following dissertation:

JNK2 INHIBITS LUMINAL CELL COMMITMENT IN NORMAL MAMMARY GLANDS AND TUMORS

Committee:

Carla L. Van Den Berg, Supervisor

Janice Fischer

Jeffrey Gross

John Richburg

Steven Vokes

JNK2 INHIBITS LUMINAL CELL COMMITMENT IN NORMAL MAMMARY GLANDS AND TUMORS

by

Michael Andrew Cantrell, B.S.

DISSERTATION

Presented to the Faculty of the Graduate School of

The University of Texas at Austin

in Partial Fulfillment

of the Requirements

for the Degree of

DOCTOR OF PHILOSOPHY

The University of Texas at Austin

May 2013

Dedication

To my mother and father, Cynthia and William Cantrell

and

Daniel Meehan – without whom I might have never started on this journey

Acknowledgments

I have many thanks to give for all the help that I have received in the past seven years at the University of Texas. However, no person deserves my acknowledgment for their assistance more so than my mentor, Carla Van Den Berg, whose foresight into potential difficulties and gut instincts of molecular interactions in the many models throughout this dissertation have been spot-on more often than I would like to admit. Pursuit of this degree has been trying at times but your thoughtful direction has always kept us on target toward our goals and led us to, what I believe is, a beautiful story.

Along the way, I have received much comfort from the commiseration and technical assistance of students and staff within and without the Van Den Berg Lab, including Shreya Mitra, Azadeh, Nasrazadani, Peila Chen, Jamye O'Neal, Everardo Macias, Irina Fernandez-Curbelo, and numerous undergraduate assistants. To my friend and lab mate, Danielle Ebelt, I owe the greatest gratitude in this regard. We have experienced triumphs and endured many small tragedies but have pulled through with, hopefully, >50% of our respective sanities intact. I'll always remember our afternoon conversations in the cell culture room and wish you the best of luck in the future.

I would also like to thank James Harman and the rest of my Austin extended family for challenging me to find life outside the lab. You have taught me a valuable lesson: that while baseball, tubing, shooting, skiing, fishing, and hiking are fun, you really only need to know one place that plays good hip-hop music to enjoy yourself.

Lastly, I would like to thank my Graduate Committee members, Janice Fischer, Jeff Gross, John Richburg, and Steve Vokes for their input and support through my several years of studies.

JNK2 INHIBITS LUMINAL CELL COMMITMENT IN NORMAL MAMMARY GLANDS AND TUMORS

Michael Andrew Cantrell, Ph.D.

The University of Texas at Austin, 2013

Supervisor: Carla L. Van Den Berg

Breast cancer is a heterogeneous disease with vastly different tumor progression kinetics and survival outcomes depending upon the differentiation state and gene expression patterns of the tumor. Effective treatments exist for patients with endocrine therapy sensitive or HER2 overexpressing tumors, but targeted treatments are not available for other tumor types. The mechanisms governing mammary tumor phenotype generation could prove critical to finding treatments. The c-Jun N-terminal kinase (JNK) pathway has recently been implicated in the inhibition of breast tumor luminal differentiation (1, 2) and JNK2, in particular, is important in mammary tumorigenesis and tumor progression (3-8). Therefore, the involvement of JNK2 in inhibition of mammary luminal cell differentiation was investigated in normal glands and tumors. Studies found that JNK2 inhibits luminal cell populations in normal mammary ducts. Additionally, JNK2 suppresses Notch activity in stem cell niche of the developing mammary gland. *In vitro* assays show that control over differentiation by JNK2 is due to suppression of p53-dependent *Notch1* expression. Inhibition of luminal cell populations by JNK2 is also

apparent in tumor cell models regardless of p53 expression. In the p53-competent Polyoma Middle T-antigen model, *Notch1* expression is suppressed by JNK2. In the absence of p53, JNK2 suppresses luminal populations independent of Notch1. In this model, decreased luminal marker expression is accompanied by increased epithelial to mesenchymal transition. It was also found that JNK2-dependent epithelial to mesenchymal transition inhibits luminal populations and is driven by JNK2-dependent suppression of *Brca1*. JNK2 also confers resistance to estrogen signaling inhibition, and increases the metastatic ability of tumor cells *in vivo*. These data establish the importance of JNK2 in mammary epithelial cell differentiation in normal glands and tumors. They also suggest that JNK2 may be an effective prognostic marker or treatment target.

Table of Contents

List of Tables

List of Figures

Chapter 1 – Introduction

1.1. Normal Mammary Differentiation

The mammary gland is the principle organ for the classification of mammals (Figure 1.1). It has evolved for the nutrition of offspring that are essentially helpless at birth. Human and mouse mammary glands carry out the same function and have remarkably similar structures. The key difference is that female mice possess ten mammary glands while humans have only two (Figure 1.2). This is presumably due to relative litter size. Lactating mammary glands release nutrients to young, in the form of milk, from external orifices called nipples. These nipples lead to a network of interconnected, epithelial, tube-like ducts that lie in a large adipose fat pad stroma. The functional portion of the gland is the duct, which undergoes periodic changes under the influence of sex hormones to prepare for potential pregnancy. Human mammary glands also possess a structure called the lobule that is present at all times and is the site of differentiation into milk-producing alveolar units during pregnancy.

Mammary ducts are bi-layered, ovular structures. Ductal layers are segregated into two distinct lineages that have similar gene expression patterns and functions in mice and humans (Figure 1.3). The inner layer confines cells of the luminal lineage and the outer layer consists of the basal/myoepithelial lineage. As the names suggest, luminal cells are directly associated with the hollow lumen while basal cells are in direct contact

with the basal lamina. Each cell type has its own specific function in the mammary gland. Cells of the luminal lineage are able to differentiate into secretory cells of the alveolar buds and produce milk proteins, while basal/myoepithelial cells provide the physical force necessary to expel milk through ducts toward the nipple. The basal compartment is less differentiated and contains stem cells, which give rise to cells of both lineages (9-11).

Luminal and basal lineages of the mammary gland can be distinguished from each other by their expression of immunohistochemical or flow cytometric markers. The markers for mammary lineages are quite similar for mice and humans. For reference, cell type markers can be found on Table 1.1. By immunohistochemistry, luminal cells can be discriminated from basal cells by their expression Cytokeratins 8 and 18, MUC1, ER, and PR, while basal cells express Cytokeratin 14, smooth muscle actin, and p63 (12). By flow cytometry, mammary lineages can be easily separated on the basis of Heat Stable Antigen (CD24) and either Integrin α6 (CD49f), or Integrin β1 (CD29) expression (10, 11, 13-16). Luminal lineages are $CD24^{hi}$ $CD49f^{lo/med}$ $CD29^{hi}$ and basal/myoepithelial cell lineages are $CD24^{lo}$ $CD49f^{hi}$ $CD29^{hi}$. Mammary stem cell populations possess an expression signature similar to the highest CD49f/CD29 expressing basal cells (9-11). It is important to note that the same markers that discriminate lineages in the normal mammary gland also define tumors that arise from a particular lineage.

In the mammary epithelial cell hierarchy, mammary stem cells divide and daughter cells either retain stem cell characteristics, through symmetric divisions, or divide asymmetrically generating a single stem cell and a daughter cell that is committed

to differentiation (Figure 1.4). One key protein that promotes mammary stem cell maintenance is Bmi-1 (17). Expression of Bmi-1 in stem cells is promoted by the process of epithelial to mesenchymal transition (EMT) (18, 19), which is, itself, a defining characteristic of adult stem cells (20). Stem cell maintenance is inhibited by p53 in a poorly understood mechanism, which involves inhibition of symmetric cell divisions (21). This mechanism may involve p53-dependent transcription of *miR200c*, as this function suppresses EMT and stem cell characteristics in mammary cells (22). Once stem cells asymmetrically divide, a bipotent progenitor is generated with the potential to maintain basal fate or adopt a luminal one (23).

Notch signaling is important for commitment of cells to the luminal lineage and inhibition of commitment to the basal lineage (24-26). Notch signaling does not promote terminal differentiation of luminal cells, however, as overexpression of Notch1 results in build-up of luminal progenitor cells (24, 25, 27). Although Notch1-3 are all expressed in the developing and adult mammary gland, *Notch1* mRNA is expressed the most differentially between luminal and basal lineages, with highest expression in luminal cells, and is considered the most important for mammary cell differentiation (25). A key function of Notch1 in luminal cell differentiation is suppression of *Trp63* (the gene encoding p63) transcription, which itself inhibits *Notch1* transcription and promotes basal lineage commitment (28-30).

Terminal differentiation along the luminal lineage depends upon the GATA3 transcription factor and Breast Cancer-associated-1 (BRCA1). Expression of both genes is stratified by cell populations, with highest expression in luminal progenitor cells (31-

33). This compartmentalization serves a functional role in allowing them to drive differentiation of luminal progenitors into mature, ER^+ luminal cells (33-35). In the absence of expression of either gene, luminal progenitor cells predominate the mammary ductal architecture.

1.2. Breast Cancer Differentiation

Despite the relatively simple structure of the mammary gland, with only two cell lineages, breast cancer is a remarkably heterogeneous disease. Historically, human breast tumors have been categorized by expression of three biomarkers in histology: ER, PR, and HER2 (36). The expression level of each marker has been used to determine treatment regimens for chemo- radiation- and endocrine therapies. While this approach has been successful in treatment of localized disease, patients with metastatic breast cancer only see 5-year survival rates of 27% (37). This demonstrates a need for better understanding of breast cancer development and gene expression.

Many other immunohistochemical biomarkers have been proposed as prognostic/predictive indicators of treatment outcome, but the heterogeneity of breast cancer has necessitated a transcriptome-wide approach to classification. Microarray-based methods have yielded several distinct subtypes with unique tumor characteristics and predictive patient outcomes (38-40). The most widely accepted subtypes of human breast tumors are luminal A, luminal B, basal-like, and $HER2^+$ (HER2-overexpressing), each named according to similarity with normal mammary lineages. A very important feature of these subtypes is that primary tumors and metastases from those tumors

possess similar gene expression patterns, a fact that suggests subtype-specific treatments may target both sites (38).

Just like the normal luminal lineage, luminal subtypes express high levels of ER, ER-target genes, luminal Cytokeratins, and luminal transcription factors such as *Gata-3*. By contrast, basal-like and $HER2^{+}$ tumors are characterized by their low or absent expression of ER and its associated transcripts (39). Luminal tumors are by far the most common subtypes and they are the most differentiated breast tumors (41). Luminal A and B differ in that Luminal A tumors proliferate and progress more slowly (41, 42). Luminal A tumors are effectively treated with endocrine therapy, whereas luminal B tumors are not responsive (43). Basal tumors progress quickly and express high levels of proliferation-related genes, EMT markers, and basal Cytokeratins (41, 44-46). There is no effective, targeted therapy currently available to patients with basal tumors. HER2 over-expressing tumors are also highly proliferative and progress quickly to metastasis (47). However, this phenotype is well-known to be dependent on the HER2 receptor—a fact that is effectively exploited by treatment of patients with the transtuzumab (Herceptin^{TM}) monoclonal antibody (48-52).

Recently, another group of tumors has been discovered with characteristics of cancer stem cells, called claudin-low. This group has been described as an "emerging" subtype and is named for it's low expression of Claudins 7 and -9, as compared to other tumor subtypes (41). Claudin-low tumors have histology characteristic of cells undergoing EMT (53). As evidence for enrichment in cancer stem cells, claudin-low tumors also express the highest levels of tumor initiating cell-related genes among all

tumor subtypes (41). Claudin-low tumors are also the least differentiated subtype, with basal, HER2, and Luminal tumors following in increasing order (33, 41).

Each subtype is hypothesiszed to be generated from aberrant expression of charcteristic gene products (41). Few mechanisms of subtype generation, however, are known. One that is well-studied is the mechanism of HER2+ subtype generation, which results from a relatively common, spontaneous, gene amplification at the erbb2 (the gene encoding HER2) locus (54). Basal tumors are not generated from a single specific mutation, as in HER2 tumors, but several potential genes that are involved in mammary cell differentiation. For example, inherited mutations in *Brca1* pre-dispose individuals to the development of basal-like breast cancers (55-57). Tumors in *Brca1* mutation carriers are generated from a build-up of luminal progenitor cells, not basal cells as the subtype name would suggest (33). This is, presumably, due to the active role of BRCA1 in terminal differentiation. Similarly, high expression of Notch1, which is involved in production of luminal progenitors, results in the generation of basal tumors in mice and humans (25, 27, 58, 59).

The generation of luminal and other tumor subtypes is more speculative. For example, GATA-3 is a master regulator of luminal cell fate and it is also one of the core genes that define luminal tumors. Thus, it is believed that GATA-3 may also be necessary for generation of luminal subtype or ER^+ tumors (60). However, additional studies must be done to better define the role of GATA-3 in luminal tumorigenesis. EMT is an important factor in maintenance of stem cell populations and as a defining characteristic of the claudin-low subtype of tumors may very well be a determinant in

their generation (33, 60). This is a question of great importance because cancer stem cell populations are hypothesized to be responsible for tumor generation and information regarding claudin-low tumors may provide insight for all tumor subtypes.

Although some of the important molecules and effectors that are involved in subtype generation are known, many remain to be discovered and the upstream elements that mediate subtype generation are even less well-described. Knowledge of these upstream effectors could prove useful in the design of targeted therapies for treating patients with metastatic disease.

1.3. C-JUN N-TERMINAL KINASES (JNKS)

One potential upstream regulator of mammary cell differentiation and tumor subtype generation is the C-Jun N-Terminal Kinase (JNK) pathway. There is evidence that the JNK pathway inhibits commitment luminal populations in breast cancer. Recent studies show that inactivating mutations in the upstream JNK activating kinases MAP3K1, MAP2K4, and MAP3K13 are prevalent in luminal breast tumors, occurring most frequently in ER^+ tumors (1, 2). Because JNKs are effectors of this pathway, these data may indicate a role for them in normal mammary lineage commitment also.

Activation of JNKs has been reported in response to a wide variety of signaling pathways and ligands including EGF (61), canonical and non-canonical Wnt signaling (62-64), FGF (65), TGFβ (66-68), TNFα (69-71), and integrins (72). These signals induce phosphorylation of JNKs, triggering their subsequent activation of nuclear and cytoplasmic substrates, including c-Jun. JNKs have been shown to possess near

ubiquitous cellular functions including apoptosis (66, 67, 73-79), cell cycle progression (71, 80-88), differentiation (64, 89-92), EMT (85, 93-96), and others.

There are three JNK genes encoding JNKs 1-3, which alternatively splice into several isoforms. Expression of *Jnk1* and *Jnk2* is widely recognized to encompass all tissues whereas *Jnk3* is thought to have a more limited expression pattern, mostly in the brain, heart and testis (97). JNKs are proline-directed serine/threonine mitogen-activated protein kinases (MAPKs) that phosphorylate substrates at (Pro)-X-Ser/Thr-Pro sequences (98)—a similar motif to the substrate of other members of the MAPK family, including ERK (99). Structures of each of the JNK proteins contain binding sites for ATP, an activation loop, and a MAPK insert domain (100-102). JNKs are phosphorylated on their respective activation loops, which require dual phosphorylation of a tyrosine and a threonine to potentiate functionality. Phosphorylation is catalyzed by MAPK kinase (MAP2K) 4 and -7 and although both kinases have dual specificity (ability to phosphorylate Ser/Thr or Tyr), MAP2K4 preferentially interacts with tyrosine residues and MAP2K7 interacts with threonine residues of JNKs (103).

Although JNKs do possess overlapping function, recent studies in JNK knockout mouse models and other specific gene targeting strategies have demonstrated that JNK proteins also possess individual, unique, substrates and cellular activities. Activator Protein 1 (AP-1) transcription factor complex proteins, including c-Jun, are bound and phosphorylated by JNK family members with varied affinity (104-106). JNK2 has the highest affinity for c-Jun and ATF2, while JNK3 binds to Elk-1 with the greatest efficiency. (106). JNK1 and JNK3 isoforms preferentially bind to c-Jun, but the affinity

of JNK2 is dependent upon isoform. JNK2α1 and -α2 preferentially bind to c-Jun while JNK2β1 and –β2 preferentially bind to ATF2. These studies and others have defined characteristic functions of each individual JNK gene. Whereas JNK1 is associated with promotion of apoptosis, JNK2 promotes the converse process of cell survival (81). JNK3 is primarily involved in apoptosis in neural tissues (76, 107).

The roles of individual JNK genes in mammary biology are not well understood. Although *Jnk1* and *Jnk2* do not seem to affect adult mammary morphology *in vivo*, double-null mammary cells display an increased branching phenotype in culture (4, 5). Additionally, inhibition of JNKs prevents AP1- and Bim-dependent acinar apoptosis and lumen clearing in 3-dimensional mammary epithelial cell cultures (108). While these studies support a role for JNKs in mammary biology, their methods prevent assignment of individual JNK gene function—further research in this area is warranted. Given that JNK isoforms perform unique functions, it is probable that the ubiquitously expressed *Jnk1* and *Jnk2* affect mammary development in different ways.

1.4. Dissertation Aims

Breast cancer is the most commonly diagnosed cancer in women of the United States (109). Early detection methods have improved overall survival, but the dismal survivorship for metastatic disease only serves to illustrate that deeper understanding is required to design reliable treatment regimens for all that are affected with breast cancer. The most effective treatments may be rationally designed by analyzing molecules and

cellular signaling pathways that are important for the development and progression of the disease.

Recent publications have shown that C-Jun N-terminal Kinase 2 (JNK2) is responsible for a range of processes in the mammary gland from normal development to tumorigenesis and tumor progression. The Van Den Berg lab and others have shown that, in breast cancer models, JNK2 promotes accumulation of replicative stress (3), tumorigenesis (4), cell motility (6, 7), and metastasis (8). These activities may be due to the promotion of EMT by JNKs (93). If this is so, the necessity for EMT in development and differentiation, points to a potential role of JNK2 in these processes, as well. This is further supported by the potential for the JNK pathway to inhibit differentiation along the luminal lineage in breast tumors (1, 2). These data led to development of the hypothesis that ***JNK2 inhibits luminal lineage commitment in mammary tumors***. Because mechanisms governing differentiation in mammary tumors are related to those in the normal mammary gland, it was also hypothesized that ***JNK2 inhibits luminal lineage commitment in the normal mammary gland***.

The studies documented herein address the role of JNK2 in mammary gland development and differentiation in normal and tumor tissues. They provide unique insight into the importance of mammary epithelial cell differentiation in tumor phenotype as tested through the following experimental aims:

Aim 1: Determine the specific alterations in luminal cell marker or lineage-specific gene expression that result from null mutation of *Jnk2* (*jnk2ko*) in normal mammary glands and tumors.

Aim 2: Define the mechanisms of luminal cell commitment that are altered by *jnk2ko.*

Aim 3: Establish a connection between alterations of luminal cell commitment to mechanisms of commitment that are altered by *jnk2ko*.

These aims were tested by the methods presented in Chapter 2. Data gained through experimentation is presented and discussed in Chapters 3, 4, and 5. A summary of results and future directions is included in Chapter 6.

Chapter 2 – Materials and Methods

Mice

All mouse experiments were performed in accordance with institutional and national guidelines and regulations. Animal procedures and experiment are pre-approved by the IACUC at the University of Texas, Austin. *Trp53*-null (*p53ko*) (110) and *jnk2ko* (111) mice were obtained from Jackson Labs and backcrossed to Balb/C strain (Jackson Labs).

Reagents

Unless otherwise stated, chemical reagents were purchased from Sigma. Antibodies used: 1:500 CK8/18 (Santa Cruz Biotechnology, Inc. #sc-52325), 1:500 p63 (Millipore #MAB4135), 1:500 Ki67 (Neomarkers, Fischer Scientific #RM-9106), 1:500 Cleaved Caspase-3 (Cell Signaling #9664) 1:500 SMA (DakoCytomation #M0851), 1:500 Notch1 (Millipore #491010), 1:500 $Notch1^{ICD}$ (Cell Signaling #2421), 0.5uL/0.5M cells CD24-PECy7 (Ebioscience #25-0242), 0.5uL/0.5M cells CD49f-PE (Ebioscience #12-0495), 1:500 Six1 (Origene #TA504057), 1:500 MMP9 (Cell Signaling #3852), 1:500 E-cadherin (Cell Signaling #3195), 1:500 Vimentin (Cell Signaling #3932), 1:500 Lef-1 (Cell Signaling #2230), 1:500 ER (Santa Cruz #sc-542), 1:500 PR (Santa Cruz #sc-539), 1:1000 GAPDH (Cell Signaling #2118), 1:500 Zeb1 (Cell Signaling #3396), Mouse HRP-conjugated secondary antibody (Santa Cruz #sc-2031), Rabbit HRP-conjugated secondary antibody (Santa Cruz #sc-2030), 1:500 Mouse lineage panel kit including

CD3e, CD11b, CD45R, Ly6G & C, Terr-119 used per manufacturer's instructions (BD Pharmingen #559971). BrdU-FITC kit was used per manufacturer's instructions, as explained below (BD Pharmingen #559619). Adenoviral MAM51 was a kind gift from Karine LeFort and G. Paolo Dotto (112). Notch1 promoter constructs were a kind gift from Takashi Yugawa (113). BRCA1 promoter constructs were a kind gift from David Rodenhiser (114).

Tissue processing and histology

Number four glands from five 3-, 4-, 5-, 6-, and 7 week-old virgin female mice were fixed with 4% paraformaldehyde and paraffin (Fisher Scientific # 23-021-401) embedded using a Leica TP1020 Tissue Processor and a Leica EG1150H/C Tissue Embedding Station. Eight unique tumors were used for each assay in tumor models. 5um sections were cut using a Leica RM2255 Microtome and placed onto slides. Tissue was treated with Citrisolv (Fisher Scientific #670209), rehydrated and boiled in 10mM Na Citrate. Tissue was permeabilized with 0.02% Triton X-100. Immunohistochemistry samples were treated with 0.3% H_2O_2 before incubation with primary antibodies and then treated according to ABC kit (Vector Labs, Mouse-#AK-5002, Rabbit #AK-5001) instructions. Samples were developed with the DAB substrate kit (Abcam #ab64238) and then mounted with VectaMount (Vector Labs #H-5000). Immunofluorescence samples were incubated with primary antibodies at concentrations listed above, overnight at 4°C. Samples were then washed with PBS (137mM NaCl, 2.7mM KCl, 10mM Na_2HPO_4, 1.8mM KH_2PO_4) and incubated with fluorescently-labeled secondary antibodies at room temperature for one hour, washed again, and mounted with VectaShield with DAPI

(Vector Labs #H-1200). Immunohistochemistry images were obtained using an Olympus CKX41 bright-field microscope with QCapture Pro software (Media Cybernetics). Immunofluorescence images were obtained on an Eclipse TE200 microscope (Nikon) using Image Pro Plus Software. Photographs were taken of 10 60X fields (immunofluorescence) or 10-40X fields (immunohistochemistry) from each gland/tumor involved in the study.

Western blot

Cell pellets were lysed in Protein Extraction Buffer (20mM Tris pH 7.6, 50mM NaCl, 3mM EDTA, 0.05% NP-40 in dH_2O) or RIPA buffer (50mM Tris pH 7.4, 150mM NaCl, 1mM EDTA, 0.1% SDS, 1% NP-40, 0.5% Sodium Deoxycholate) with protease inhibitor cocktail (5ug/mL Leupeptin, 1mM DTT, 1mM PMSF, 1% Aprotinin, 368ug/mL Na-Orthovanadate). Samples were frozen at -20°C and thawed on ice to allow lysis. Following lysis, samples were centrifuged in a micrcentrifuge at full speed for 15 minutes at 4°C. Concentrations were calculated based off of a BSA standard curve, using DC Protein Assay System (Bio-Rad #500-0111). Protein samples were prepared in 4X SDS loading buffer (40% glycerol, 50mM Tris pH 6.8, 8% SDS, 0.4% Bromophenol blue). Gels were cast at 8-12% polyacrylamide, using the Protean III system (Bio-Rad). Gels were run at 200V in Tris-Glycine (25mM Tris, 0.2M Glycine, 0.1% SDS, pH 8.3) and then transferred to 0.2um pore nitrocellulose (Bio-Rad #162-0112) in Tris-Glycine with 20% Methanol. Blots were then blocked with 4% powdered milk in TBS-T (50mM Tris, 150mM NaCl, 0.05% Tween-20, pH 7.6), washed in 1X TBS-T and then probed with primary antibodies overnight at 4°C. After washing with three times in TBS-T, blots were

incubated with HRP-conjugated secondary antibodies for 1 hour at room temperature. Blots were developed using ECL-Plus Reagent (Amersham #PRPN2132) on a STORM 860 Molecular Imager (Amersham).

Primary Mammary Epithelial Cell Culture and Imaging

Mammary Glands from three adult (8-10 week-old) virgin female mice were extracted and minced and treated with 5 mg/mL collagenase for 1.5 hours at 37°C with rocking, until well-digested. Mammary organoids were isolated by four rounds of differential centrifugation at 500xg for 30 seconds. Organoids were disaggregated with 0.025% trypsin/EDTA (Invitrogen #R-001-100). Cells were filtered through 40um cell strainers (Fisher Scientific #08-771-1). 3-dimensional cultures were seeded on Matrigel (BD Biosciences #356234) according to established protocols (115, 116). 50 Acinar diameters for each treatment were measured at 24-hour intervals from bright field images with QCapture Pro Software. Immunofluorescence images were obtained using an SP2 AOBS Confocal Microscope (Leica) from a minimum of 15 acini per treatment. Differentiation assays were performed on isolated mammary epithelial cells after sorting for colony forming units ($CD24^{hi}$ $CD49f^{lo}$) or mammary repopulating units ($CD24^{lo}$ $CD49f^{hi}$) with flow cytometer. 4000 mammary epithelial cells were then plated in 60mm dishes in triplicate with 40,000 NIH3T3 cells that had previously been cell cycle arrested by γ-irradiation at 50 Gy. Cells were plated in Epicult B Medium (Stem Cell Technologies #05610) according to the manufacturer's protocol. After eleven days, cell media was removed and cells were fixed in 4% paraformaldehyde, washed with 1X PBS, then cells were stained with Geimsa and cells were imaged by brightfield microscopy as above.

qPCR

RNA was isolated from cells or tissue as described in text using Trizol Reagent (Invitrogen #15596). Primers were designed using PerlPrimer with at least one primer of each pair spanning an intron. RNA was reverse-transcribed using MMLV High Performance Reverse Transcriptase (Epicentre #RT80110K). 0.005ug of cDNA for each well, in triplicate, was amplified using specific primers and SYBR Green SuperMix-UDG (Invitrogen 11733-038) at 1/8X concentration in 96-well plates. Fluorescence was measured in a Stratagene Mx3005p qPCR Thermal Cycler (Agilent Technologies). Relative expression was calculated against standard curves with glyceraldehyde-3-phosphate dehydrogenase (GAPDH) as normalizer, using MxPro Software (Agilent Technologies). All primers can be found in Appendix D. Normal mammary assays examined organoid preparations from three glands of each genotype. Tumor assays examined RNA from eight tumors of each genotype.

Flow Cytometry

Single cell suspensions were isolated from mammary glands as above or from culture and incubated with fluorescently tagged antibodies, listed in reagents. Antibody incubations were carried out on single cell suspensions for one hour at 4℃ in cell staining buffer (2% Bovine Serum Albumin, 2mM EDTA, in 1X PBS). Cells were then washed in cell staining buffer, centrifuged at 300xg for 5 minutes and resuspended in cell staining buffer. Labeled experimental cells, unlabeled control, and singly labeled compensation controls were then run in triplicate on Millipore Guava Easy Cyte 8HT or BD Biosciences FACSAria II and analyzed using FloJo 9.3.1 software (Treestar Inc). For

normal mammary assays, lineage panel-negative cells were gated to analyze CD24 and CD49f populations. For BrdU assay, cells were gated against CD24 to analyze $CD24^+$ and $CD24^-$ populations.

p53ko Mammary Gland Transplants

Mammary glands from sexually mature *p53ko;jnk2wt* or *p53ko;jnk2ko* female (five of each genotype) mice were transplanted as $5mm^2$ pieces into cleared fat pads of 25 3 week-old wildtype females per genotype, with an average of five transplants per donor. Transplant surgeries were carried out under anesthesia with 500uL of 0.2% Avertin Tribromoethanol solution for recipients and 750uL for donors. Two weeks after transplantation, pituitary glands were extracted from sexually mature female mice (one whole pituitary gland per mammary transplant recipient) and placed within the kidney capsule of each mammary transplant recipient, under anesthesia, as described (117). Mammary transplants were palpated three times weekly until tumors were palpated and tumors were measured with caliper until they reached a target size of 1.5cm diameter. Tumors were then harvested and cut into pieces and flash frozen for RNA, fixed in 4% paraformaldehyde for histology, or minced for cell line generation.

Cell lines

MT^+*jnk2ko* cell lines were previously generated from MT tumors and GFP and GFP-JNK2 genes were stably integrated (3). Cell lines from p53ko tumors were generated after harvest from transplant recipient mice at target size. Whole tumors were minced and treated with 5 mg/mL collagenase, then rocked at 37℃ for four hours or until suitably digested—prior to single cell suspension. Tumor organoids were then enriched by four

rounds of differential centrifugation at 500xg with PBS washes. Cells were plated in eight 10cm diameter dishes in DMEM/F12 with 1% FBS. Cells were treated with 2.5mg/mL Dispase to remove fibroblasts and cultures were combined after crisis to generate immortalized cell lines. MT cells and *p53ko* cells were maintained in DMEM/F12 medium (Mediatech Inc.#10-090) supplemented with 10% Benchmark FBS (Gemini #100-106), 10μg/ml Humulin® R U-100 (Lilly #0002-8215-01), 5ng/ml EGF (Peprotech AF-100-15), penicillin/streptomycin (Life Technologies #15070-063). GFP and GFP-JNK2 constructs were stably expressed p53ko cells by using the GP2-293 cell retroviral packaging system (Clontech). GP2-293 cells were plated on 10cm dishes at a density of 800,000 cells. After attaching, cells were transfected with 10ug total DNA (5ug construct plus 5ug VSV-G) using 20 uL of Lipofectamine 2000 Reagent (Life Technologies #11668) in DMEM without serum or antibiotics. Media was replaced, after four hours of incubation, with target cell media and viral media was placed onto target cells at 48 hours and 72 hours post-transfection. Cells were selected with 5ug/mL Puromycin and populations were assessed for construct expression.

Luciferase assay

MT+*jnk2ko* GFP and GFP-JNK2 cells were plated at 400,000 cells per 10cm dish and allowed to attach overnight. Cells were transfected with 5ug total DNA of both luciferase constructs and CMV-Beta-galactosidase or CMV-Luciferase as positive control, using 10uL Lipofectamine 2000 Reagent. Cells were harvested using Reporter Lysis Buffer (Promega #E3971). Lysates, in quadruplicate, were exposed to Luciferase

Assay Reagent (Promega #E1483) or w-nitrophenyl-β-D-galactopyranoside (Fisher Scientific PI-34055) and read on a Synergy 4 Plate reader (BioTek).

Chromatin Immunoprecipitation Assay

20 million cells of each genotype, in 10cm cell culture dishes, were fixed at room temperature in 1% formaldehyde to facilitate cross-linking of protein-DNA complexes. Cross-linking reactions were stopped after 10 minutes with 125mM glycine (added directly to media) then cells were washed with ice cold 1X PBS three times before scraping into 1mL 1X PBS with protease inhibitor cocktail. Cells were then centrifuged at 400xg for 5 minutes and supernate removed. Cells were then lysed for 10min on ice in 600uL 5mM Pipes (pH 8.0), 85mM KCl, 0.5% NP-40 with protease inhibitor cocktail minus DTT. Then cells were pelleted at 5000 RPM in microcentrifuge at 4°C. Supernate was removed and DC Protein Assay was performed on this liquid to normalize sample concentrations. Then nuclei were lysed on ice in 200uL of 50mM Tris (pH 8.1), 10 mM EDTA, 1% SDS with protease inhibitor cocktail, while vortexing every 30 seconds at full speed for 10 minutes. Then chromatin was sheared by bath sonication in an Episonic Bioprocessor (Epigentek), at Amplitude 56, 8 times for 20 seconds with 20 second rests on ice. Samples were then centrifuged in a microcentrifuge at 4°C and full speed for 10 minutes. Supernate containing chromatin fragments was removed diluted by adding 450uL of 0.01% SDS, 1.1% Triton X-100, 1.2mM EDTA, 16.7mM Tris (pH 8.1), 167 mM NaCl with protease inhibitor cocktail. Samples were divided approximately into thirds (~200uL) in microcentrifuge tubes. One tube was frozen for use as input and 30uL of 50% protein A sepharose beads (Fisher Scientific #26159) that had been pre-cleared

with sonicated salmon sperm DNA (Amresco 309-566-6) was then added to the sonicated chromatin samples along with either 1:500 anti-mouse p53 antibody (Cell Signaling #2524) or 1:50,000 IgG (Calbiochem NI03) were added. Samples were then rocked on a rotary nutator overnight at 4°C. Samples were then centrifuged at 5000RPM in centrifuged for one minute, then washed with the following solutions plus protease inhibitor cocktail: 0.1% SDS, 1% Triton X-100, 2mM EDTA, 20mM Tris (pH 8.1), 150mM NaCl, then 0.1% SDS, 1% Triton X-100, 2mM EDTA, 20mM Tris (pH 8.1), 500mM NaCl then 0.25M LiCl, 1% NP-40, 1% deoxycholate, 1mM EDTA, 10mM Tris (pH 8.1) then twice with 1X TE Buffer (10mM Trist pH 8.1, 1mM EDTA pH 8.0). Samples were then eluted from beads by adding 250uL 1% SDS, 0.1 NaHCO3 and incubating samples at 65°C for 40 minutes, with shaking. Samples were flicked every 10 minutes during this incubation to resuspend bead/chromatin complexes. Next, samples were centrifuged at full speed in a microcentrifuge for 3 minutes at 4°C and supernate with liberated chromatin was moved to a fresh tube. Input samples were then thawed and cross-links of all samples were reversed by addition of 1uL 20mg/mL RNase A (Life Technologies 12091-039), 17.5uL of 5M NaCl, and incubation at 65°C for five hours with shaking. 750uL of 100% ethanol was then added and samples were precipitated overnight at -20°C. DNA was then centrifuged at full speed in a microcentrifuge and supernate removed. The resulting pellets were resuspended in 100uL of dH2O, 2uL 0.5M EDTA, 4uL 1M Tris (pH 6.5), and 1uL 20mg/mL Proteinase K (Fisher Scientific #BP1700). Then samples were incubated for 2 hours at 45°C. After digestion, DNA was isolated using a DNEasy kit (Qiagen #69504) according to manufacturer's instructions

with 50uL final elution volume. 2uL of final input samples and 15uL for immunoprecipitated samples were amplified by PCR using specific primers, listed in the appendix.

Microarray Analysis

Cell pellets were collected for *p53ko* cell lines and tumors (10 *p53ko;jnk2ko* and 4 *p53ko;jnk2wt*), then lysed and processed using the RNEasy Kit (Qiagen #74104), to purify total RNA. RNA was sent to the Charles Perou Lab at the University of North Carolina at Chapel Hill, where probe labeling and hybridization was carried out by Adam Pfefferele, using Agilent custom 4X180K microarrays as previously described (118). The microarray data was uploaded to the University of North Carolina Microarray Database (UMD) (https://genome.unc.edu/pubsup/breastGEO/clinicalData.shtml) and to the Gene Expression Omnibus (GEO) under accession number GSE40226. Hierarchical clustering was performed using Gene Cluster 3.0 (119) and the data was viewed using Java Treeview version 1.1.5r2 (120). Statistically significant expression changes between tumor genotypes were determined using a 2-class unpaired significance analysis of microarray (SAM) analysis, with genes having a false discovery rate (FDR) ≤5% considered statistically significant.

BrdU Assay

600,000 cells were plated onto 10cm dishes then allowed to attach and recover for 23 hours in full media (as described above). Cells were then incubated with a 1mM BrdU solution (BD Biosciences BD Biosciences #550891) at a 1:100 dilution. Cells were then harvested with trypsin-EDTA and quenched with full media, strained through a 40um

strainer, and then counted. Live cells were next incubated with a CD24-PE-Cy7 antibody in cell staining buffer. After washing, cells were incubated with fixation/permeabilization buffer (BD Biosciences #554714) for 30 minutes at room temperature. Cells were then washed with 1X PBS and incubated with 300ug/mL in 1X PBS for 1 hour at 37°C. Cells were then washed with 1X PBS and resuspended in 1X Perm/Wash Buffer (BD Biosciences #554723) and BrdU-FITC antibody and incubated 1 hour at 4°C. Cells were then washed with 1X PBS and resuspended in cell staining buffer and plated in triplicate in a 96-well plate for analysis by flow cytometer.

Limiting Dilution Tumor Assay

Cell lines were trypsinized and recovered in full media counted, before passing through a 40um cell strainer and counting. Serial dilutions of 10,000, 1,000, and 100 cells per 50uL of sterile filtered normal saline (Biochemika #07982). 50uL of cells were then injected of cells into #2 mammary glands of nude mice using a Hamilton syringe (Hamilton Company #7638-01). Tumors were palpated thrice weekly. To determine tumor initiating cell frequency, L-Calc v1.1 (Stemsoft Software) was used.

Statistics

Statistical analyses were performed using Prism Software (GraphPad). Student's T-test was employed to determine significance of single variable data. Significant data from T-test is indicated on figures as follows: * for $0.05 \geq p \geq 0.01$, ** for $0.01 > p \geq 0.0001$, *** for $p < 0.0001$. Significance for survival data was determined using Logrank test, where $p < 0.05$ was considered significant. 2way ANOVA with Bonferroni Post-test was

employed to determine significance of multi-variable data. Data was considered significant if $p<0.05$. Error bars are shown as standard deviation.

Chapter 3 – JNK2 Inhibits Notch-Dependent Mammary Luminal Cell Differentiation

3.1. JNK2 Inhibits Mammary Luminal Cell Differentiation *in vivo*

To test if mammary cell differentiation is altered in the absence of JNK expression, seven week-old virgin mammary glands from *Jnk2*-null (*jnk2ko*)and wildtype (*jnk2wt*) female mice mammary glands were harvested, paraffin-embedded and examined for discrepancies in expression of myoepithelial (p63) and luminal markers (Cytokeratin 8/18 and ER), p63 in histologic samples. This time point was used to ensure counting of only mature ducts in fully invaded fat pads of both genotypes.

Analyses of lineage markers showed that *jnk2ko* ducts possess 35% fewer $p63^+$ myoepithelial cells than *jnk2wt* (Figure 3.1, p=0.0078), trend toward increased luminal cells by Cytokeratin 8/18 (Figure 3.2A), significantly higher proportion of ER^+ luminal cells (Figure 3.3, p=0.011) staining. In histology samples, the observation was also made that Cytokeratin 8/18 staining is more intense in *jnk2ko* ducts than *jnk2wt*. To confirm this observation, mammary glands from both genotypes were harvested from seven week-old virgin females. Cells were then processed and digested with collagenase to yield mammary organoids, which consist of fat pad-free mammary epithelial cells with their underlying extracellular matrix and few stromal cells. Organoids were then lysed for western blot to examine Cytokeratin 8/18 expression. Western blot confirmed that higher

expression of Cytokeratin 8/18 is induced by loss of JNK2 expression in the mammary epithelium (Figure 3.2B).

To better quantify the luminal and basal cell populations, individual cell CD49f and CD24 expression levels were measured using flow cytometry. For this assessment, mammary glands from *jnk2ko* and *jnk2wt* mice were dissociated to organoids and then trypsinized to create a single cell suspension. Stromal cells, such as fibroblasts and immune cell populations were negatively selected using a lineage panel of antibodies. As seen in the above experiments, *jnk2ko* glands contain a larger proportion of $CD49f^{Lo}$ $CD24^{+}$ luminal cells (61%) as compared *jnk2wt* glands (36%, Figure 3.4, $p<0.0001$). A corresponding decrease in the $CD49f^{hi}$ $CD24^{lo}$ basal/myoepithelial cell population was also seen in *jnk2ko* mammary epithelial cell preparations ($p<0.0001$).

3.2. Inhibition of Luminal Populations by JNK2 is Cell Autonomous

Development and differentiation of the mammary gland is highly dependent upon the influence of hormones such as ER (see section 1.1). The mice analyzed in the above experiments possess a systemic knockout of *Jnk2*, therefore there is a potential that the differentiation phenotype is caused by an alteration of the endocrine system. In order to act within the mammary gland in a cell autonomous fashion, JNK2 must be expressed by mammary epithelial cells or cells of the stroma. To determine the expression pattern of JNK2 in the mammary gland, adult glands were examined by immunofluorescence using an anti-JNK2 antibody. This analysis shows that JNK2 is expressed in *jnk2wt* mammary glands and not in *jnk2ko* glands, throughout the mammary epithelium (Figure 3.5). This

indicates that JNK2 is available and may act cell autonomously to prevent luminal cell differentiation.

To further test if JNK2 affects differentiation and mammary growth independent of hormonal influence, mammary epithelial cells from both genotypes were isolated and cultured on Matrigel™ using defined growth media. This method has been shown to allow growth of single cells into spherical mammary 3-dimensional cultures that possess differentiative capability and recapitulate effects of gene targeting *in vivo* (25, 116). Cultures were allowed to grow and differentiate prior to analysis of cell populations. Consistent with observations that JNK2 inhibits luminal cell populations *in vivo*, the resulting *jnk2ko* cultures show fewer smooth muscle actin positive myoepithelial/basal cells and more Cytokeratin $8/18^{+}$ cells than *jnk2wt* controls (Figure 3.6).

To determine the level of the mammary epithelial cell hierarchy is affected by JNK2, *in vitro* differentiation assays were performed. Mammary glands from *jnk2ko* and *jnk2wt* mice were minced and sorted for mammary repopulating unit (stem cell enriched) and colony forming unit (progenitor enriched) populations, representing stem and progenitor fractions, respectively. These were plated and allowed to grow and differentiate thus producing colonies of cells that define the particular lineage path that was taken by stem cells or revealing whether the progenitor was of bipotent, luminal, or basal lineage in the case of colony forming units. Mixed-, luminal-only-, and basal-only colonies were produced from mammary repopulating- and colony forming units of both genotypes. Mammary repopulating unit-enriched populations from *jnk2ko* were found to produce significantly more luminal colonies (Table 3.1, 2way ANOVA with Bonferroni

Post-test) and significantly fewer basal+mixed colonies, representing the sum of both basal groups. There were no significant differences found in proportions of basal or mixed colonies. Colony forming units-enriched populations from *jnk2ko* produced a lower proportion of basal-only colonies (Table 3.2, 2way ANOVA with Bonferroni Post-test), but there were no other significant differences in luminal colony proportions. These data further support that JNK2 promotes population of the mammary gland with the basal lineage while suppressing luminal populations. Suppression of luminal lineage proportions appears to cause an effect at both stem and progenitor levels of the mammary hierarchy.

3.3. JNK2 INHIBITS NOTCH-DEPENDENT LUMINAL CELL DIFFERENTIATION

Lineage commitment and differentiation within the mammary gland is highly dependent upon the p63/Notch1 interaction (30). When p63 expression is elevated, myoepithelial populations increase and when Notch1 expression increases, so do luminal cell populations. In *jnk2ko* mammary glands, luminal populations are increased as compared to *jnk2wt* controls. The proportion of cells expressing p63 is also decreased by loss of JNK2. Because, like Notch1, JNK2 appears to be important for regulation of luminal cell differentiation in both stem and progenitor levels of the mammary hierarchy, it was hypothesized that increased luminal populations in *jnk2ko* mammary glands are due to increased Notch activity.

In order to become activated, transmembrane Notch receptors that are bound by their ligands must be cleaved at intracellular and extracellular domains (121). The

intracellular cleavage event is mediated by Gamma Secretase, which allows the Notch intracellular domain ($Notch^{ICD}$) to translocate into the nucleus to de-repress promoters of target genes, such as Hes1. Highest levels of transcriptional activation are achieved by association with Mastermind-like proteins (122).

To find if Notch signaling is increasing luminal differentiation in the *jnk2ko* model, were fixed and stained for fluorescence microscopy with cell lineage markers. To determine if Notch signaling promotes proliferation and/or differentiation of *jnk2ko* 3-dimensional cultures, primary mammary epithelial cells were seeded in Matrigel™ and treated with Gamma Secretase IX (GSI), an inhibitor of Notch receptor cleavage and activation. GSI treatment trends toward increases in the proportion of $p63^+$ myoepithelial cells in both *jnk2wt* and *jnk2ko* cultures compared to DMSO controls but only *jnk2ko* groups vary significantly (Figure 3.7, 2way ANOVA with Bonferroni Post-test). The proportion of $p63^+$ cells is similar in *jnk2ko* and *jnk2wt* GSI treated cultures, which indicates that treatment has successfully eliminated effects of Notch signaling on differentiation. Similar to results gained in assessment of Notch-dependent growth, the increase of myoepithelial cell proportion is greatest in *jnk2ko* cultures. This indicates a greater dependence on Notch signaling for differentiation in these cells, as compared to *jnk2wt*.

To evaluate the proportions of luminal cells that are affected by GSI treatment, 3-dimensional cultures were stained with a Cytokeratin 8/18 antibody and positive cells were counted. Consistent with the increase in myoepithelial cell proportion observed in the presence of GSI, proportions of *jnk2ko* luminal populations significantly decreased in

jnk2ko cultures (Figure 3.8, 2way ANOVA with Bonferroni Post-test). No significant alteration in luminal cell populations was observed in *jnk2wt* cultures.

These data were further confirmed using a Adenoviral introduction of a dominant negative Mastermind gene (AdMAM51) (112). In this experiment, normal mammary epithelial cells were isolated from *jnk2ko* and *jnk2wt* glands and then infected with adenoviruses encoding GFP (AdGFP) or AdMAM51 to reduce Notch-dependent transcription. RNA harvested from 3 dimensional cultures showed a reduction in expression of the Notch target gene, *Hes1*, in response to AdMAM51 expression (Figure 3.9A, 2way ANOVA with Bonferroni Post-test). This finding confirms efficacy of the AdMAM51 activity. Similar to GSI treatment, infection of *jnk2ko* mammary cells with AdMAM51 significantly decreased the diameter of cultures (Figure 3.9B, 2way ANOVA with Bonferroni Post-test). AdMAM51 treatment also significantly decreased luminal cell populations of *jnk2ko* cultures (2way ANOVA with Bonferroni Post-test) without significantly affecting populations in *jnk2wt* cultures (Figure 3.10). Collectively, these data indicate that *jnk2ko* MECs are more sensitive to Notch signaling inhibition, and JNK2 regulates mammary epithelial cell differentiation through the Notch pathway.

3.3. JNK2 INHIBITS NOTCH-DEPENDENT MAMMARY CELL GROWTH

Other reports show that increased Notch signaling leads to increased acinar growth (24, 25). To see if this is true in the jnk2ko model, mammary cells were grown in 3-dimensional culture in the presence of GSI, as above. At nine days post-seeding, cultures were imaged and measured. As expected, GSI treatment significantly decreases

the final diameter of *jnk2wt* and *jnk2ko* 3-dimensional cultures, relative to the vehicle controls (Figure 3.11, 2way ANOVA with Bonferroni Post-test). Treatment with GSI causes *jnk2wt* and *jnk2ko* cultures to become essentially equal in diametric size. The fact that *jnk2ko* cultures show a larger reduction in diameter with GSI than *jnk2wt* implies that they are more reliant on Notch signaling. This could potentially be caused by an increase in magnitude of Notch signaling within *jnk2ko* mammary epithelial cells.

3.5. JNK2 INHIBITS NOTCH1 EXPRESSION AND CLEAVAGE *IN VIVO*

The importance of Notch signaling in mammary epithelial cell differentiation is well known. The fact that Notch activity is highest in the terminal end buds of pubertal mammary glands also supports a role for Notch during pubertal mammary development (30). Moreover, all Notch receptors are expressed in the developing mammary gland but it is *Notch1* that is temporally and spatially expressed in a pattern that best facilitates the process of differentiation (25). As mentioned previously, Notch1 efficiently promotes luminal cell populations over myoepithelial/basal populations—similar to the effect of *jnk2ko*. Since 3-dimensional culture experiments demonstrate that Notch signaling drives luminal commitment, Notch activity was assessed throughout puberty by performing immunohistochemistry, using a $Notch1^{ICD}$ antibody. Because highest levels of Notch signaling occur in the terminal end buds, analyses were divided between mature ductal regions and terminal end buds themselves. No differences in $Notch1^{ICD}$ expression are detected in mature ducts (Figure 3.12). However, within the putative mammary stem cell niche of terminal end buds, the proportion of cells staining positive for $Notch1^{ICD}$ is

higher in *jnk2ko* glands, compared to *jnk2wt*, throughout puberty (Figure 3.13, 2way ANOVA with Bonferroni Post-test).

To validate that increased Notch1^{ICD} expression in *jnk2ko* pubertal glands results in higher Notch-dependent transcription, mammary organoids were isolated from *jnk2ko* and *jnk2wt* mammary glands and harvested to collect RNA. The expression of *Hes1* was measured using qPCR. This experiment revealed that *jnk2ko* organoids express 10.5 times more *Hes1* mRNA than *jnk2wt*, thus confirming increased Notch activity in the absence of JNK2 expression (Figure 3.14A, $p=0.0093$). Further qPCR experiments revealed that *Notch1* mRNA is also significantly elevated in *jnk2ko* organoids (Figure 3.14B, $p<0.0001$), and western blotting of protein isolated from mammary organoids shows an increase in full-length Notch-1 protein as compared to *jnk2wt* (Figure 3.14C).

3.6. DISCUSSION

Our data are consistent for a role of JNK2 in negative regulation of Notch1-dependent luminal cell differentiation. However, the *jnk2ko* phenotype observed does not agree with all reports of increased Notch signaling in the mammary gland. For example, mammary-specific overexpression of active Notch-1, -3, or -4 leads to tumorigenesis through overgrowth of luminal progenitors (123, 124). Many generations of *jnk2ko* mice have been observed and these mice to not show a propensity to develop mammary tumors, in spite of the increased luminal populations observed in the above experiments. This is likely due to disparate levels of Notch signaling in the *jnk2ko* and Notch receptor overexpression models. A recent study examining the effect of Notch1^{ICD}

expression in 3-dimensional cultures revealed a dose-dependent mammary growth phenotype (125). The highest levels of Notch1^{ICD} expression are associated with small and abortive cultures that were not seen in our experiments. The *jnk2ko* 3-dimensional culture phenotype is more reminiscent of large, hyper-proliferative cultures that were associated with lower Notch1^{ICD} overexpression. This level of expression may be more physiologically relevant and give a more appropriate picture of the role of Notch in mammary development.

Spatio-temporal localization of Notch1^{ICD} is also of critical importance in differentiation of mammary epithelial cells. Reports show that highest *Notch1* expression in the mammary gland is during puberty with the most intense activity in terminal end buds (30). Because terminal end buds are the site of mammary stem cells, they are an ideal structure for differentiation to begin. Consistent with this, highest levels of Notch1^{ICD} expression is localized to the terminal end buds in *jnk2ko* mice. Because of the biphasic nature of Notch1-dependent luminal commitment, in promotion of stem cell differentiation and at the level of progenitor expansion, further experiments into the precise steps affected by JNK2 may be warranted. Although mammary repopulating unit populations were not validated by *in vivo* transplantation experiments, they agree with our differentiation data and show that this enriched population results in the production of luminal cells at a higher frequency in *jnk2ko* as compared to *jnk2wt* mammary glands. Colony forming unit results also support our *in vivo* differentiation results, but in an unexpected way. Here, equal numbers of luminal colonies and fewer basal colonies were seen in *jnk2ko* preparations. The remaining colonies were of mixed lineage, supposedly

bipotent progenitor enriched. *Jnk2ko* cultures had significantly more of these mixed colonies and presumably, a higher proportion of luminal cells as a result. The presence of JNK2 protein in all cell types of the mammary epithelium and the role of Notch1 in both stem cell- and progenitor differentiation processes support JNK2 regulates both levels of the mammary hierarchy as well.

JNK-Notch interactions have been studied in a variety of tissues with unique results depending upon the system. The results point to a dichotomous relationship wherein JNKs regulate Notch signaling differentially depending upon whether or not it has been activated by an external stimulus. For example, treatment of mice by intraperitoneal injection of JNK inhibitor induces cleavage of the Notch-1 receptor in normal brain tissues (126). Similarly inhibition of JNK in macrophage cell lines induces increased Notch signaling by upregulating Jagged-1 (127). Conversely, treatment of HEK293 cells with various cytokines induces Notch1 cleavage and requires JNK (128). In this system, JNK activity was induced by the cytokines. In Kaposi's sarcoma endothelial cells, JNK is induced by contact inhibition to promote *Hes1* transcription, independent of Notch receptor activation (129). Notch also reciprocally regulates JNK activity in HEK293 cells by preventing UV-induced activation of JNK1 and JNK3 by binding to and inhibiting the scaffold activity of JIP-1 (130). This prevents JNK-induced apoptosis. Our model required no external input of stimulus and seems to be in agreement with reports that basally active JNKs inhibit Notch signaling.

Our model indicates that the highest level of regulation over the Notch pathway, by JNK2, is in transcription of the *Notch1* gene. A recent report in keratinocytes has

suggested a potential mechanism for this interaction. This showed that MAPK signaling negatively regulates expression of *Trp53* mRNA through AP-1 (131). In this report, EGF-induced ERK signaling was the regulating MAPK, but JNKs have been cemented as key regulators of AP-1 and they are, themselves, activated in response to EGF. This may be a potential mechanism, but in light of the previous paragraph may present mixed results because active JNKs seem to promote Notch1 activity.

Chapter 4 – JNK2 Inhibits Luminal Differentiation and Notch signaling in the Polyoma Virus Middle T Antigen (MT) Model

4.1. JNK2 Inhibits Luminal Cell Differentiation in MT Tumors

In order to characterize the signaling involved in JNK2-dependent inhibition of *Notch1* mRNA expression, cell lines and tumors that were developed while studying the MT model of mammary tumorigenesis were utilized (3, 6). Because normal mammary and tumor differentiation are controlled by similar mechanisms, it was hypothesized that JNK2 inhibits luminal lineage commitment in MT tumors through inhibition of Notch signaling. To test this hypothesis, tumors from MT^+ *jnk2ko* and MT^+ *jnk2wt* mice were sectioned and immunostained with p63 or Cytokeratin 8/18 antibodies to identify basal/myoepithelial and luminal cells, respectively. Results show that a high proportion of tumor cells do not express either p63 or Cytokeratin 8/18, an indication that these tumors became less differentiated as they developed—a characteristic that is typical of advanced tumors. Of cells that did show positive staining, MT^+ *jnk2ko* tumors have a significantly smaller proportion of cells with nuclear p63 staining (Figure 4.1, p=0.0079) and a greater proportion of Cytokeratin $8/18^+$ cells than MT^+ *jnk2wt* tumors (Figure 4.2, p=0.0411 Mann Whitney test). These results suggest that, akin to the normal mammary gland, JNK2 promotes basal lineage commitment while suppressing the luminal lineage in MT tumors.

4.2. JNK2 INHIBITS EGF-DEPENDENT NOTCH SIGNALING IN MT TUMORS AND CELLS

Next, MT tumors sections were immunostained for Notch1^{ICD} to address the hypothesis that Notch signaling is suppressed by JNK2 in MT tumors. This analysis reveals that while MT^{+} *jnk2wt* tumors are virtually Notch1^{ICD} negative, MT^{+} *jnk2ko* tumors express the cleaved Notch1 receptor in nearly all cells (Figure 4.3). Additionally, qPCR shows that *Notch1* mRNA expression is four times higher in MT^{+} *jnk2ko* tumors as compared to MT^{+} *jnk2wt* tumors (Figure 4.4, p=0.0101). This assessment verifies that Notch signaling is inhibited by JNK2 in cells of MT tumors, similar to normal mammary epithelial cells.

Further exploration of the mechanism by which JNK2 inhibits *Notch1* mRNA expression and activity was performed using an MT^{+} *jnk2ko* cell line that was previously generated (3). This cell line is modified to express a GFP-JNK2 fusion protein or GFP control. RNA was isolated from confluent cells in culture and assessed by qPCR. Consistent with results found in normal glands and MT tumors, GFP-JNK2 expression suppresses *Notch1* by 42% (Figure 4.5A, p=0.0005). Western blotting confirmed that GFP-JNK2 expression suppresses full-length Notch1 receptor at the protein level in MT cells (Figure 4.5B). Additionally, there is a trend toward reduction of *Hes1* mRNA in GFP-JNK2 cells (Figure 4.5C). These results show that expression of and signaling through Notch1 is inhibited by JNK2 expression in MT cells.

Previous work in keratinocytes showed that MAPK signaling inhibits *Notch1* mRNA expression through transcriptional repression of *Trp53*, the gene encoding p53 (131). These experiments show that MEK-1 and ERK suppress *Notch1* expression in

response to EGF-mediated activation. Although the authors did not observe any effects after JNK inhibition, this may have been a tissue specific interaction. Because JNKs have been shown to become activated in response to EGF in breast cancer cells (61), I hypothesized that JNK2 inhibits Notch1 expression through suppression of *Trp53* transcription. To test this hypothesis, expression levels of *Trp53* mRNA in MT cells were examined. RT-PCR showed that GFP-JNK2 inhibits *Trp53* expression (Figure 4.6A). To verify that this also occurs in normal mammary glands, organoid mRNA was assessed by qPCR for *Trp53* expression. This showed that *jnk2ko* mammary glands express nearly three times more *Trp53* mRNA than *jnk2wt* glands (Figure 4.6B, p=0.0004).

To determine if suppression of p53 by JNK2 is through EGF signaling, MT cells were treated with 50ng/mL EGF and harvested for mRNA. In this experiment, qPCR was performed to examine expression levels of *Trp53* and *Notch1*. Expression of *Cyclind1* was also assessed as a positive control for EGF-dependent transcription (132). As expected, EGF treatment significantly increased expression of *Cyclind1* in both MT^+ GFP-JNK2 and MT^+ GFP cells against serum free media controls (Figure 4.7A, 2way ANOVA with Bonferroni Post-test), thus showing that EGF treatment is successfully inducing EGFR activity. EGF treatment did not significantly affect expression of either *Notch1* or *Trp53* in MT+ GFP-JNK2 cells, but instead induced 2.11 times more expression of *Trp53* and 30.6 times more *Notch1* in MT^+ GFP cells (Figure 4.7B and C, 2way ANOVA with Bonferroni Post-test). Serum free media controls were not

significantly different from each other. These data show that JNK2 suppresses EGF-dependent promotion of *Trp53* and *Notch1* mRNA expression.

4.3. JNK2 INHIBITS EGF-DEPENDENT ACTIVATION OF *NOTCH1* PROMOTER ACTIVITY THROUGH P53 RESPONSE ELEMENTS

To assess whether JNK2-dependent inhibitions of *Trp53* and *Notch1* expression are related, notch1 promoter assays were performed. The *notch1* promoter contains two p53 response elements that are bound by p53 to potentiate its transcription (113). Because MT tumors and cell lines express wildtype p53 (3), I hypothesized that p53 binds to the promoter of *notch1* in MT cells in a manner that is suppressed by JNK2 expression. This mechanism was explored by transfecting MT^+ GFP and MT^+ GFP-JNK2 with *Notch1* promoter constructs driving expression of luciferase. These plasmids were previously designed and assessed for activity (113). Three constructs were transfected into cells, individually: full-length *Notch-1* promoter (N1PR), *Notch-1* promoter with mutated p53 response elements (N1PRmut), or a control promoterless construct (N1PRless). As expected, MT^+ GFP cells have higher *Notch1* promoter activity than MT^+ GFP-JNK2 cells (Figure 4.8A, 2way ANOVA with Bonferroni Post-test). This higher expression was significantly decreased to MT^+ GFP-JNK2 levels in cells transfected with N1PRmut. Promoter activity in MT^+ GFP cells was not affected by mutation of the p53 response elements, indicating that these are not important in promotion of *Notch1* in these cells. These data support that JNK2 inhibition of *Notch1* requires the p53 response elements within its promoter.

Next, the effect of EGF treatment on *Notch1* promoter activity was assessed. Similar to data gained in the qPCR experiment above, EGF-stimulated N1PR activity was suppressed by expression of GFP-JNK2 (Figure 4.8B, 2way ANOVA with Bonferroni Post-test). Additionally, EGF-stimulated N1PR activity was abolished by mutation of p53 response elements in the *Notch1* promoter in MT^+ GFP cells. Surprisingly however, was the finding that mutation of p53 response elements in serum free media caused significant increases in *Notch1* promoter activity in both MT^+ GFP-JNK2 and MT^+ GFP cells. These data suggest that the *Notch1* promoter is both positively and negatively regulated through its p53 response elements. Negative regulation appears to be EGF and JNK2-dependent, but positive regulation is JNK2-independent.

To determine if decreased expression of *Trp53* mRNA in MT^+ GFP-JNK2 cells also leads to decreased binding of p53 to the *Notch1* promoter, chromatin immunoprecipitation was performed. Primers were designed using the sequence of the *Notch1* promoter and aligned around the p53 response elements. As a positive control for p53 binding, primers were also designed around p53 response elements of the *Cdkn1a* (the gene encoding the cyclin-dependent kinase inhibitor, p21) promoter and the glyceraldehyde phosphate dehydrogenase (*Gapdh*) promoter was used as negative control. Chromatin was purified from MT^+ GFP and MT^+ GFP-JNK2 cell lysates and Chromatin immunoprecipitation was performed using an anti-p53 antibody or IgG control. Input controls show similar loading of MT^+ GFP and MT^+ GFP-JNK2 samples and IgG antibody control shows no amplification, as expected (Figure 4.9). Amplification with *Cdkn1a* promoter positive control primers shows that p53 was

successfully immunoprecipitated and that GFP-JNK2 inhibits binding of p53 to the *Cdkn1a* promoter. *Notch1* promoter primers show that p53 binds to the *Notch1* promoter at a greater frequency in MT^+ GFP cells than MT^+ GFP-JNK2 cells, thus demonstrating that JNK2 inhibits binding of p53 to the *Notch1* promoter. Experiments above suggest that decreases in binding of p53 to the *Notch1* promoter, in the presence of GFP-JNK2, are caused by inhibition of transcription of *p53* mRNA.

4.4. DISCUSSION

Data presented in this chapter support that JNK2-dependent differentiation mechanisms that are present in the normal mammary gland are also present in tumors. Specifically, these data show that JNK2 inhibits luminal populations in the MT model. Our results were limited by the overall lack of differentiation in archived tumors, presumably because of the advanced size and subsequent dedifferentiation. However, a sufficient proportion of cells maintained expression of Cytokeratin 8/18 and p63 to produce a meaningful result that mirrors the effects of JNK2 in normal mammary tissue.

In other mouse models, overexpression of $Notch1^{ICD}$ has been shown to cause the generation of tumors due to a build-up of luminal progenitor cells. Given the decreased tumor latency phenotype observed (3) and preponderance of $Notch1^{ICD}$ positive cells in MT^+ *jnk2ko* tumors, it is reasonable to hypothesize that Notch signaling plays a role in increasing the susceptibility to tumorigenesis in this model. This may be a direct effect, such as increasing the proliferative capacity of cells or an indirect effect, through modulation of the differentiation programme. A larger luminal population in *jnk2ko*

glands may enhance tumor susceptibility when confronted with oncogenic stimuli, as luminal cells are the target for tumorigenesis in the MT model. This could lead to both the decreased tumor latency and increased multiplicity phenotypes of MT^+ *jnk2ko* mice.

Our results show that *Trp53* mRNA is upregulated by *jnk2ko* in both normal mammary and MT tumor cell models. This contrasts with a recent result that MKK7 ablation in *Kras* induced lung tumors and NeuT oncogene induced tumors causes destabilization and degradation of p53 (133). The results in this report were corroborated using *jnk1*+/- *jnk2ko* mice, but *jnk2ko* alone had no effect on p53 protein expression. The oncogenic stimuli used in these experiments are unique from ours and it is worth noting that MT expression is silenced in our MT^+ cell lines due to methylation (unpublished data). This means that our signaling mechanism exists in the absence and presence of oncogenic activation, thus showing that the JNK2/*Notch1* interaction is the result of basal JNK activity.

The question of whether p53 is the protein mediating *Notch1* upregulation in the absence of *jnk2* expression has not been answered by these experiments completely. We have shown conclusively that the p53 response elements within the *Notch1* promoter are essential for upregulation and that p53 binding is increased to the promoter. However, p63 is also able to bind to the p53 response elements (113) and is known to counteract *Notch1* expression (30). Because p63 expression is decreased by *jnk2ko* in both the normal and MT models, there remains the potential that *Trp63* expression may be promoted by JNK2 and the absence of JNK2 decreases its expression thus allowing *Notch1* expression to rise.

Chapter 5 – JNK2 Inhibits ER$^+$ Luminal Cell Differentiation Through Promotion of EMT in a Tr*p53*-null Model

5.1. JNK2 Promotes Proliferation of *Trp53*-null Tumors

In order to test the hypothesis that JNK2 inhibits Notch-dependent luminal cell differentiation through the inhibition of *Trp53* transcription, the *Trp53*-null model was used. Mice harboring *p53ko* mutations have a propensity toward development of lymphoma and sarcoma but few develop mammary tumors (110, 134, 135). To circumvent the lethality caused by tumors of other types, *p53ko* mammary glands were isolated from sexually mature *p53ko* females and transplanted into fat pads of 3 week-old wildtype virgin female mice. Tumors generated by *p53ko* transplants have been shown to differentiate into most of the tumor subtypes, so this an ideal model for assessing JNK2-dependent lineage regulation (53).

Jnk2wt and *jnk2ko* mice were crossed with *p53ko* mice to obtain *p53ko*;*jnk2ko* mammary glands for transplantation. Similar to data recently reported comparing *p53ko*;*jnk2wt* and *p53ko*;*jnk2ko* systemic mutant mice (5), no significant difference in tumor latency was noted (Figure 5.1). However, *p53ko*;*jnk2ko* tumors grow significantly faster than *p53ko*;*jnk2wt* tumors (Figure 5.2A, $p<0.0003$, Logrank Test). Histology confirms that increased tumor growth is due to elevated proliferation rate, as *p53ko*;*jnk2ko* tumors exhibit 2.9 times more Ki-67 positive cells compared to

p53ko;jnk2wt (Figure 5.2B, p=0.0159). Microarray analysis found that expression of Prediction Analysis of Microarray (PAM)50 Proliferation genes (136) is higher in the *p53ko;jnk2ko* tumors, which further supports that JNK2 inhibits *p53ko* tumor proliferation (Figure 5.2C, p=0.0101). These data indicate that while JNK2 does not have a role in promoting or suppressing tumorigenesis, it is important for suppressing tumor growth in later stages of tumor progression.

5.2. JNK2-DEPENDENT INHIBITION OF NOTCH SIGNALING REQUIRES P53

As is characteristic of the *p53* null transplant model, gene expression is quite heterogeneous among tumors generated. Because JNK2 inhibits *notch1* expression in normal mammary glands and MT tumors that express wildtype p53, it was hypothesized that *notch1* expression would not be suppressed in the absence of p53. Analysis by qPCR shows that expression of *Notch1* is highly variable in *p53ko* tumors and does not significantly differ between tumor genotypes (Figure 5.3A). Microarray analysis also failed to detect significant differences in *Notch1* expression (1.1-fold increase, FDR 54%, data not shown). This demonstrates that JNK2 no longer suppresses expression of *Notch1* in *Trp53*-null tumors.

To look at JNK2/*Notch1* interactions in a system with lower variability, a primary cell line was generated from one of the *p53ko;jnk2ko* tumors. As with the MT cell lines, GFP-JNK2 or GFP alone were stably expressed using lentiviral infection and selected for highest the expressing clone. As with MT tumor cells, *p53ko;jnk2wt* and *p53ko;jnk2ko* cells were transfected with either N1PR, N1PRp53mut, or N1PRless and CMV-beta

galactosidase control plasmid. As seen in tumors, *Notch1* promoter activity is not affected by expression of GFP-JNK2 (Figure 5.3B). These data further support that inhibition of *p53* is necessary for JNK2 to reduce *Notch1* transcription.

5.3. JNK2 Inhibits Luminal Cell Differentiation of *p53* Null Tumors

Since *Notch1* expression is not inhibited by JNK2 in the absence of p53, it was hypothesized that tumor histology does not differ between *p53ko*;*jnk2ko* and *p53ko*;*jnk2wt* tumors. To assess if luminal lineages are altered by JNK2 expression in these tumors, sections were immunostained with a Cytokeratin 8/18 antibody. As with MT tumors, a large proportion of cells within tumors are negative for this marker. Surprisingly, the proportion of Cytokeratin $8/18^{+}$ cells is significantly elevated in *p53ko*;*jnk2ko* tumors as compared to *p53ko*;*jnk2wt* (Figure 5.4A, p=0.0159). This is similar to our findings in normal mammary glands and MT tumors.

To confirm that luminal cell populations are elevated in *p53ko*;*jnk2ko* tumors, lineage markers were assessed by qPCR. This approach revealed that loss of *jnk2* causes a trend toward down-regulation of basal related genes (*Trp63* and *Krt14*) and significant up-regulation of the luminal marker, *Brca1* (Figure 5.4B, p=0.05). Expression of *Brca1* differed most strongly between the two genotypes and was also noted by tumor microarray (BRCA1 elevated 2.16-fold, 4.38% FDR) along with alterations in the ATM/BRCA1 pathway using Gene Set Enrichment Analysis (GSEA) (Figure 5.5). These data suggest that even in the absence of p53/*Notch1* interactions, loss of JNK2 increases luminal populations.

Further exploration of the mechanism behind JNK2-dependent differentiation in the absence of p53, the *p53ko*;*jnk2ko* cell line with GFP or GFP-JNK2 expression was used. RNA was isolated from cell lines and assessed for expression of *Trp63*, *Krt14*, and *Brca1*. Similar to tumors, GFP cells trend toward expression of lower levels of *Krt14* and *Trp63*, as well as significantly increased expression of *Brca1* (Figure 5.6A, p=0.0205). To confirm that BRCA1 transcription is inhibited by JNK2, *p53ko*;*jnk2ko* GFP and GFP-JNK2 cells were transfected with either a *brca1* promoter plasmid (BRCA1 PR) driving expression of luciferase or PRless control plasmid. Again, this revealed that GFP-JNK2 reduces *Brca1* promoter activity compared to the GFP control (Figure 5.6B, 2way ANOVA with Bonferroni Post-test). To assess the role of p53 in this process, *Brca1* expression was examined by qPCR in MT tumors. This revealed no significant difference in expression (Figure 5.7), further suggesting that *Brca1* is a JNK2 target in the absence of p53 expression. These data show that JNK2 inhibits luminal lineage commitment independent of p53/*Notch1* interactions.

5.4. *BRCA1* EXPRESSION AND EMT GENE SIGNATURE ARE ANTI-CORRELATED

To explore potential mechanisms that contribute to the suppression of luminal characteristics by JNK2, human breast tumor datasets were consulted. Given the established role of BRCA1 in the luminal differentiation, the correlation between *Brca1*mRNA expression and a stem/EMT signature was examined in human datasets. For this analysis, the average value of a set of genes that increase in expression during EMT was calculated for each individual tumor in the datasets and then tumors were

ranked by expression level (137). Each tumor's specific expression level of *Brca1* expression was then plotted against these values to see the correlation between EMT and *Brca1*. Figures 5.8A and B show that there is a significant anti-correlation between *Brca1* and EMT in both the UNC308 (Pearson correlation -0.215, p=0.000147) and COMBINED855 (Pearson correlation -0.246, $p=2.75e^{-17}$) human datasets. To verify that this same relationship occurs in our mouse tumors, this comparison was again made using microarray data from both *p53ko*;*jnk2ko* and *p53ko*;*jnk2ko* transplanted mice. The same trend was observed, although not significantly due to low numbers of tumors assessed (Figure 5.8C, Pearson correlation -0.444). These data are consistent with the role of BRCA1 in later stages of mammary cell differentiation and suggest the potential that EMT genes and BRCA1 antagonize the transcription of each other.

5.5. JNK2 PROMOTES EMT AND TUMOR INITIATING POPULATIONS

It was next hypothesized that if EMT and *Brca1* have opposing functions, JNK2 must promote EMT. To test this hypothesis, mRNA expression differences of select EMT/stem-related genes were then assessed by qPCR in *Trp53*-null tumors and cell lines. In these experiments, *p53ko*;*jnk2ko* tumors show trends toward lower expression of *Twist1*, *Snai1*, and *Klf4* and significantly downregulated *Zeb1* (p=0.0105) and *Snai2* (Figure 5.9A, p=0.0336). Expression of *Cdh1* (the gene transcribing e-cadherin) was significantly elevated in *p53ko*;*jnk2ko* tumors (p=0.0268). Comparison of *p53ko*;*jnk2ko* GFP and GFP-JNK2 cell lines further support that JNK2 promotes EMT. This

experiment showed that expression of *Zeb1* is significantly decreased by GFP-JNK2 expression ($p=0.0315$), however remaining genes appear unchanged (Figure 5.9B).

More comprehensive analysis of EMT-related genes was carried out with microarray-based comparison of the GFP and GFP-JNK2 cell lines. This analysis identified several other EMT-related gene targets (Figure 5.10A) that were validated by western blot (Figure 5.10B). GFP-JNK2 promotes higher expression of Zeb1, Six1, Lef1, Vimentin, and MMP9. Notably, although full length e-cadherin protein and its cleavage products are present in both GFP and GFP-JNK2 cells, it is less abundant in GFP-JNK2 cells. These data show that JNK2 promotes expression of genes that are associated with EMT.

The presence of e-cadherin in both cell lines necessitated that the expression pattern be visualized in cells by immunofluorescence to see if it is homogeneous or segregated into discrete populations. This experiment showed that two distinct populations exist within the GFP-JNK2 expressing cell line: one that expresses e-cadherin and one that does not (Figure 5.11A). Similarly, two populations can be discerned when analyzing Vimentin expression (Figure 5.11B). Bright field microscopy also revealed that GFP-JNK2 cells in culture grow as foci, thus demonstrating they are less prone contact inhibition than GFP cells—further supporting that an EMT population exists in the GFP-JNK2 cell line (Figure 5.12).

E-cadherin and Vimentin expression appear to discriminate between two separate populations in GFP-JNK2 cells, but immunocytochemistry could not confirm this because the primary antibodies were raised in the same species. To test the possibility

that two distinct populations exist in GFP-JNK2 cells, CD24 and CD49f expression levels were measured. $CD24^{-/Lo}$ and CD49f+ populations have been identified by many as a mesenchymal population in mouse mammary tumor models (138, 139). CD49f positivity does not differ between GFP and GFP-JNK2 cells, whereas CD24 expression is markedly different. GFP cells are almost exclusively $CD49f^{+}/CD24^{+}$ (98%) whereas GFP-JNK2 cells contain a $CD49f^{+}/CD24^{+}$ (21%) population and a significant $CD49f^{+}/CD24^{-}$ (77%) population (Figure 5.13). The $CD49f^{+}/CD24^{-}$ population is significantly larger in GFP-JNK2 cells than in GFP cells (2way ANOVA with Bonferroni Post-test). To find if the two populations are generated due to differential expression of GFP-JNK2, flow cytometry was performed comparing GFP levels to CD24 expression. When cells are gated for medium and high GFP intensity, high GFP-JNK2 expression is associated with $CD24^{-}$ cells (Figure 5.14). These data show that high expression of JNK2 leads to induction of EMT and a putative tumor initiating cell population in *Trp53*-null cells.

We next wished to verify that the $CD24^{+}$ population is less mesenchymal than the $CD24^{-}$ population. To accomplish this, GFP-JNK2 cells were sorted on the basis of CD24 positivity and then each population was lysed for RNA isolation. The same gene panel as above was used in this analysis. We found that the $CD24^{+}$ population has lower expression of markers Mesenchymal cells, *Twist1* (p=0.0484), *Klf4* (p=0.0439), and *Snai2* (p=0.0233) and higher levels of markers of differentiation—*Brca1* (p=0.05 Mann Whitney test), *Krt14* (p=0.0018, Mann-Whitney test) and *Cdh1* (Figure 5.15A, p=0.0131, Mann-Whitney test). We also assessed expression of *Gata-3*, a transcription factor that

promotes luminal cell commitment (35), using RT-PCR. Like other markers of differentiation, its expression is higher in the $CD24^+$ population (Figure 5.15B). This data show that the CD24+ population consists of cells with both luminal and basal characteristics, but low expression of EMT genes. This population is thus more differentiated than the EMT-rich $CD24^-$ population with low expression of luminal and basal genes. Because GFP-JNK2 expression is highest in the CD24- population, this data also shows that JNK2 antagonizes differentiation by inducing EMT in the absence of p53.

5.6. JNK2 Promotes Metastasis and Tumor Initiating Cell Populations

EMT promotes tumor initiating cell populations that are comparatively less differentiated than other non-EMT populations (140). Because GFP-JNK2 expression promotes an EMT populations, I hypothesized that it might also enrich the *p53ko;jnk2ko* cells in tumor initiating cells. To test this hypothesis, limiting dilutions of GFP and GFP-JNK2 cells were made and delivered to nude mice. The dilutions selected were 10,000-, 1,000-, and 100 cells per mouse. All mice from both genotypes produced palpable tumors at the 10,000 cell dilution (Table 5.1). Only one of four mice injected with GFP-JNK2 cells produced a palpable tumor while no GFP cell injected mice produced tumors at this dilution. No mice injected with either genotype of cell line produced palpable tumors at the 100 cell dilution. No metastases were produced from palpable tumors of GFP cell injected mice, but two metastases were detected by GFP fluorescence in GFP-JNK2 injected mice.

After six months, many mice from each genotype had not produced palpable tumors. To assess the potential that injected cells were still viable and had produced non-palpable tumors, mice were harvested and examined with fluorescence microscopy (Table 5.2). No additional tumors were detected in GFP cell injected mice, but one contra-lateral gland metastasis was seen at 100 cell dilution without a primary tumor. Five more tumors were found in GFP-JNK2 injected mice, with one at 1000 cell dilution and four at 100 cell dilutions. One contralateral gland metastasis was seen in each of the 1000 and 100 cell dilution groups. Additionally, ascites developed in one of the 1000 cell injected GFP-JNK2 group. This was detected in the absence of a primary tumor.

Data from this experiment were used to calculate tumor initiating cell frequency using calculation software (Table 5.3). This showed that the GFP cell line has an average of 1 tumor initiating cell in 5,116 cells. This is considerably lower than the GFP-JNK2 cell line, where tumor initiating cells were found at a frequency of 1 in 569 cells ($p=0.0305$, Pearson's Chi-squared Test). This experiment shows that GFP-JNK2 expression not only promotes tumor initiating cell populations, but also metastasis. As previously shown by other groups, these two characteristics are likely a result of the role of JNK2 in promotion of EMT.

5.7. BRCA1 ANTAGONIZES JNK2-DEPENDENT TUMOR INITIIATING CELL POPULATIONS

To directly assess the potential that BRCA1 and EMT antagonize each other, *p53ko*;*jnk2ko* cells were co-infected with either GFP-JNK2 and BRCA1 viruses or

transiently transfected with GFP and Zeb1. Zeb1 and BRCA1 were chosen because they are the genes that are most consistently affected by JNK2 expression and BRCA1 was shown to antagonize EMT *in silico* (see section 5.4). Cells were selected and then analyzed by flow cytometry for variable expression of CD24 and CD49f against GFP-JNK2 alone cells. It was hypothesized that ZEB1 expression would increase the $CD24^-$ population of GFP cells while BRCA1 expression would decrease the $CD24^-$ population of GFP-JNK2 cells. We found, remarkably, that expression of BRCA1 in GFP-JNK2 cells is sufficient to lower the $CD24^-$ population from 77% to <1% (Figure 5.16, $p<0.0001$). ZEB1 expression decreased the magnitude of CD24 positivity in GFP cells but did not significantly affect the proportion of CD24- cells. This may be due to the transient nature of the ZEB1 expression and insufficient selection as a result. This experiment shows that BRCA1 is sufficient to suppress JNK2-dependent EMT populations and suggests that it may be a major target of downregulation by JNK2 to bring about this phenotype.

To see if EMT is affected by JNK2 expression in the absence of *Brca1* expression changes, MT tumor RNA from MT^+ *jnk2wt* and MT^+ *jnk2ko* mice was analyzed for expression of select EMT markers by qPCR. No significant differences in *Cdh1*, *Snai1*, *Snai2*, or *Klf4* were seen by this analysis (Figure 5.17A-D). These data support that p53 inhibits promotion of EMT populations by JNK2.

5.8. JNK2 INHIBITS ER-DEPENDENT GROWTH OF *TRP53*-NULL CELLS

As with *p53ko* tumors, proliferation is inhibited by expression of GFP-JNK2 in *p53ko*;*jnk2ko* cells (Figure 5.18A, 2way ANOVA with Bonferroni Post-test). These findings are consistent with the properties EMT/tumor initiating cell populations that are induced by JNK2. To examine if the JNK2-dependent effects on proliferation are secondary to its ability to induce EMT, cells were pulse labeled with BrdU for 24 or 48 hours and sorted into $CD24^-$ and $CD24^+$ populations. Results were similar for both time points. In both GFP and GFP-JNK2 samples, the $CD24^+$ population constitutes a higher fraction of $BrdU^+$ cells than the $CD24^-$ population (Figure 5.18B, 2way ANOVA with Bonferroni Post-test). Moreover, both the $CD24^+$ and $CD24^-$ GFP-JNK2 cells incorporate less BrdU compared to GFP cells, indicating that JNK2 slows proliferation in both an EMT-dependent and -independent fashion.

In rationalizing why the $CD24^+$ population displays a higher proliferation rate in spite of showing evidence of more luminal differentiation, it was suspected that ER could modulate this response, especially given its elevated expression in GFP cells (Figure 5.19A). GFP cells also express higher levels of the ER target gene, PR, as compared to GFP-JNK2. As in human tumors, co-expression of ER and PR in GFP cells potentially indicates ER-responsiveness in these cells. To validate this functional importance of ER, cells were cultured in 5% charcoal stripped serum and exposed to estradiol (E2) or E2+fulvestrant, a drug that degrades ER protein. After 24 hours of treatment, ER protein is notably reduced in GFP cells treated with E2+fulvestrant, whereas E2+fulvestrant treatment of GFP-JNK2 cells show no change in ER (Figure 5.19B). This data show that

GFP cells are more ER responsive than GFP-JNK2 cells and that JNK2 inhibits ER expression.

To evaluate the effect of JNK2 on ER-dependent proliferation, GFP and GFP-JNK2 cells were cultured in 10% FBS with or without fulvestrant for several days. Fulvestrant significantly inhibits GFP cell viability on day 3 and 6 of treatment, but GFP-JNK2 cells show no significant growth inhibition (Figure 5.19C, 2way ANOVA with Bonferroni Post-test). These data indicate that JNK2 inhibits ER expression and ER-associated proliferation. Since ER expression is uncommon in mouse derived mammary tumors, its expression was measured in paraffin embedded *p53ko* tumors and did not identify any other tumors with ≥10% ER+ cells (data not shown). No tissue is available for the tumor from which the cell line was derived, but protein lysate from the first passage confirms ER expression.

5.9. DISCUSSION

The majority of breast tumors possess a mutation in the gene encoding p53 or regulators of its activity. Breast tumors with these mutations are commonly undifferentiated and invasive (39, 55, 118, 141-143). The role of p53 in inhibition of stemness is a likely contributor to this association because cancer stem cells are involved in generating tumors and progression to metastasis (21, 144-146). Because of this, the role of p53 in differentiation may provide an equal impact on tumor progression as its role in DNA damage response. Therefore, the ability of JNK2 to inhibit luminal cell differentiation in spite of the p53/*Notch1* interaction not having an effect is an important

discovery. This means that JNK2 regulates luminal differentiation of mammary tumors independent of Notch signaling.

Contrary to the MT tumor model, the *p53ko* transplant model showed no difference in tumorigenesis between *jnk2ko* and *jnk2wt* groups. Differences in tumorigenesis in the MT model were attributed to the function of JNK2 in suppression of replicative stress (3). Because this role requires p53 (133), its absence may have neutralized differences. Alternatively, increased *Brca1* expression in *p53ko*;*jnk2ko* tumors may have alleviated stress by potentiating DNA damage response.

It is interesting to note that the *p53ko* mutation in these tumors exposed the ability of JNK2 to regulate *Brca1* expression. It is not surprising, however, that *Brca1* expression is affected in the *p53ko* model, as p53 is a known inhibitor of *Brca1*transcription (147). Because BRCA1 is an important protein for the differentiation of normal mammary glands and tumors, it is a strong candidate to potentiate luminal differentiation in the absence of *Jnk2* expression.

Induction of EMT is a key process in tumorigenesis and metastasis. Cells that have undergone an EMT are more motile because of decreased cell-cell interactions and increased expression of extracellular matrix degrading enzymes. JNK inhibition has been shown to prevent AP-1-dependent polarization and tight junction assembly in 3-dimensional cultures of mammary epithelial cells, indicative of the role of JNKs in EMT (148). Our studies highlight specific proteins involved in this process, such as Vimentin, Zeb1, Snail, and others. Other tumor models have shown that inhibition of JNK2 by siRNA causes upregulation of claudins 4, 7, and 9 that are critical for the definition of

claudin-low tumors (53, 149). Because these are important genes for breast tumor subtype, they merit further study.

The fact that EMT is not affected in the MT model, with wildtype *p53* expression may be due to the p53-dependent *brca1* suppression. Using the *p53ko* tumor model effectively unmasked the downregulation of JNK2 thus revealing a secondary mode of luminal cell suppression that it regulates. Our data did not show a direct mechanism for positive regulation of EMT by JNK2, but the ability of *brca1* expression to suppress EMT accompanied with the ability of JNK2 to suppress *brca1* offers a clue. The large array of protein targets that are affected by JNK2 expression may be a result of either its interaction with *brca1*—alternatively, potential interactions with miRNAs such as mir200 or miRNA pathways may have a similar effect.

Level of differentiation and expression of ER is of paramount importance in prognosis of breast cancer patients. While poorly differentiated, claudin-low human tumors are known for their high expression of EMT, stem cell related genes and poor patient prognosis, those tumors expressing ER provide comparatively better outcomes (41). The finding that these two phenotypes are anti-correlative demonstrates their relevance in tumor classification. Additionally, the preceding results establish JNK2 to be a critical mediator between EMT and differentiation within *Trp53* null tumors. Recent reports that JNK signaling is inactivated at high frequency in human luminal, ER^+ tumors lend support to our data (1, 2), although a significant frequency of mutations *Jnk2* was not noted. This may be because higher complexity within the heterogeneous human model or that not enough tumors were included in studies to reach statistical significance.

Our results have higher resolution in this regard because use of specific *Jnk2ko* cell lines allowed less heterogeneity to observe direct JNKs effects.

Our results suggest that BRCA1 controls ER^+ $CD24^+$ populations in the *p53ko* model. BRCA1 is able to sufficiently suppress $CD24^-$ tumor initiating cell populations and, presumably, its absence promotes them through upregulation of EMT. The control of this interaction by JNK2 is novel; as is its control over vital ER target genes including *Gata-3* and *Pr*. The functional significance of this interaction was found that JNK2 significantly reduces ER-dependent growth. Others have shown that high JNK activity correlates with tamoxifen resistance in human breast tumors and this provides a potential mechanism (150, 151). Further study could show BRCA1 to be a key target for re-initiating endocrine therapy sensitization, as well.

The integral role of BRCA1 in differentiation of luminal cells is well known in both normal and tumor contexts but the demonstration that EMT and BRCA1 antagonize each other is of particular interest. This is because of BRCA1's established role in DNA damage response. This means that undifferentiated cells within mammary tumors may have a higher propensity toward double strand DNA breaks and greater chance of acquiring mutations to evolve toward metastasis. This serves to show that differentiation may have greater importance than simply changing motile characteristics and growth factor receptor expression, but also in slowing cancer progression.

The overall effect of the BRCA1/EMT interaction is not entirely clarified by tumor initiating cell experiments. Because both $CD24^+$ and $CD24^-$ populations were injected, it is uncertain if increases in tumor initiating capacity is a consequence of

intrinsic capacity for the $CD24^-$ population to seed tumors and metastasize or if $CD24^-$ populations promote tumor seeding and metastasis of $CD24^+$ populations. In the setting of the tumor, EMT not only affects tumor populations, but the tumor microenvironment and allows for remodeling by stromal cells. The potential exists that $CD24^-$ populations are responsible for remodeling and are not the tumor initiating/metastasizing cells themselves. This question merits further examination.

Chapter 6 – Summary and Future Directions

This project has demonstrated that JNK2 is involved in the suppression of luminal populations in both normal mammary and tumor contexts. Regulation of this process involves mechanisms that are both dependent on and independent of *Trp53* expression. In the p53-dependent mode of luminal cell differentiation, JNK2 inhibits the ability of EGF signaling to induce expression of p53 and, subsequently, *Notch1* expression. Notch1 is well-known to promote luminal populations, and 3-dimensional culture models in this report show that elevated Notch signaling is responsible for increased luminal populations in *jnk2ko* mammary epithelial cell preparations. In the p53-independent mode of luminal cell differentiation, JNK2 inhibits luminal differentiation through induction of EMT and suppression of luminal differentiation mediators. BRCA1 is downregulated by JNK2 and is sufficient to suppress JNK2-dependent EMT. This is a potential feedback mechanism, as Slug represses *Brca1*mRNA expression in response to Wnt signaling (152). The particular levels of the stem cell hierarchy that are altered to lead to inhibition of luminal populations in our model have not yet been elucidated but may be found through higher resolution methods such as those mentioned below.

In p53-competent normal mammary glands, the manifestation of *jnk2ko* on lineage commitment is increased proportions of Cytokeratin $8/18^{+}$ and ER^{+} luminal cell populations. This is accompanied by decreased expression of the basal marker, *Trp63*.

Assessment of these markers in whole glands does not give information of the level in the hierarchy that is affected by *jnk2ko* as both Cytokeratin 8/18 and p63 are lineage restricted markers but may be expressed by progenitors or mature, differentiated cells. The fact that the proportion of ER^+ cells changes does not indicate a change at any specific point in the hierarchy, either, because these cells are highly differentiated and only a result of changes occurred earlier in the hierarchy. It is likely that JNK2 affects the hierarchy at multiple levels because *notch1* is important for the differentiation of stem cells and commitment to the luminal lineage. Differentiation assays performed on putative mammary stem cell- and progenitor-enriched populations support that JNK2 may inhibit luminal cell commitment and differentiation at both the stem and progenitor levels, but results are inconclusive because stem fractions were not validated and further assessment of progenitor populations is required.

Roles for p53 and Notch1 in the promotion of stem cell differentiation are well-known, thus it is likely that high expression of these proteins in *jnk2ko* cells will increase the propensity for stem populations to differentiate (21, 26, 153). In contrast, if JNK2 is not expressed in mammary stem cells, then levels of *Trp53* and *Notch1* mRNA would remain unaltered and stem cell populations would not be affected as a result. Histology shows that JNK2 is expressed by both the luminal and basal lineages, thus the basally located stem cells might also express JNK2. If this is true, decreased mammary repopulating potential and self-renewal capacity are likely consequences of *jnk2ko*. Whether *notch1* is dispensable for this response due to p53-dependent downregulation of EMT would be interesting to assess. Mammary repopulating potential could be tested

through limiting dilution mammary epithelial cell transplantation experiment using cells isolated from *jnk2wt* and *jnk2ko* glands. Additionally, real time *in vitro* assessment of self-renewal would give a higher resolution picture of the effect of JNK2 on stem cell commitment and determine if potential effects are due to this stem-related process (21).

JNK2 may also affect stem cell maintenance independent of its role in suppression of *Trp53* and *Notch1* transcription. It is unclear, from experiments, if JNK2 directly promotes EMT independent of BRCA1 or if *Brca1* downregulation by JNK2 is the direct mechanism of EMT promotion. If a direct interaction leads to EMT, then JNK2 would likely have a role in the promotion of normal mammary stem cell populations in the absence of p53 expression. If the interaction requires downregulation of *Brca1* mRNA expression, *jnk2ko* may not have any effect due to luminal lineage-restricted expression of *Brca1* (32, 33, 154). In this case, BRCA1 expression could not be induced in stem cell populations and EMT would not be inhibited. However, *jnk2ko* may promote ectopic BRCA1 expression and, in turn, promote differentiation. This requires further clarification in normal mammary models. A mammary specific, inducible shBrca1 would be useful in determining the role of *brca1* in this process.

A role for JNK2 in lineage commitment is supported by evidence provided in this report—both Notch1 and BRCA1 are critical for the appropriate lineage proportions in the mammary gland. The fact that high expression of $Notch1^{ICD}$ leads to a build-up of luminal progenitors (24, 25, 27), whereas the same phenotype is seen in mutants lacking expression of BRCA1 (33, 155) illustrates that these genes function at different stages of differentiation in the mammary cell hierarchy—because Notch1 is responsible for effects

in earlier progenitors than BRCA1, luminal lineage inhibition by JNK2 could produce varied results in overall differentiation of the normal mammary gland depending upon p53 status (156). In p53-competent mice, JNK2-dependent inhibition of Notch1 expression suppresses mammary luminal cell proportions. The precise cellular mechanism of notch1 in this context is not known. Presumably, *Notch1* mRNA expression increases luminal cell proportions by promoting luminal lineage commitment or expansion of luminal progenitors but it could also promote opposing effects in the basal lineage. To assess progenitor expansion, differentiation assays could be performed using *jnk2wt* and *jnk2ko* cells. The key to this experiment is to examine the size of colonies produced—smaller/larger colonies resulting from each lineage-restricted progenitor type would indicate a change in progenitor expansion. It is expected that progenitor expansion is the step that is affected by Notch1, as $Notch1^{ICD}$ overexpressing mice exhibit hyperproliferation of luminal progenitor cells. Thus, a similar, but blunted, phenotype is expected in differentiation assays of *jnk2ko* cells. If this is not the case, then lineage commitment must be the step that JNK2 mediates. Of note, while several markers have been defined to evaluate the various steps of luminal cell differentiation, essentially no markers, aside from p63, have been published that allow elucidation of basal/myoepithelial cell differentiation steps. Therefore, a role for JNK2 in the promotion of basal cell differentiation could be an important observation.

In the absence of *p53* expression, *jnk2ko* may cause a decrease in luminal cell proportions. This is because BRCA1 promotes terminal differentiation of luminal mammary cells in the normal mammary gland—contrary to its role in the more plastic

environment of a tumor where cells continue to proliferate in the face of differentiation. The expected normal mammary phenotype is also different from the *p53*-competent phenotype because Notch1 affects progenitor populations and does not promote terminal differentiation. This could be assessed by comparing non-tumor-bearing *p53ko*;*jnk2wt* and *p53ko*;*jnk2ko* mature mammary ducts. Results that are found from this approach could be mechanistically evaluated with differentiation assays to find the specific cause of increases/decreases in luminal cell proportions as with Notch1 experiments. To assess the importance of BRCA1 in this model, *p53ko;jnk2ko* could be combined with conditional *brca1ko*.

Increased proliferation is also an effect of *jnk2ko* in the *p53ko* cells and tumors. In normal cell populations, high levels of differentiation are often associated with slowed or stalled proliferation. This does not necessarily hold true in mammary tumors. Relatively highly differentiated subtype tumors (Luminal B) are highly proliferative, whereas the least differentiated tumors (high EMT) are more slowly proliferating. Therefore, use of differentiation as a means of therapy could pose a potential conundrum. Undifferentiated tumors are slowly proliferating but invasive and may harbor metastatic cancer stem cells but more differentiated tumors are comparatively highly proliferative that may quickly progress toward metastasis. The true measure of benefit, however, is patient outcome and targeted therapies with demonstrable efficacy exist for the more differentiated tumors such as Luminal A and $HER2^{+}$ while no such therapies exist for their undifferentiated counterparts.

The importance of differentiation for treatment efficacy is well-illustrated when comparing the *p53ko;jnk2ko* GFP and GFP-JNK2 cell lines. GFP-JNK2 expression induces EMT and dedifferentiation as evidenced by downregulation of ER and PR. This also causes a reduction in responsiveness to the ER inhibitor fulvestrant. If this mechanism exists in human systems, it could provide great benefit to patients whose tumors are either unresponsive (Luminal B) or potentially have become resistant to endocrine therapies. Evidence to support these effects are in recent reports that point to a potential role for the JNK pathway in suppression of luminal differentiation (1, 2). However, in order to fully establish JNKs, or JNK2 in particular, as important in this process, human cell lines or primary cells must be manipulated to explore alterations in differentiation and/or EMT characteristics.

As with the costs and benefits that must be weighed with pharmacologically inducing differentiation of tumor cells, the potential draw-backs of JNK2 inhibition must be considered. We have found that loss of JNK2 in the MT model is associated with increased susceptibility to replicative stress, increased tumor multiplicity, and increased tumor latency (3). This was reinforced by studies of oncogene induced tumorigenesis in *map2k7* (MKK7)-null mice and *jnk2ko* in combination with *p53*+/- (5, 133). In the p53 study, *Trp53*-null mice were also examined and there was no effect on tumor latency with *jnk2ko*, but latency was greatly decreased in *p53*+/-*;jnk2ko* mice. This result is particularly interesting given that *jnk2ko* in the absence of p53 causes increased *Brca1*mRNA expression. Because this may cause increased DNA damage response in the face of p53 loss, mutation frequency may be decreased in *p53ko;jnk2ko* tumors as

compared to *jnk2wt* counterparts. Therefore, although JNK2 inhibition in tumors expressing wildtype *p53* may cause a reduction in DNA damage response and increase in mutation frequency, it could be potentially beneficial in basal tumors where a high frequency of *p53* mutation is seen. The benefit of differentiation and potential ER responsiveness when JNK2 expression is absent cannot be overlooked, either.

These results suggest that JNK2 expression could be used as a predictive marker of luminal differentiation and as a potentially important prognostic marker for ER responsiveness. If insights gained using mouse models and various cell lines hold true for human models, JNK2 may also be an attractive target for differentiation therapy in undifferentiated tumors or tumors that are resistant to endocrine therapies. There are several competitive JNK inhibitors that are commercially available (157-159), although the most widely used inhibitor, SP600125, has known cross-reactivity with other MAPKs (160). Newer inhibitors show higher specificity toward JNKs. One JNK inhibitor by Celgene is in clinical trials for treatment of autoimmunity associated with pulmonary fibrosis and discoid lupus, but this compound inhibits all JNK proteins and may not have a similar effect to *jnk2ko* when administered. A more recent approach is development of compounds the covalently bind to JNKs with much improved specificity over previous drugs (161). These should be developed and implemented to assess their efficacy and this approach will hopefully, one day, lead to increased survival of breast cancer patients everywhere.

Appendix A – Tables

1.1. Mammary Epithelial Cell Lineage Markers

lineage	markers
luminal	cytokeratin 8/18, MUC1, ER, PR, CD24, EpCAM (human), CD61, GATA-3, BRCA1
basal	cytokeratin 14, smooth muscle actin (SMA), p63, CD49f, CD29
stem cells	bmi-1, epithelial to mesenchymal transition, klf4, oct4, sox2, cmyc, aldh activity

*while all mammary epithelial cells express CD24, CD29, and CD49f, luminal cells express the highest levels of CD24 and basal cells express the highest levels of CD29 and CD49f.

3.1. Colony Forming Assay – Mammary Repopulating Units

	jnk2wt	jnk2ko
luminal	23.8%	38.8%
basal	7.5%	7.3%
mix	68.7%	53.9%
basal+mix	76.2%	61.2%

3.2. Colony Forming Assay – Colony Forming Units

	jnk2wt	jnk2ko
luminal	18.2%	21.2%
basal	19.05%	9.3%
mix	62.75%	69.5%
basal+mix	81.8%	78.8%

5.1. Limiting Dilution Assay – Palpable Tumors

Cell # inject.	GFP		GFP-JNK2	
	tumors	metastasis	tumors	metastasis
10^4	4/4	0/4	4/4	2/4
10^3	0/6	0/6	1/4	0/4
10^2	0/6	0/6	0/9	0/9

5.2. Limiting Dilution Assay – Non-palpable Tumors

Cell # inject.	GFP		GFP-JNK2	
	tumors	metastasis	tumors	metastasis
10^4	0/0	0/0	0/0	0/0
10^3	0/6	0/6	1/3	2/3*
10^2	0/6	1/6	4/9	1/9

*** Ascites developed in 1/3 of GFP-JNK2 1000 cell dose**

5.3. Limiting Dilution Assay – Tumor Initiating Cell Proportions

	GFP	GFP-JNK2
Frequency	1 in 5116	1 in 569
- S.E.M.	1 in 8605	1 in 937
+ S.E.M.	1 in 3042	1 in 346

Appendix B – Figures

1.1. Human vs Mouse Mammary Gland Structure

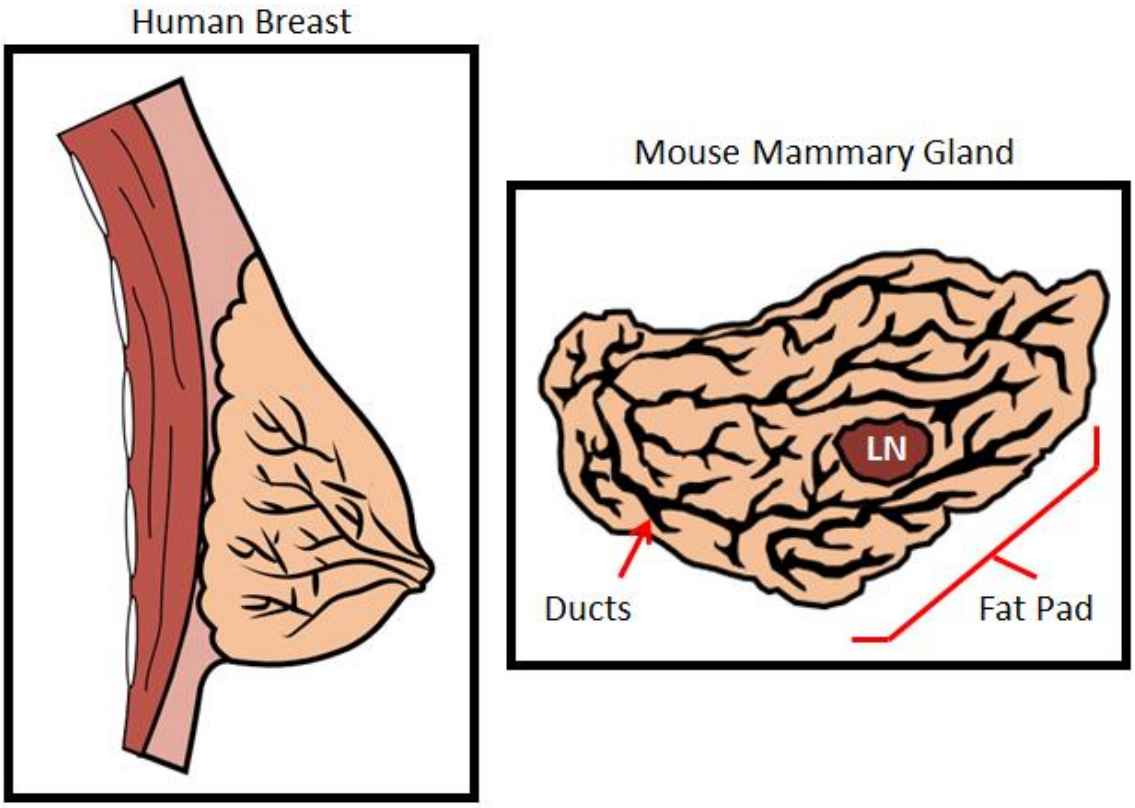

1.2. Mouse Mammary Gland Locations

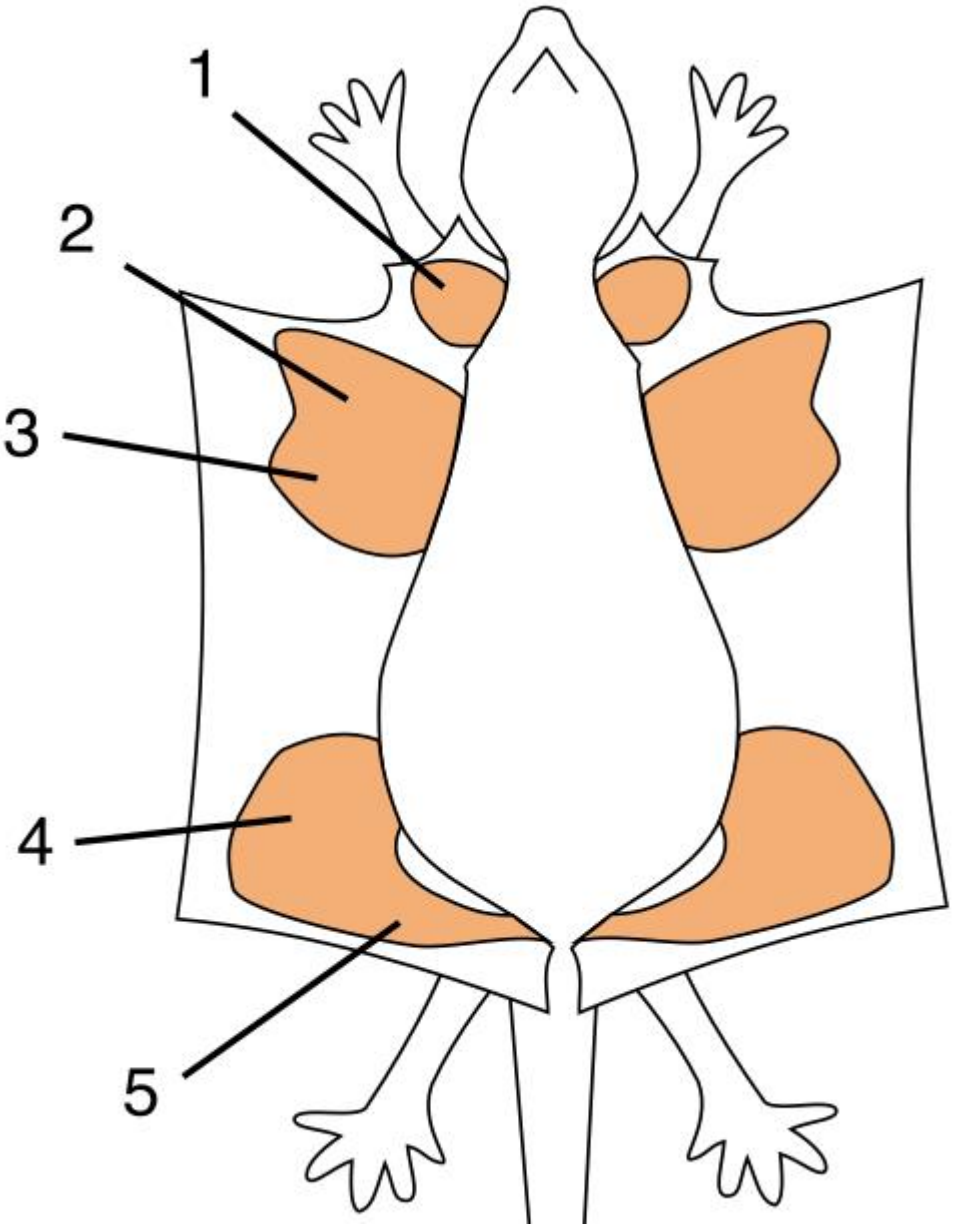

1.3. Mammary Ductal Structure

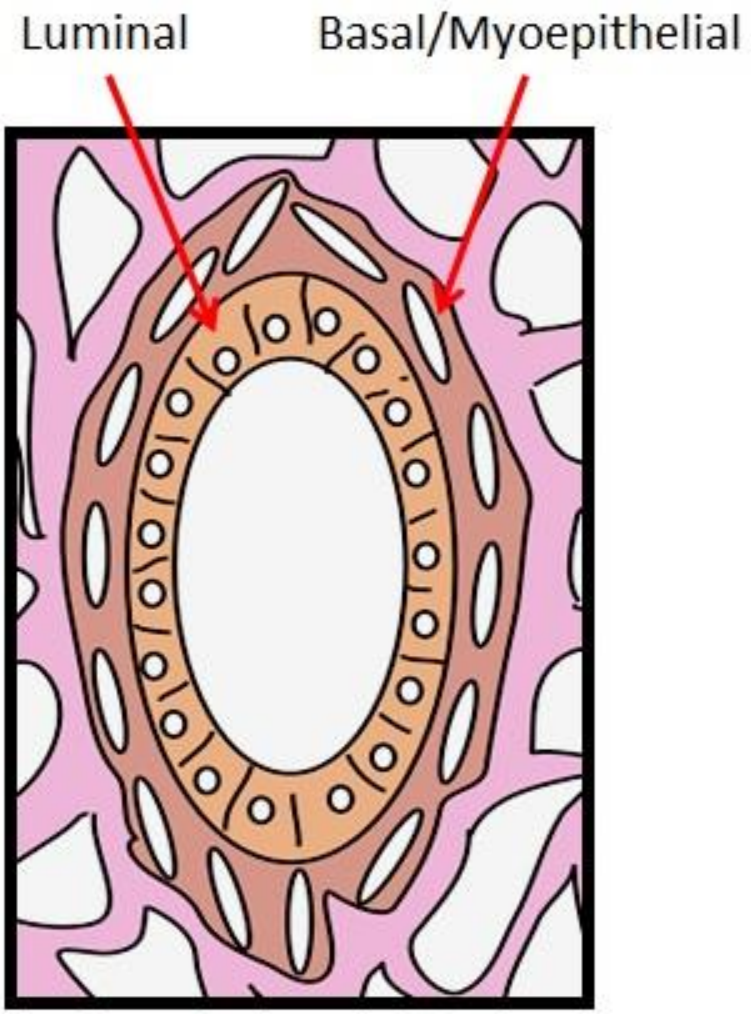

1.4. Simplified Mammary Hierarchy

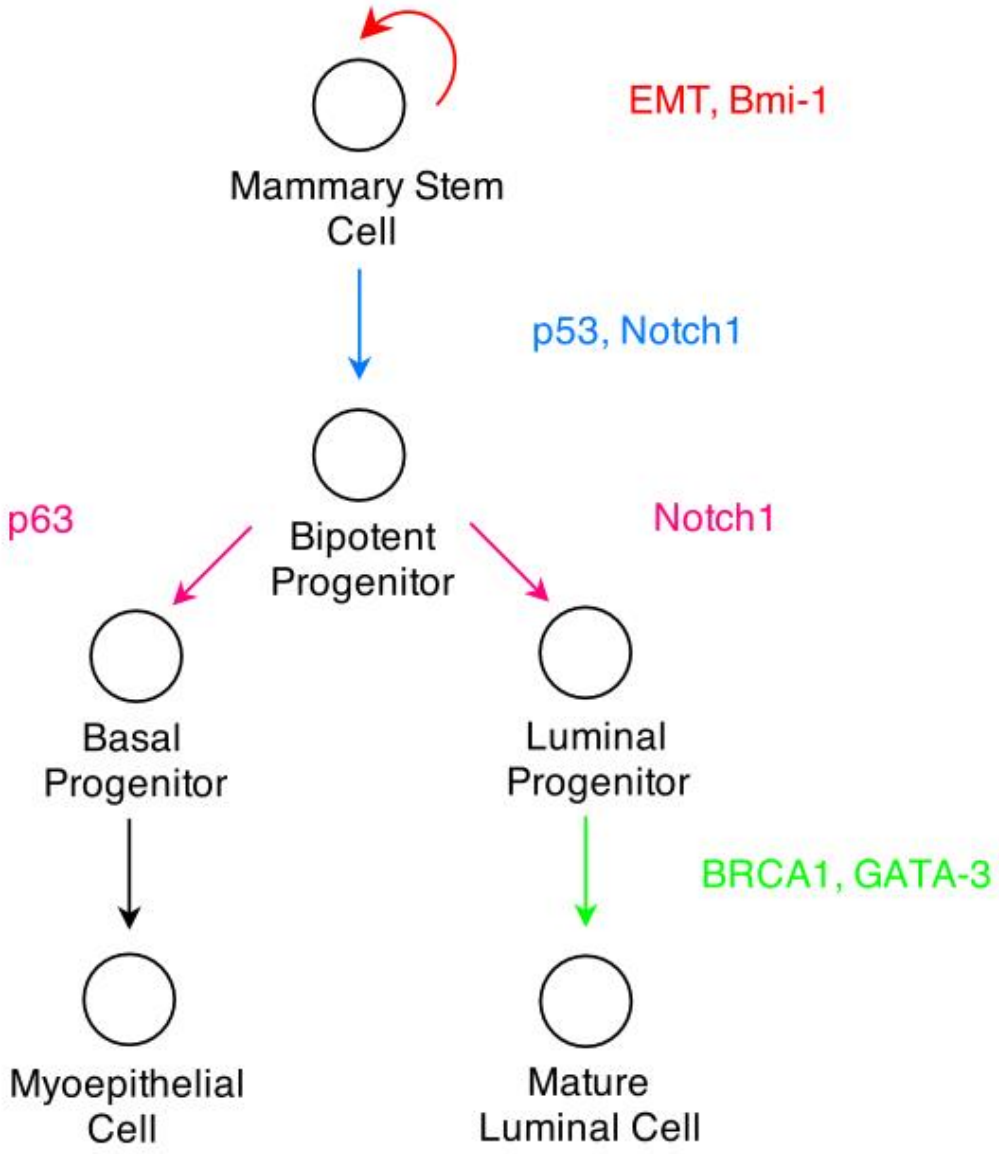

3.1. JNK2 Promotes p63^{+} Myoepithelial Cell Populations

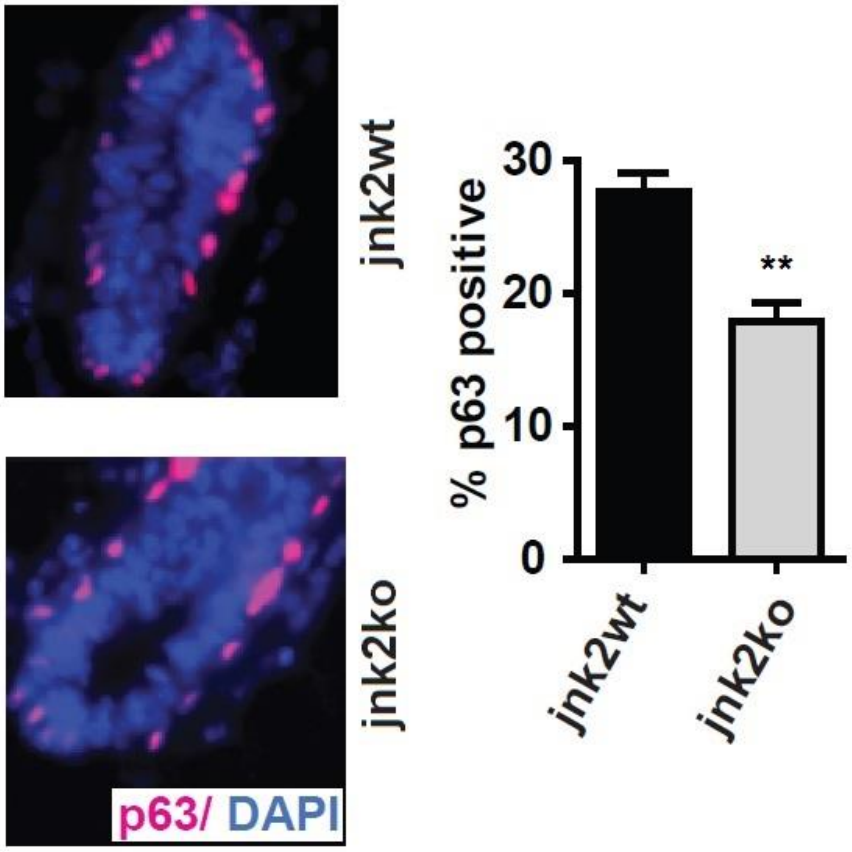

Mammary glands from seven week-old virgin, adult, female mice were harvested, fixed, and embedded in paraffin. Slides were prepared from these blocks and immunostained to analyze p63-positive myoepithelial cell populations. Significance between groups was determined by T-test. Results are indicated on the figure as follows: * for $0.05 \geq p \geq 0.01$, ** for $0.01 > p \geq 0.0001$, *** for $p < 0.0001$.

3.2. JNK2 Inhibits Cytokeratin 8/18^{+} Luminal Cell Populations

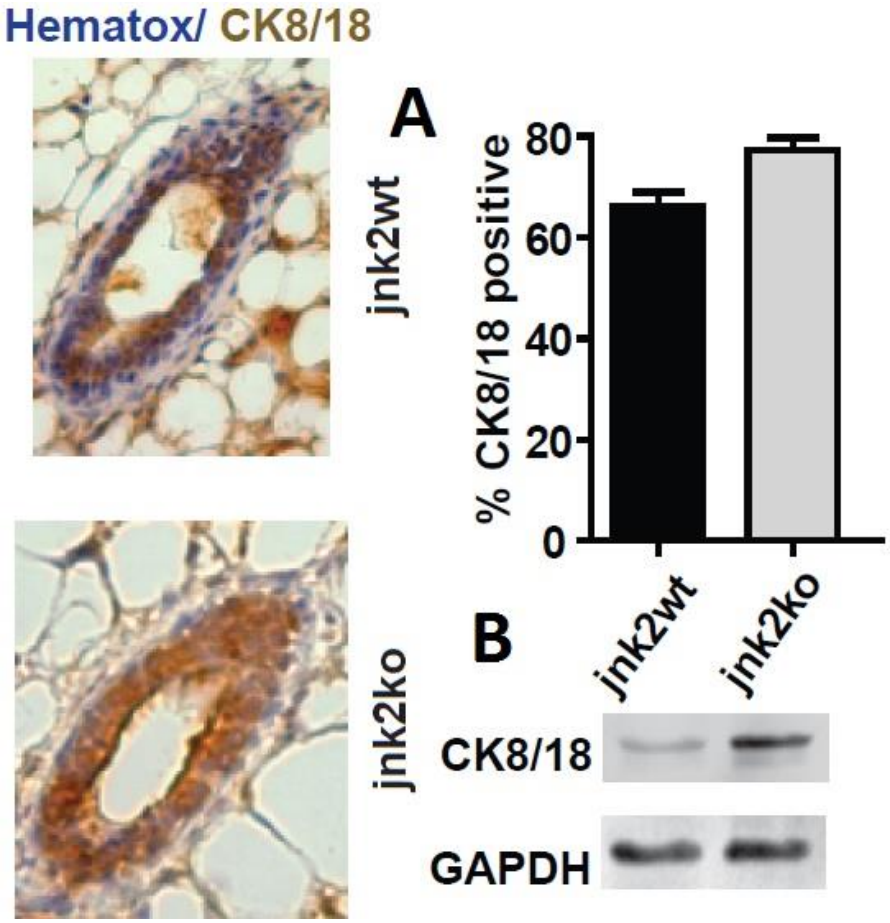

A: Mammary glands from seven week-old virgin, adult, female mice were harvested, fixed, and embedded in paraffin. Slides were prepared from these blocks and immunostained to analyze Cytokeratin 8/18 (CK8/18)-positive luminal cell populations. B: Isolated mammary epithelial cells were lysed and protein lysates were analyzed for CK8/18 expression by western blot. Significance between groups was determined by T-test. Results are indicated on the figure as follows: * for $0.05 \geq p \geq 0.01$, ** for $0.01 > p \geq 0.0001$, *** for $p < 0.0001$. No significant difference was found for CK8/18 expression.

3.3. JNK2 Inhibits ER^+ Luminal Cell Populations

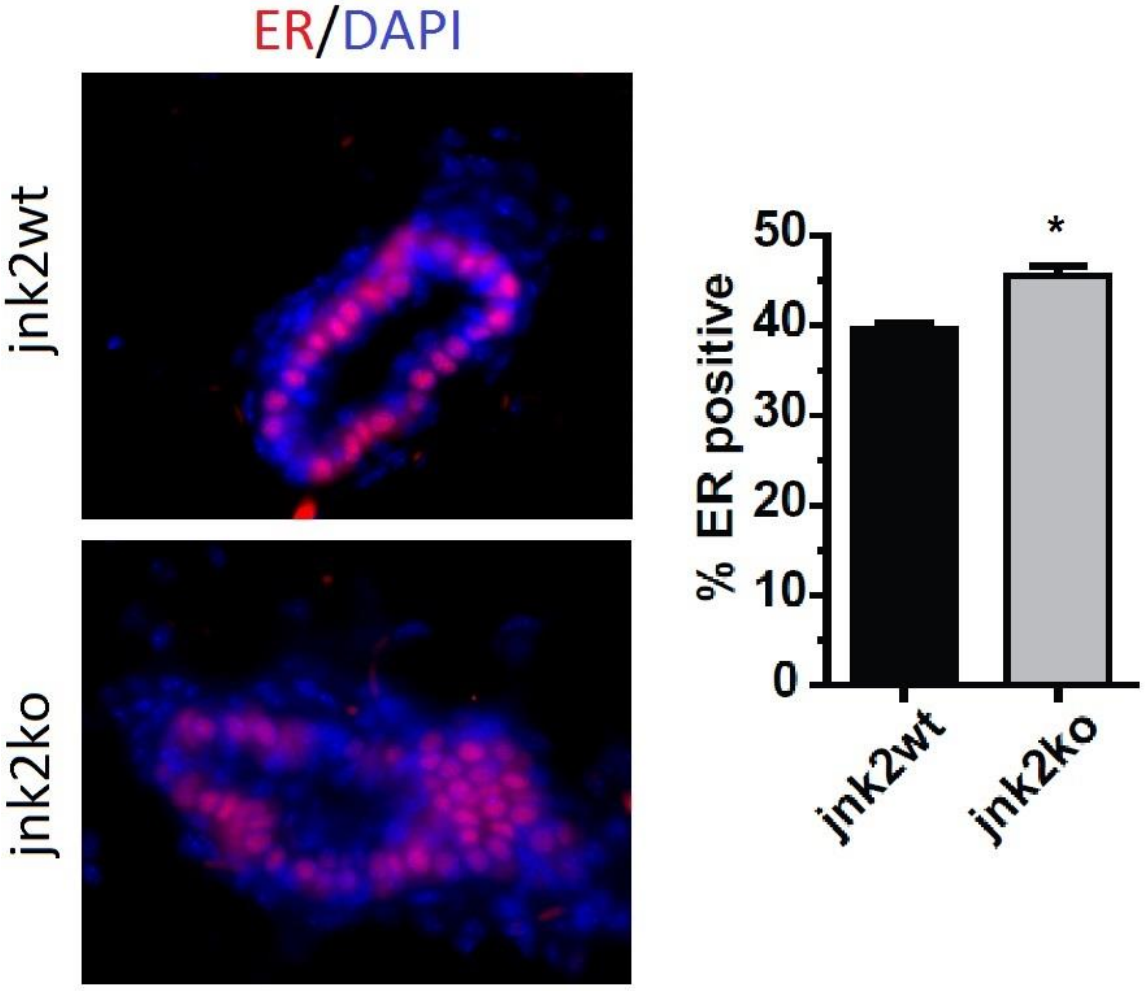

Mammary glands from seven week-old virgin, adult, female mice were harvested, fixed, and embedded in paraffin. Slides were prepared from these blocks and immunostained to analyze estrogen receptor (ER)-positive luminal cell populations. Significance between groups was determined by T-test. Results are indicated on the figure as follows: * for $0.05 \geq p \geq 0.01$, ** for $0.01 > p \geq 0.0001$, *** for $p < 0.0001$.

3.4. JNK2 Inhibits $CD24^{hi}$ $CD49f^{lo}$ Luminal Cell Populations

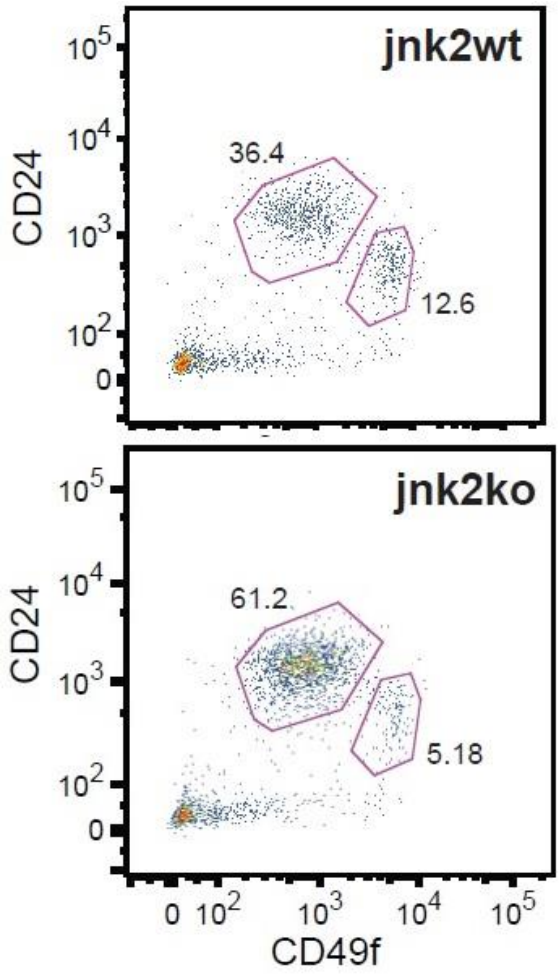

Mammary glands were harvested from adult virgin, female mice and mammary epithelial cells were isolated. Cells were incubated with CD24 and CD49f antibodies and then examined by flow cytometry to evaluate proportions of basal/myoepithelial ($CD24^{+}$ $CD49f^{hi}$) and luminal ($CD24^{hi}$ $CD49f^{lo}$) cell populations.

3.5. JNK2 is Expressed in the Mammary Gland

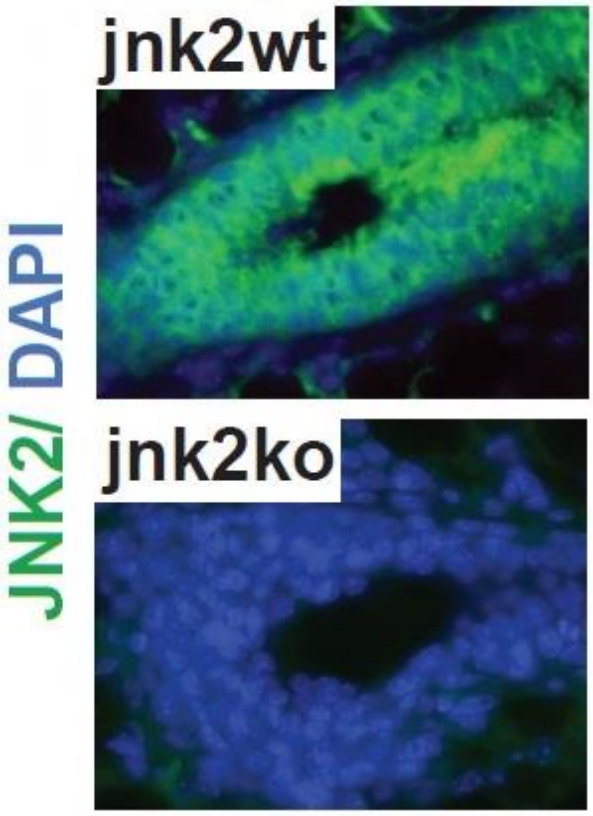

Mammary glands from seven week-old virgin, adult, female mice were harvested, fixed, and embedded in paraffin. Slides were prepared from these blocks and immunostained to analyze the localization of JNK2 expression.

3.6. JNK2 Alters Mammary Cell Differentiation *in vitro*

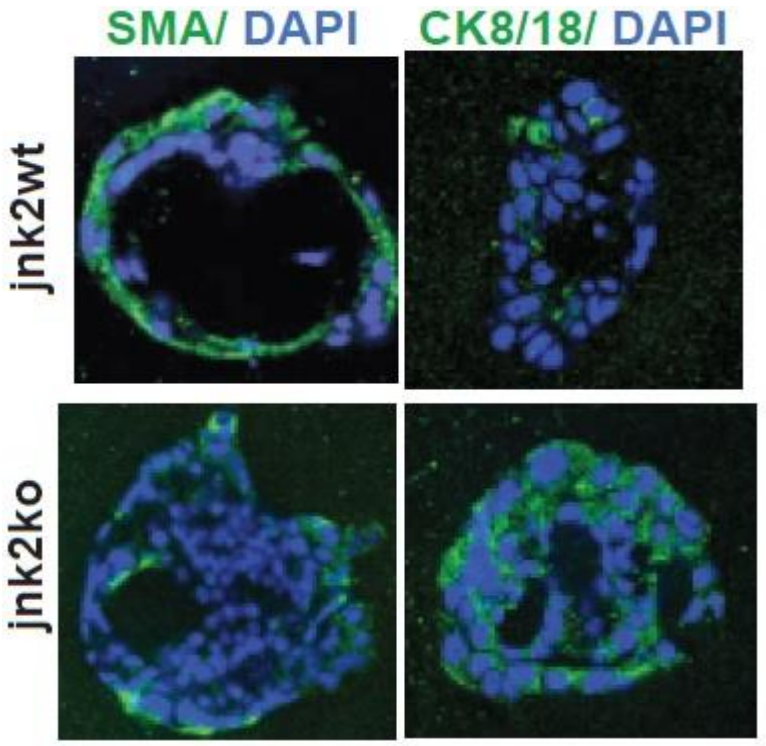

Mammary glands were harvested from adult virgin, female mice and mammary epithelial cells were isolated. Cells were then seeded onto beds of Matrigel in defined media and allowed to grow and differentiate prior to fixation and immunostaining with smooth muscle actin (SMA) or Cytokeratin 8/18 (CK8/18) antibodies to recognize differentiated basal/myoepithelial and luminal cell populations, respectively

3.7. JNK2 Inhibits Notch-dependent Myoepithelial Cell Suppression

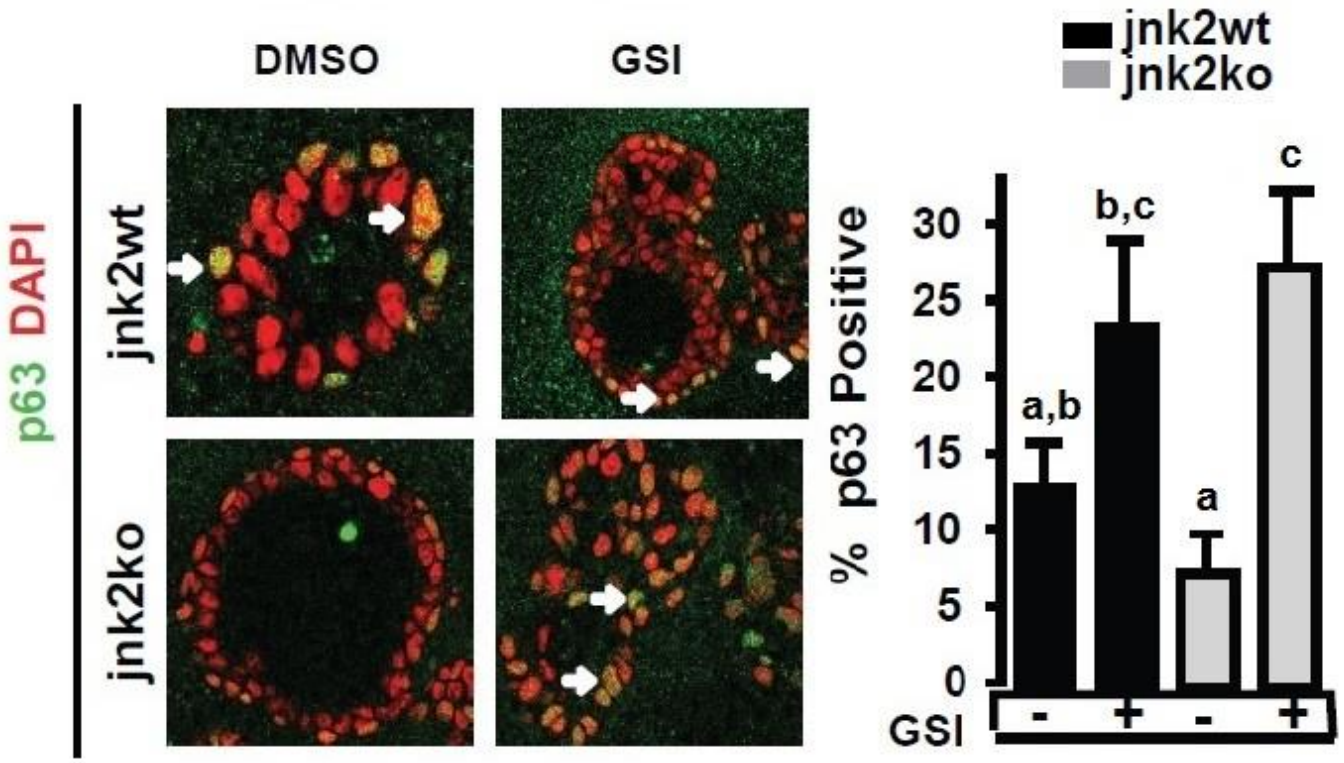

Mammary glands were harvested from adult virgin, female mice and mammary epithelial cells were isolated. Cells were then seeded onto beds of Matrigel in defined media with either gamma secretase inhibitor (GSI) or vehicle control (DMSO) and allowed to grow and differentiate. The resulting 3-dimensional structures were immunostained to analyze p63 positive basal/myoepithelial cell populations. 2way ANOVA with Bonferroni Post-test was performed and significant values are indicated by unique letters. Ex: a is significantly different ($p<0.05$) from b.

3.8. JNK2 Inhibits Notch-dependent Luminal Cell Differentiation

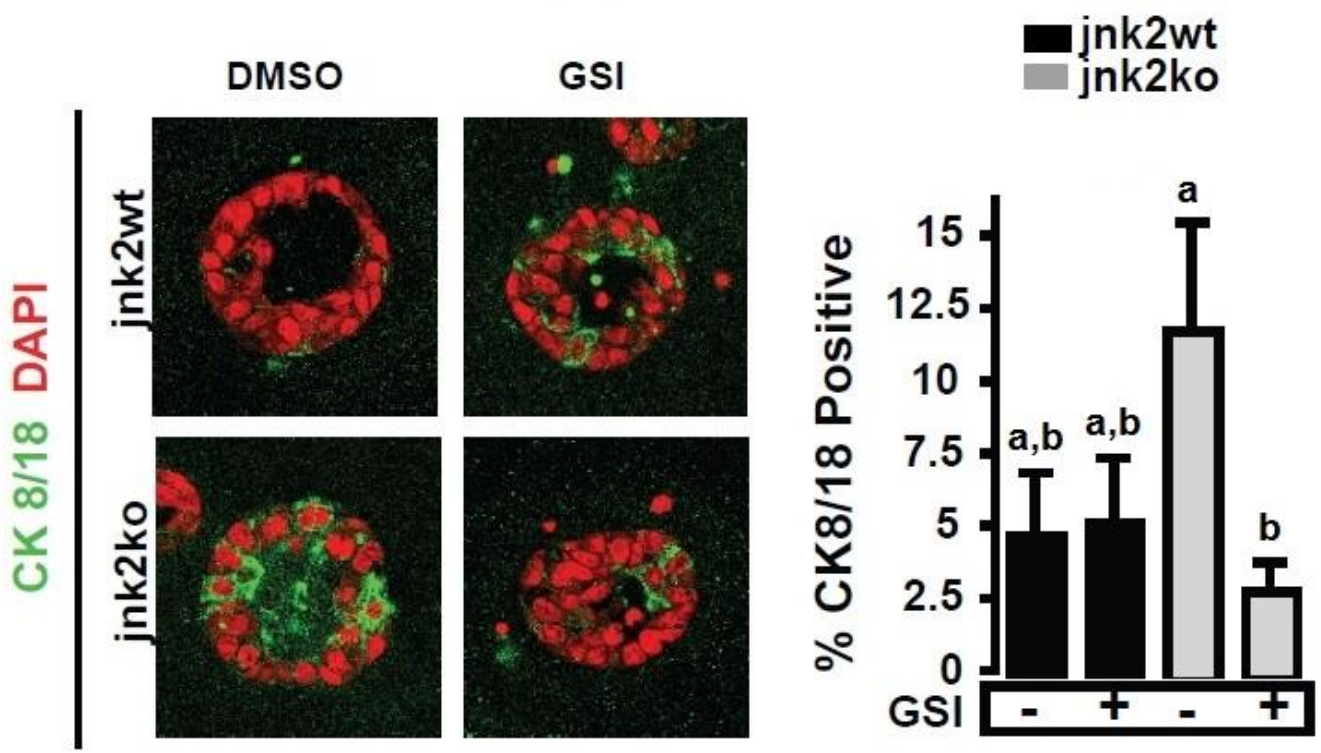

Mammary glands were harvested from adult virgin, female mice and mammary epithelial cells were isolated. Cells were then seeded onto beds of Matrigel in defined media with either gamma secretase inhibitor (GSI) or vehicle control (DMSO) and allowed to grow and differentiate. The resulting 3-dimensional structures were immunostained to analyze Cytokeratin 8/18 (CK 8/18) positive luminal cell populations. 2way ANOVA with Bonferroni Post-test was performed and significant values are indicated by unique letters. Ex: a is significantly different ($p<0.05$) from b.

3.9. JNK2 inhibits Notch-dependent Mammary Cell Growth

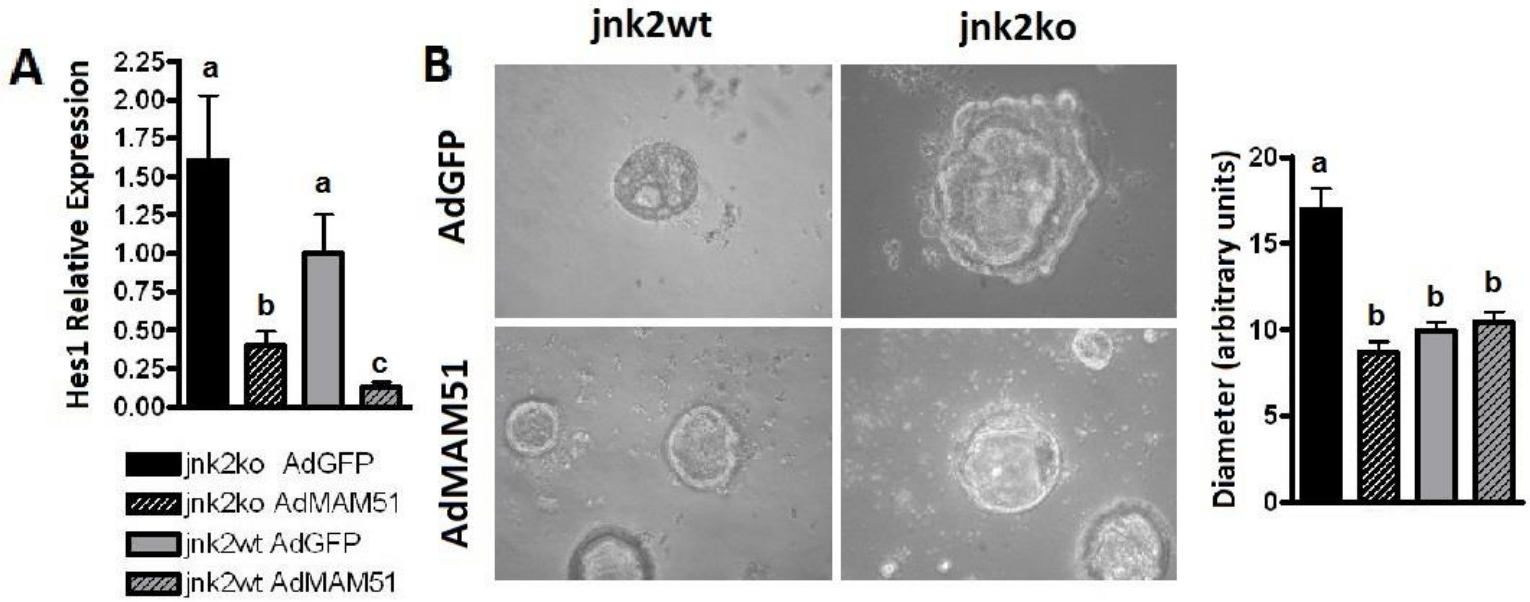

Mammary glands were harvested from adult virgin, female mice and mammary epithelial cells were isolated. Cells were then infected with Adenoviruses encoding GFP (AdGFP) or a dominant negative Mastermind-like construct. Cells were then seeded onto beds of Matrigel in defined media and allowed to grow and differentiate. The resulting 3-dimensional structures were either harvested for RNA isolation and *hes1* qPCR (A) or photographed for diameter measurement (B). 2way ANOVA with Bonferroni Post-test was performed and significant differences ($p<0.05$) are indicated between columns with different letters.

3.10. JNK2 inhibits Notch-dependent Luminal Cell Differentiation

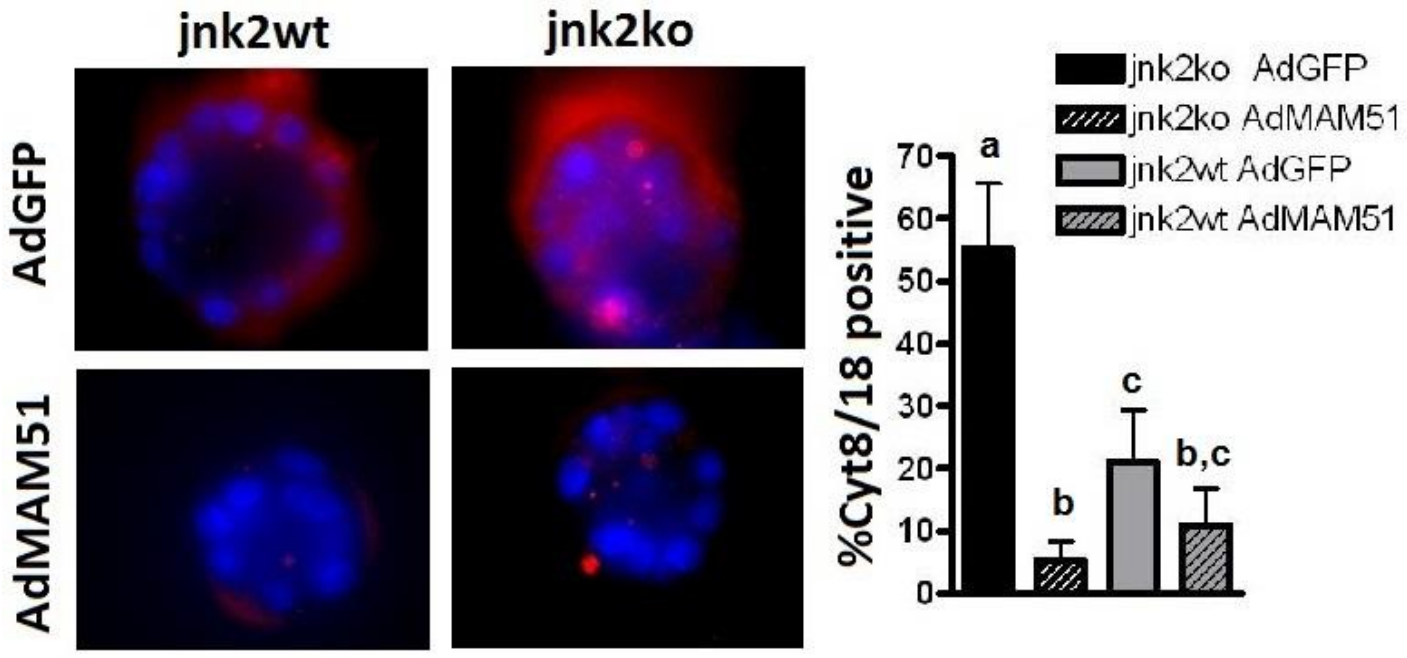

Mammary glands were harvested from adult virgin, female mice and mammary epithelial cells were isolated. Cells were then infected with Adenoviruses encoding GFP (AdGFP) or a dominant negative Mastermind-like construct. Cells were then seeded onto beds of Matrigel in defined media and allowed to grow and differentiate. The resulting 3-dimensional structures were fixed and then luminal populations were assessed by immunofluorescence using an anti-Cytokeratin 8/18 (cyt8/18) antibody. 2way ANOVA with Bonferroni Post-test was performed and significant differences ($p<0.05$) are indicated between columns with different letters.

3.11. JNK2 Inhibits Notch-dependent Mammary Cell Growth

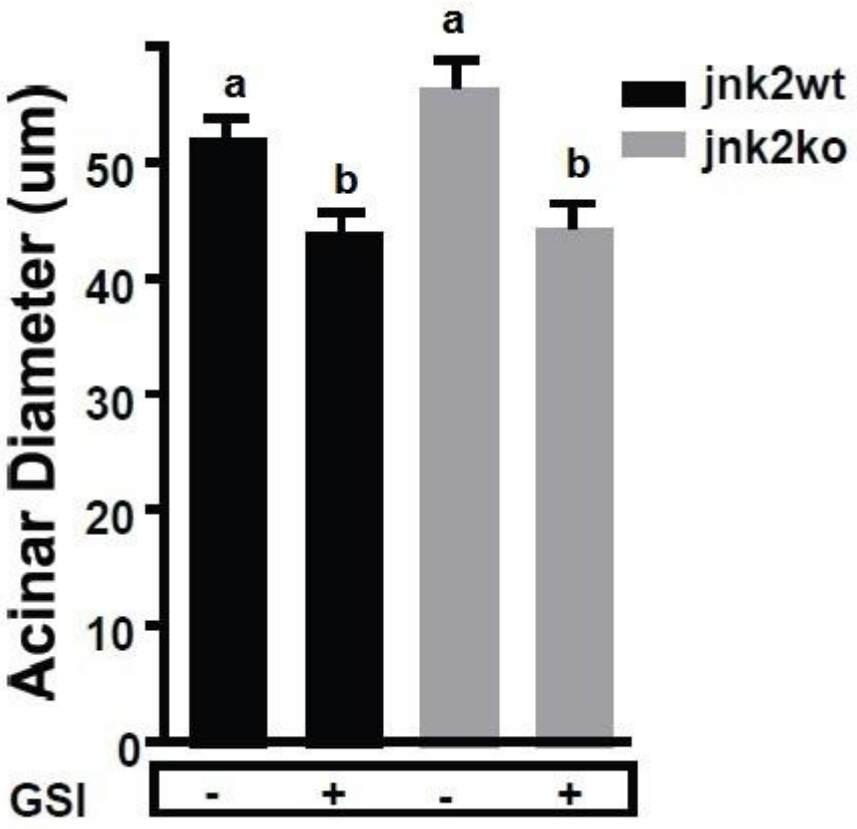

Mammary glands were harvested from adult virgin, female mice and mammary epithelial cells were isolated. Cells were then seeded onto beds of Matrigel in defined media with either gamma secretase inhibitor (GSI) or vehicle control (DMSO) and allowed to grow and differentiate. The resulting 3-dimensional structures were measured using images taken with light microscopy. 2way ANOVA with Bonferroni Post-test was performed and significant differences ($p<0.05$) are indicated between columns with different letters.

3.12. JNK2 Does Not Affect Notch Activity in Differentiated Mammary Ducts

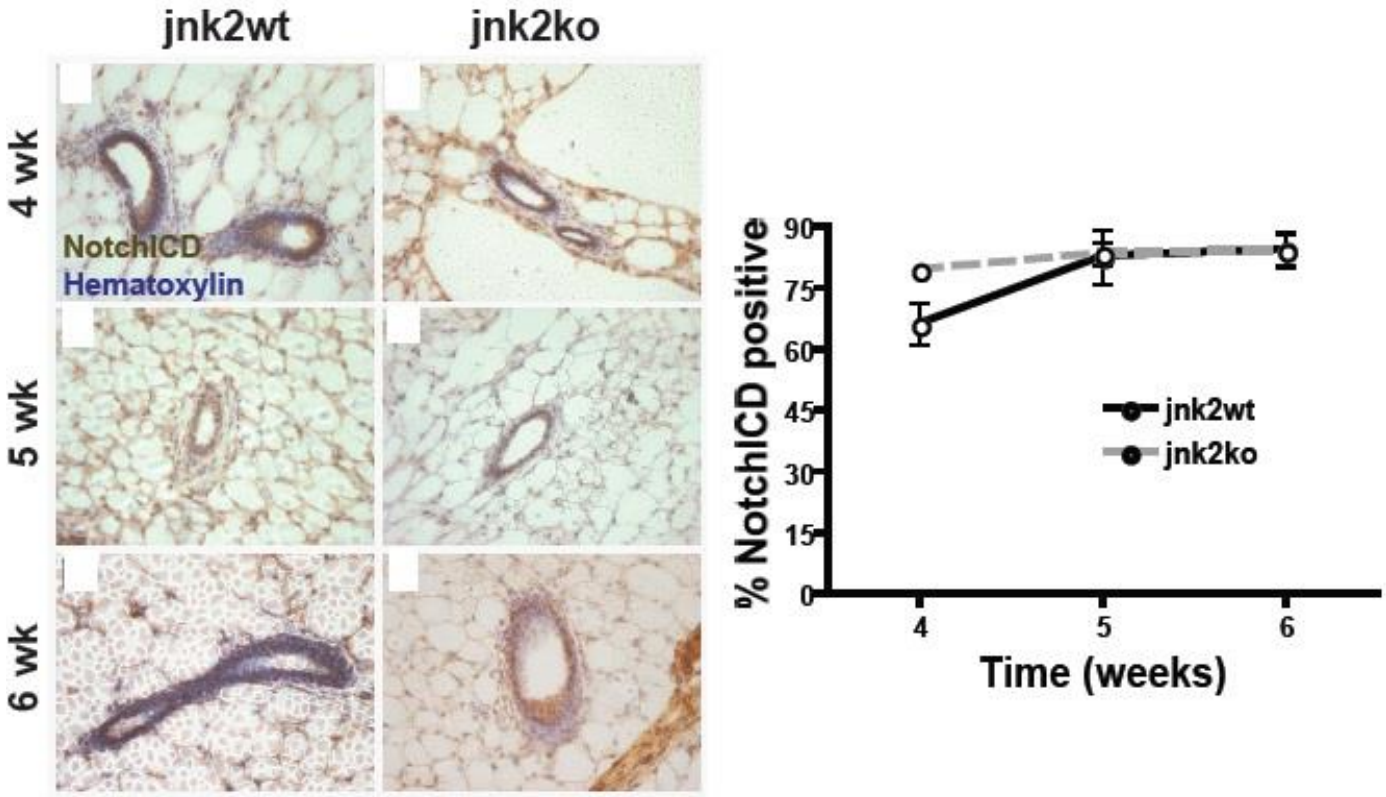

Mammary glands were harvested from virgin female mice at pubertal time points, then fixed and embedded in paraffin for sectioning. Slides were prepared and immunohistochemistry performed to examine Notch1^{ICD} expression in mammary ducts. 2way ANOVA with Bonferroni Post-test was performed and no significant differences ($p<0.05$) were found.

3.13. JNK2 Inhibits Notch Activity in Adult Mammary Terminal End Buds

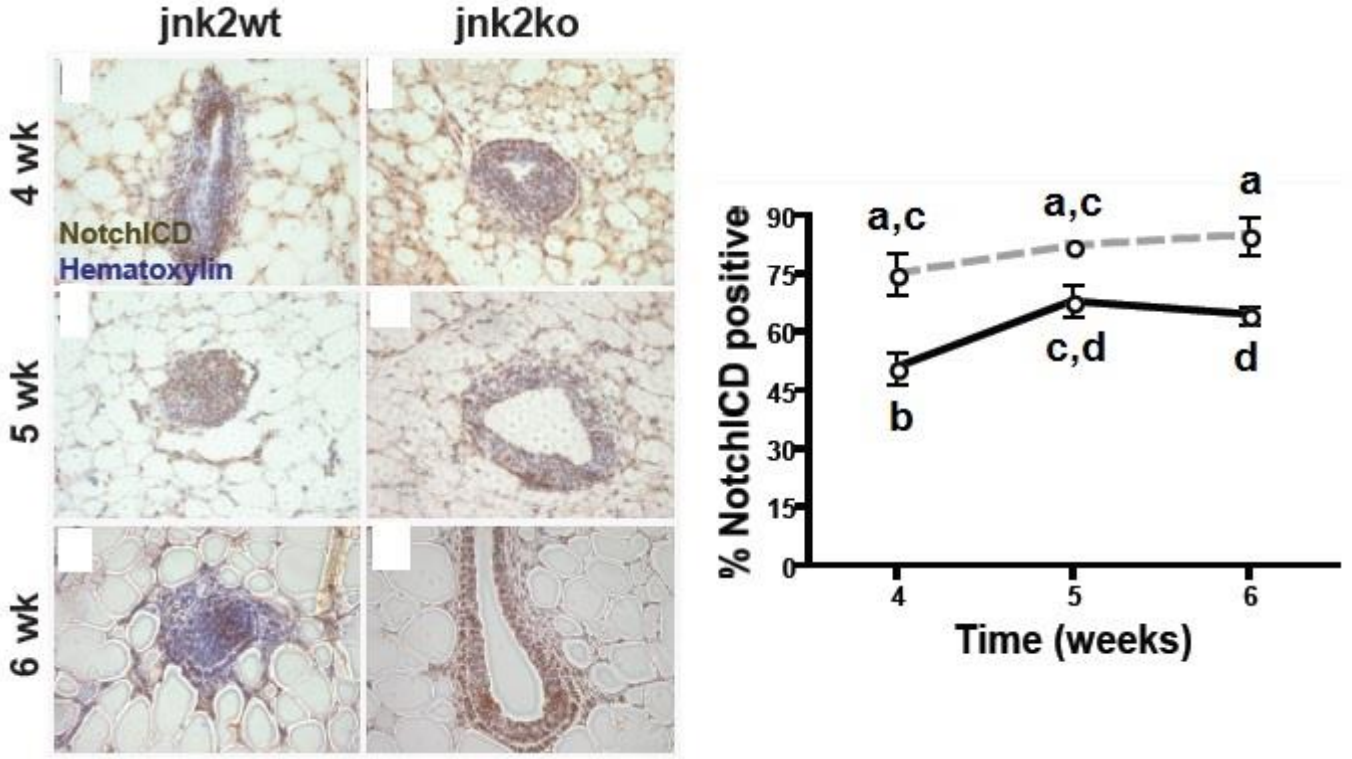

Mammary glands were harvested from virgin female mice at pubertal time points, then fixed and embedded in paraffin for sectioning. Slides were prepared and immunohistochemistry performed to examine Notch1^{ICD} expression in terminal end buds. 2way ANOVA with Bonferroni Post-test was performed and significant differences ($p<0.05$) are indicated between columns with different letters.

3.14. JNK2 Inhibits Expression and Activity of *Notch1* in Mammary Cells

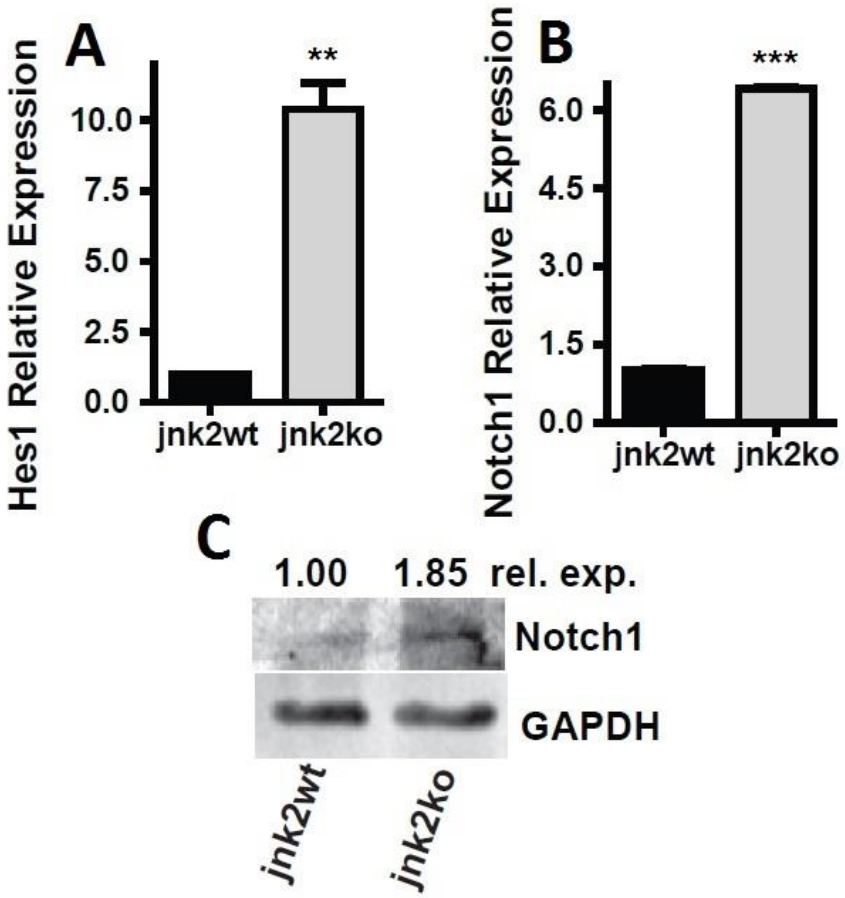

Mammary glands were harvested from virgin mice and treated with collagenase to dissociate adipocytes from mammary epithelium. Resulting mammary organoids were lysed with either Trizol reagent or protein lysis buffer. Isolated RNA was analyzed for *hes1* (A) and *notch1* (B) expression. C: Expression of full length Notch1 protein was assessed by western blot. Significance between groups was determined by T-test. Results are indicated on the figure as follows: * for $0.05 \geq p \geq 0.01$, ** for $0.01 > p \geq 0.0001$, *** for $p < 0.0001$.

4.1. JNK2 Promotes p63^{+} Basal Populations in MT Tumors

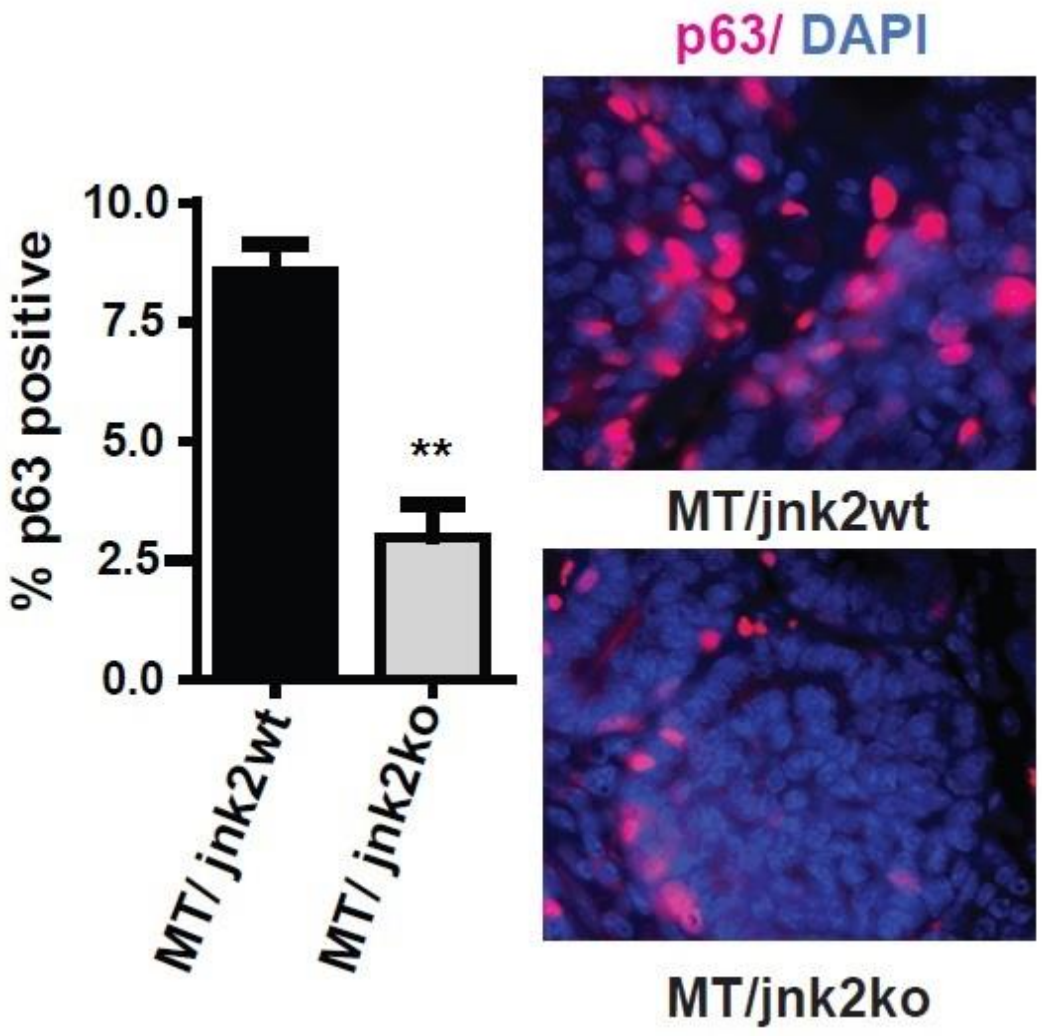

Tumors from MT+ *jnk2wt* and *jnk2ko* mice were previously generated and harvested for histology (3). Sections were cut from these tumor blocks and immunostained to examine p63^{+} basal populations. Significance between groups was determined by T-test. Results are indicated on the figure as follows: * for $0.05 \geq p \geq 0.01$, ** for $0.01 > p \geq 0.0001$, *** for $p < 0.0001$.

4.2. JNK2 Inhibits Cytokeratin 8/18^{+} Luminal Populations in MT Tumors

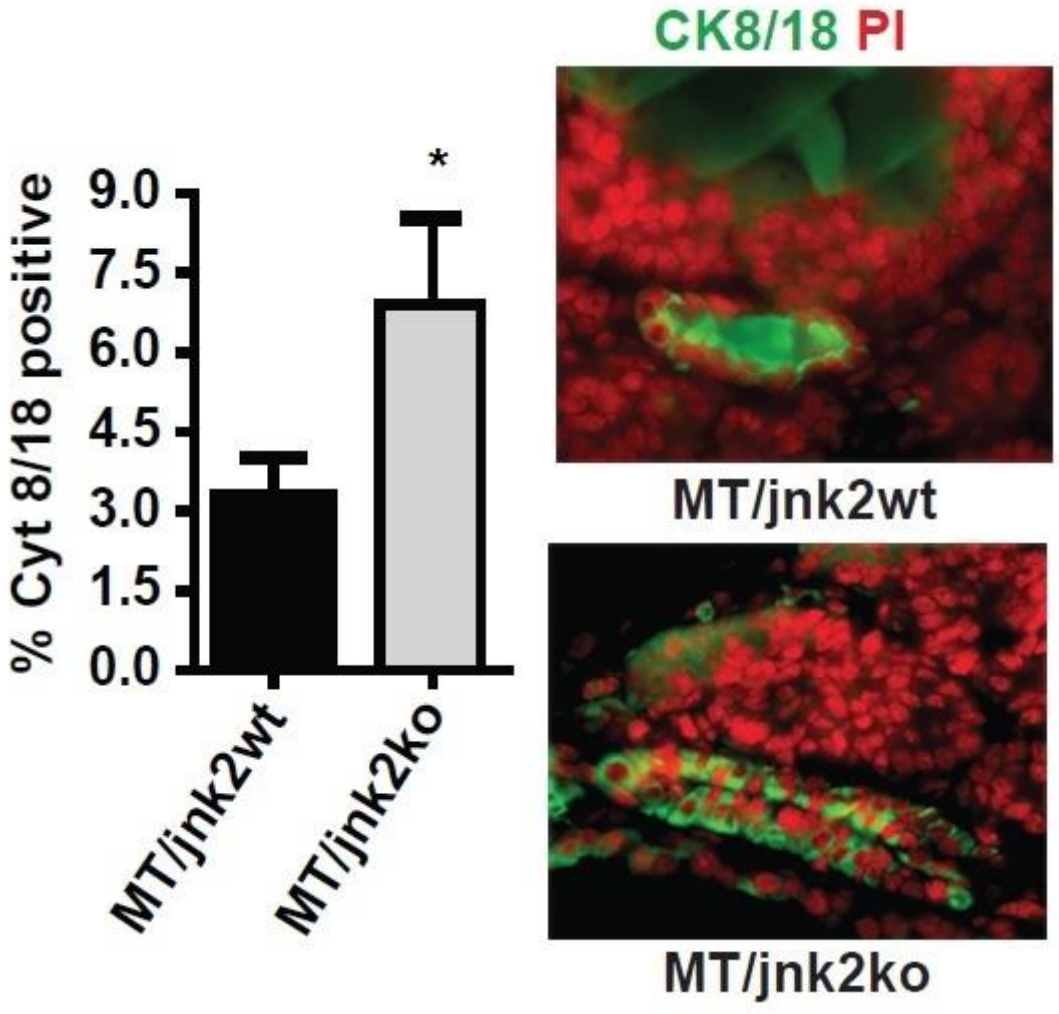

Sections of MT tumors were immunostained to examine Cytokeratin8/18^{+} (Cyt 8/18) luminal populations. Significance between groups was determined by T-test. Results are indicated on the figure as follows: * for $0.05 \geq p \geq 0.01$, ** for $0.01 > p \geq 0.0001$, *** for $p < 0.0001$.

4.3. JNK2 Inhibits Notch1 Activity in MT Tumors

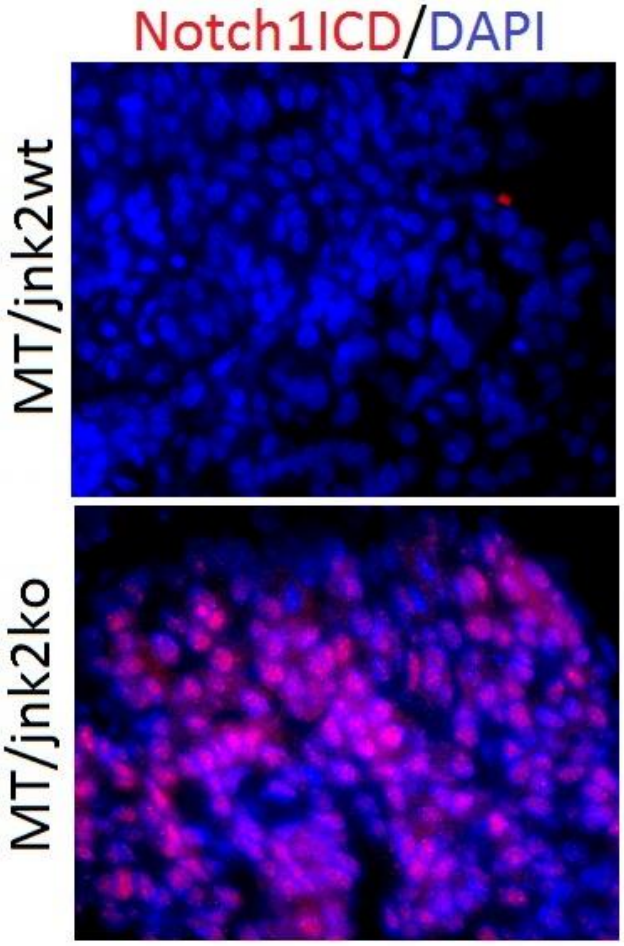

Sections of MT tumors were cut and immunostained to examine Notch1^{ICD} expression.

4.4. JNK2 Inhibits Expression of *Notch1* in MT Tumors

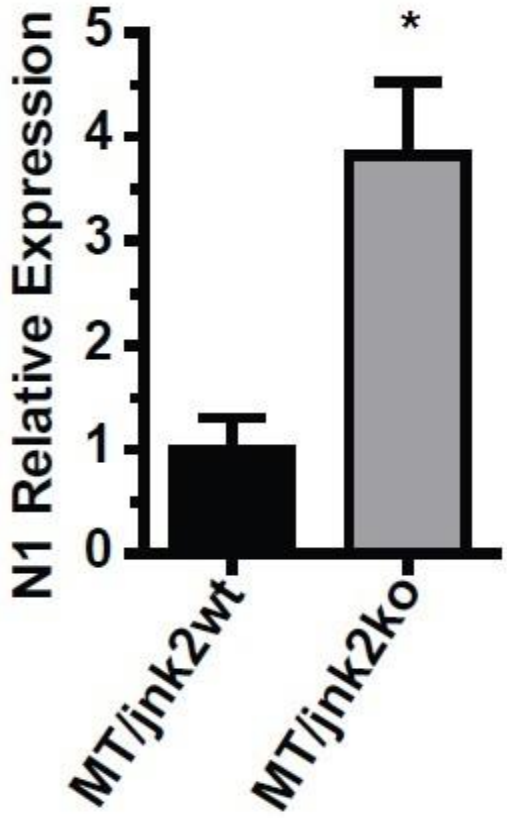

RNA from MT+ *jnk2wt* and *jnk2ko* tumors was previously isolated (3). Expression of *notch1* was analyzed by qPCR using these samples. Significance between groups was determined by T-test. Results are indicated on the figure as follows: * for $0.05 \geq p \geq 0.01$, ** for $0.01 > p \geq 0.0001$, *** for $p < 0.0001$

4.5. JNK2 Suppresses Notch Signaling in MT Cells

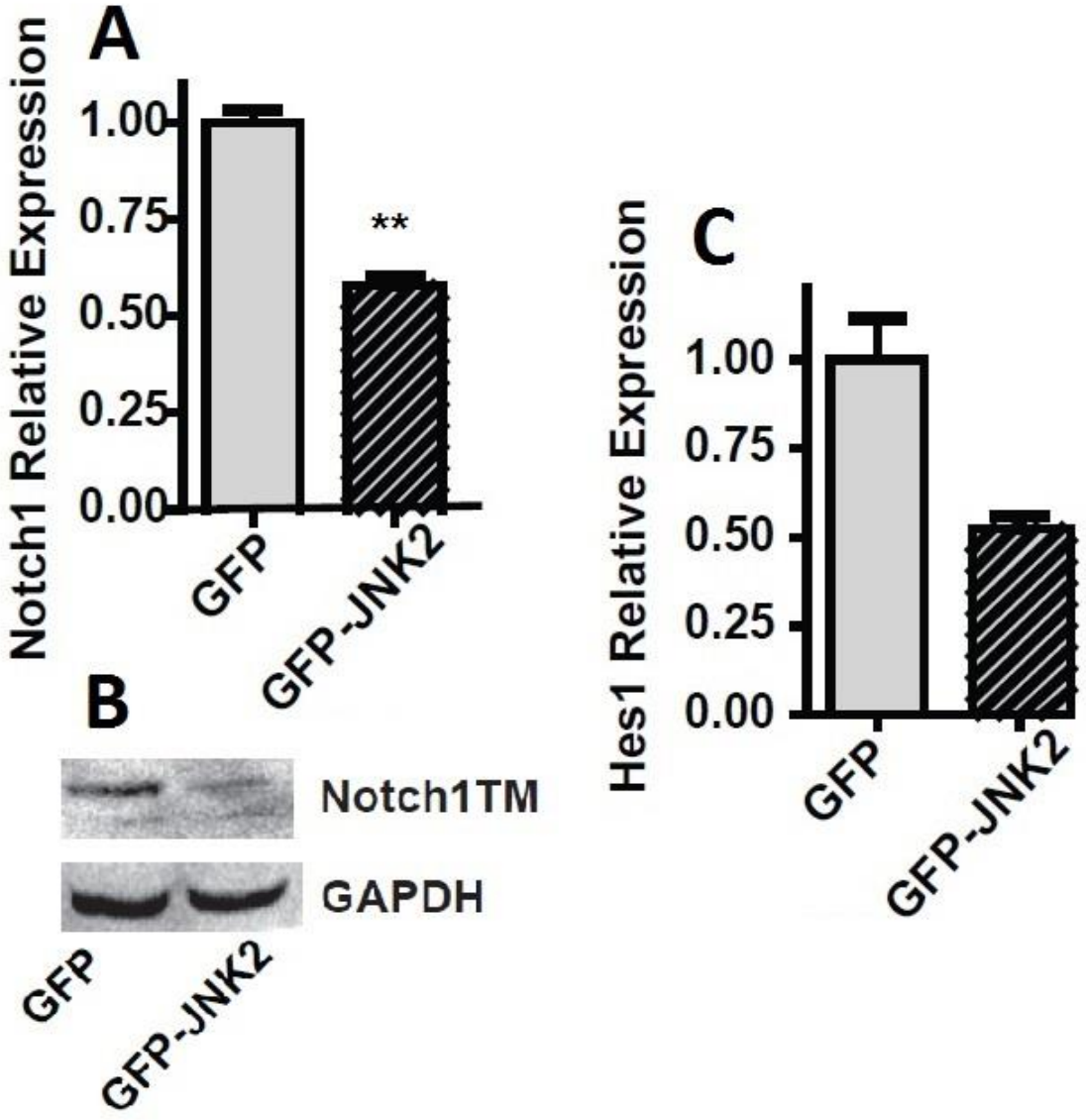

Cell lines were previously established from a MT+ *jnk2ko* tumor and infected with viruses encoding either GFP or GFP-JNK2 (3). These cells were lysed with either Trizol reagent or protein lysis buffer. Isolated RNA was analyzed for *notch1* (A) and *hes1* (B) expression. C: Expression of full length Notch1 protein was assessed by western blot. Significance between groups was determined by T-test. Results are indicated on the figure as follows: * for $0.05 \geq p \geq 0.01$, ** for $0.01 > p \geq 0.0001$, *** for $p < 0.0001$.

4.6. JNK2 Inhibits Expression of *Trp53* mRNA

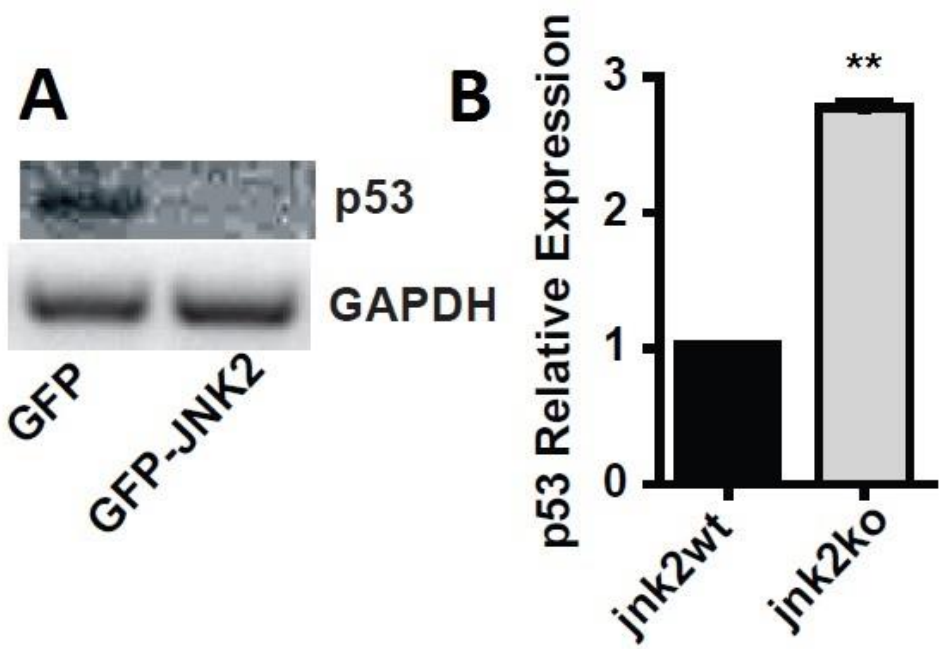

A: RNA was isolated from MT cells and expression of *p53* was assessed by RT-PCR. B: RNA was isolated from mammary organoids and expression of *p53* was assessed by qPCR. Significance between groups was determined by T-test. Results are indicated on the figure as follows: * for $0.05 \geq p \geq 0.01$, ** for $0.01 > p \geq 0.0001$, *** for $p < 0.0001$

4.7. JNK2 Inhibits EGF-dependent Transcription of *Notch1* and *Trp53*

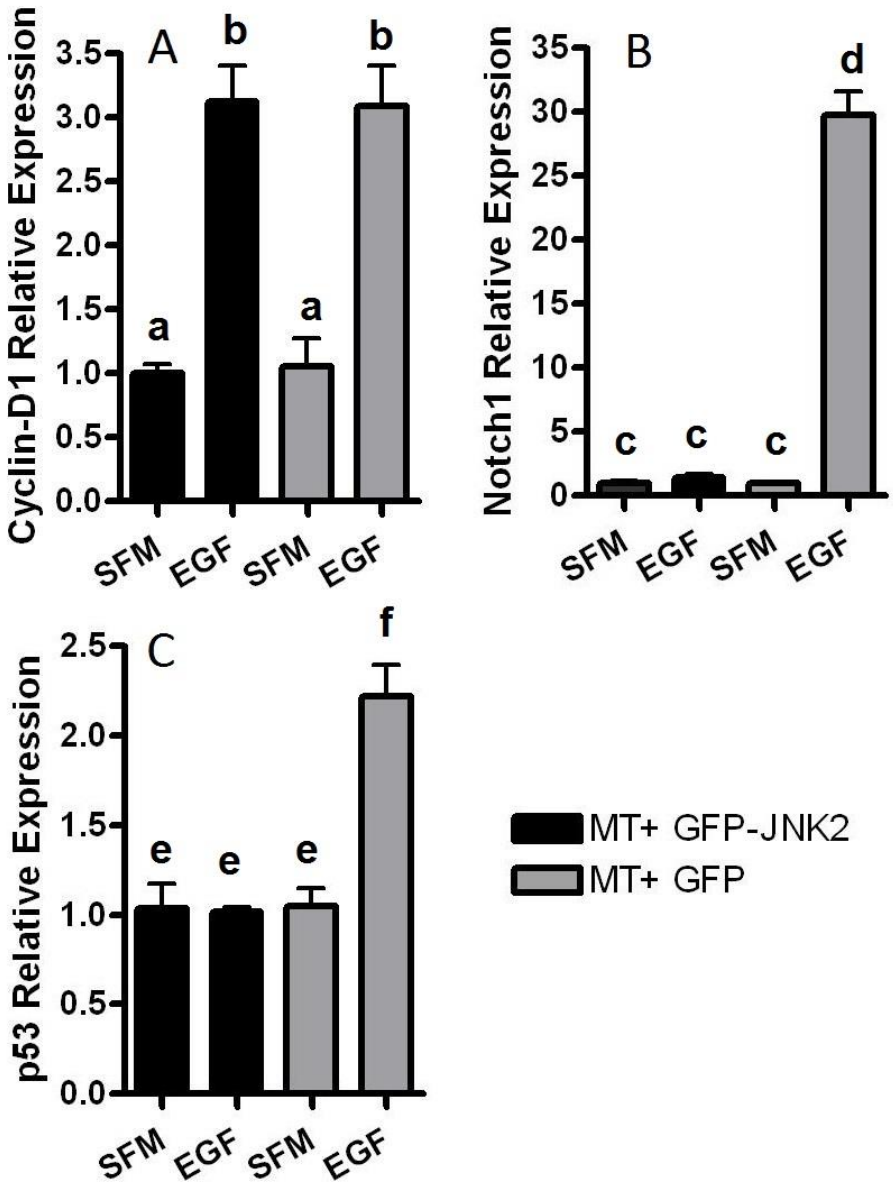

MT cells were placed in serum-free media (SFM) to deplete growth factors. Media was then replaced with fresh SFM or SFM supplemented with EGF. Cells were harvested for RNA isolation and expression levels of *cyclin-d1* (A), *notch1* (B), and *p53* (C) were examined by qPCR. 2way ANOVA with Bonferroni Post-test was performed and significant differences ($p<0.05$) are indicated between columns with different letters.

4.8. JNK2 Suppresses EGF-dependent *Notch1* Promoter Activity

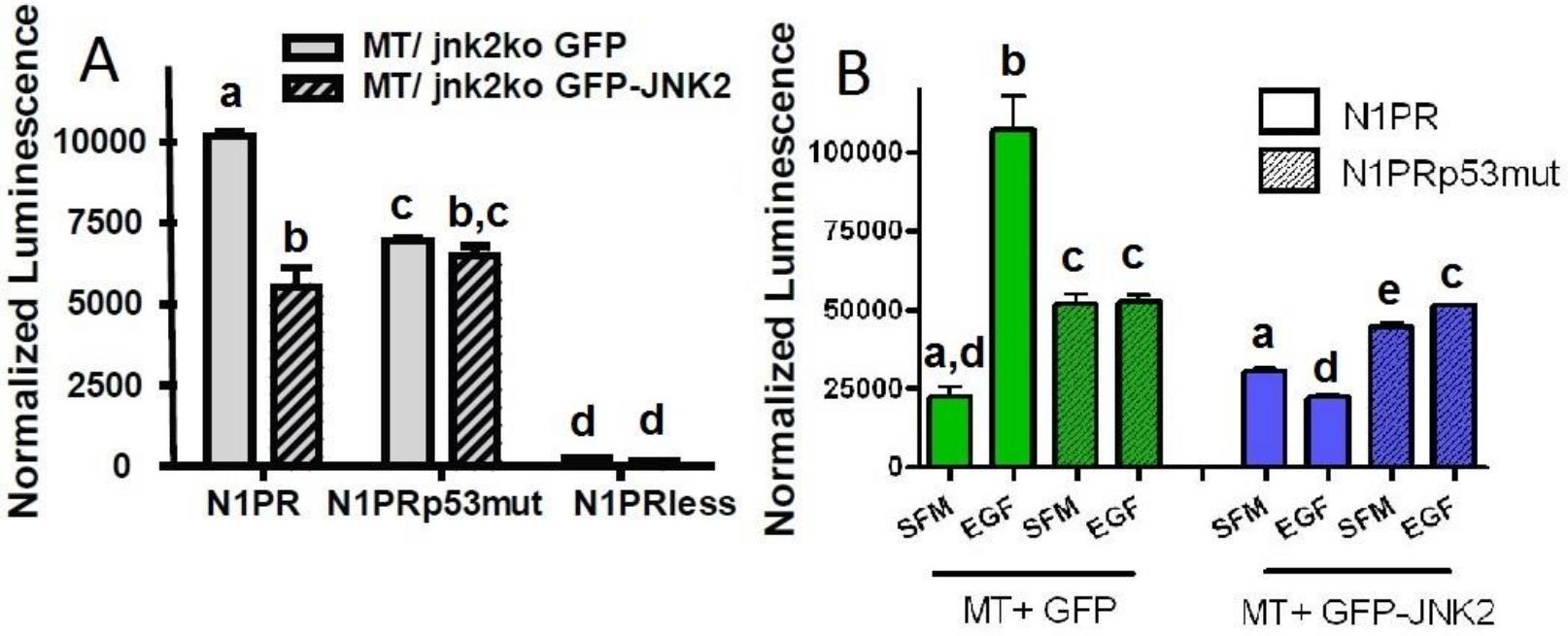

MT cells were transfected with plasmids containing either a wildtype *notch1* promoter (N1PR), a *notch1* promoter with mutated p53 response elements (N1PRp53mut) , or no promoter (N1PRless) attached to *luciferase*. Cells were incubated in full media (A) or SFM vs EGF (B) and then harvested for luciferase assay. 2way ANOVA with Bonferroni Post-test was performed and significant differences ($p<0.05$) are indicated between columns with different letters.

4.9. JNK2 Decreases p53 Binding to the *Notch1* Promoter

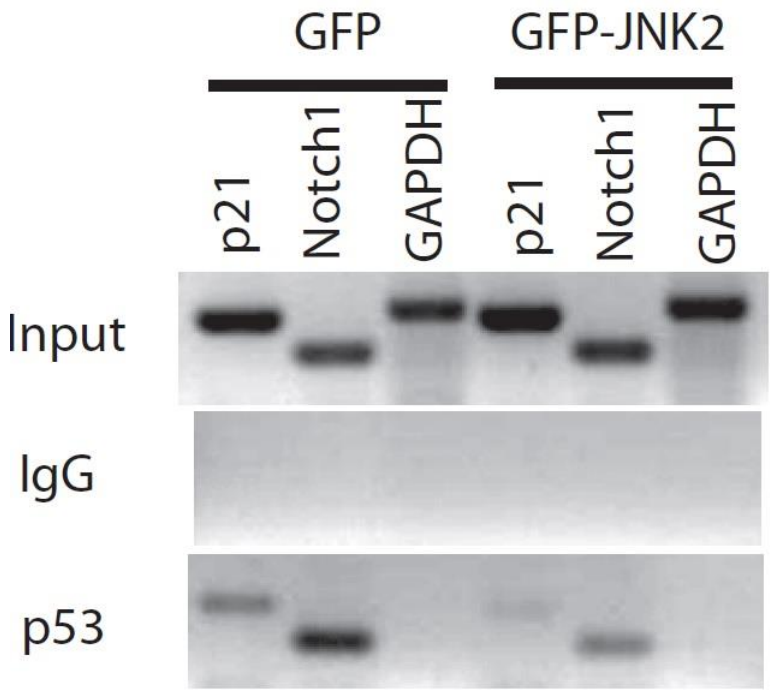

MT cells were fixed in formaldehyde and lysed to release chromatin. Chromatin was then sonicated and immunoprecipitated with p53 or IgG as negative control. Resultant DNAs were then amplified by PCR with specific primers surrounding p53 response elements within the promoters of *p21* (positive control) or *notch1*. Glyceraldehyde 3-Phosphate Dehydrogenase (*gapdh*) promoter was amplified as a negative control.

5.1. JNK2 Does Not Affect Tumor Latency in *Trp53-n*ull Tumors

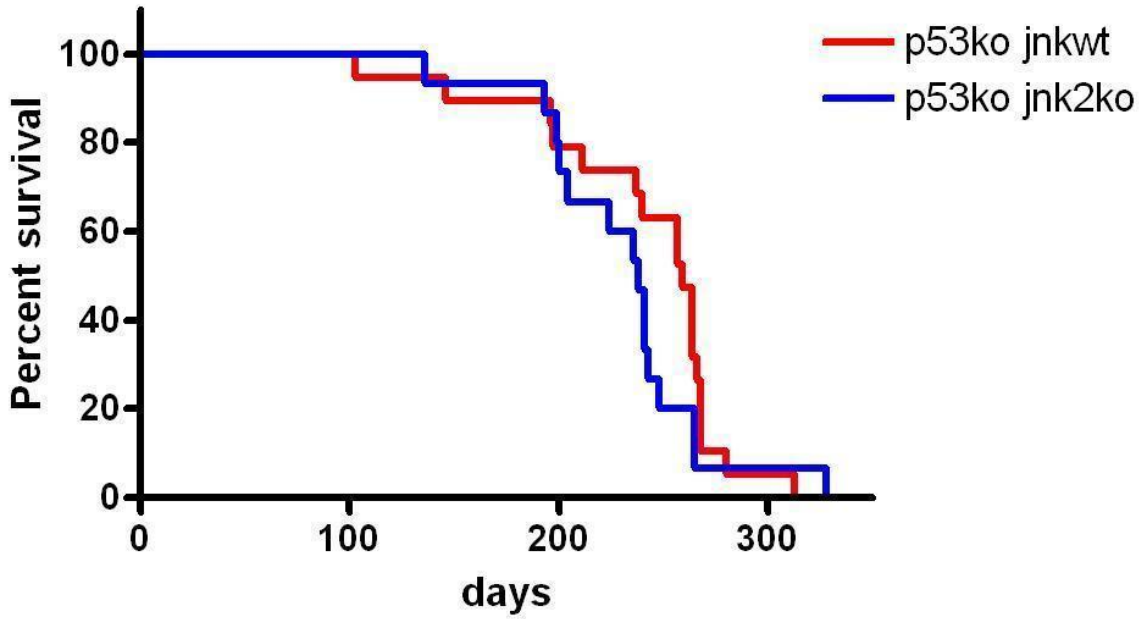

Mammary glands from *p53ko*;*jnk2wt* or *p53ko*;*jnk2ko* female mice were transplanted into cleared fat pads of 3 week-old female mice. Growth of mammary tissue was potentiated by pituitary isograft. Time from transplant to tumor palpation is shown. Logrank test showed no significant differences among groups.

5.2. JNK2 Inhibits Growth and Proliferation of *Trp53*-null Tumors

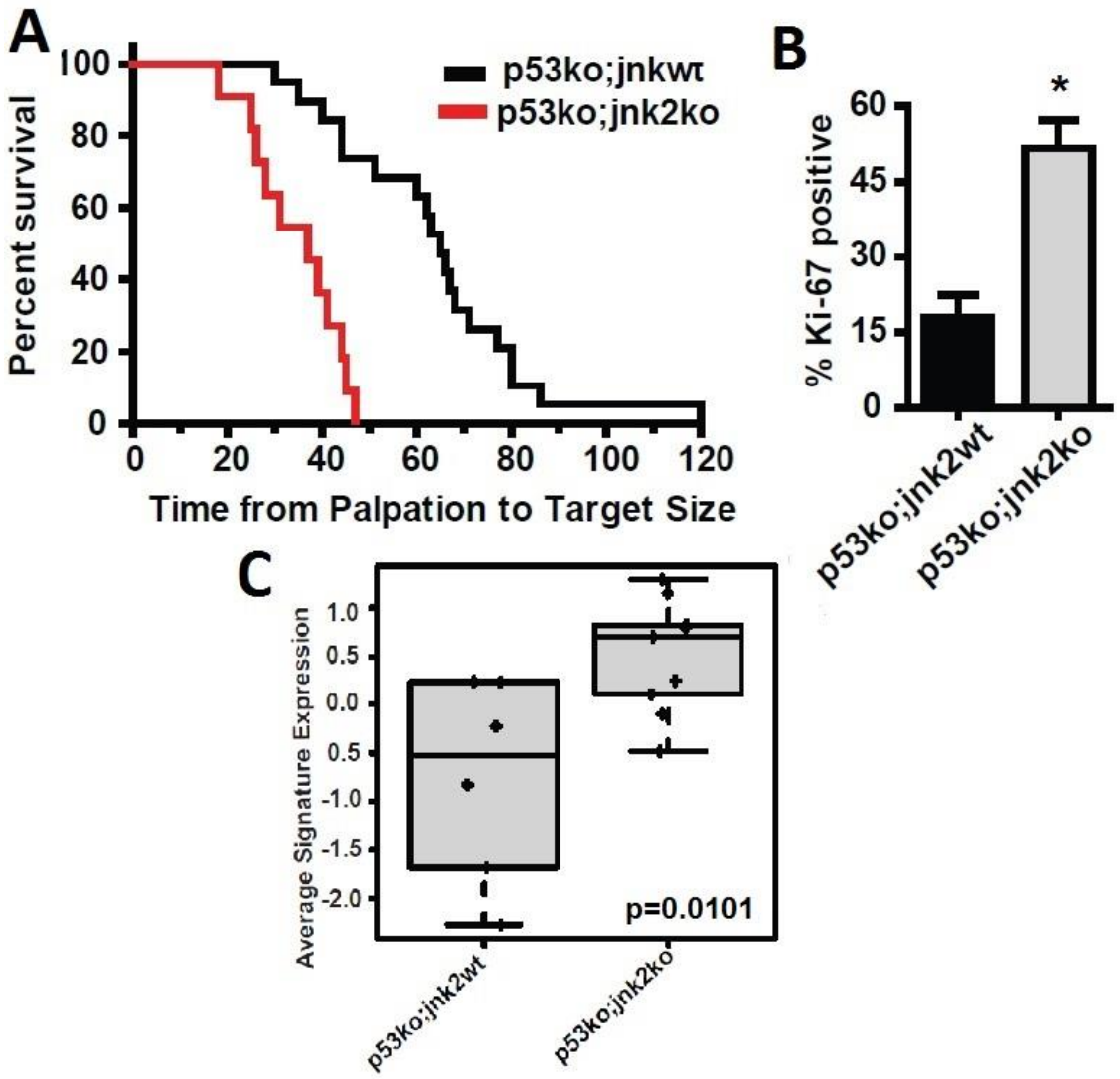

A: Transplant tumors were measured and harvested at 1.5 cm^2. Time from tumor palpation to harvest at target size is shown in the Kaplan Meier chart. Logrank shows significant difference in tumor growth ($p<0.05$) B: Harvested tumors were divided into pieces with parts of each being fixed for histology. Tumor sections were stained with Ki67, a marker of proliferation, and then quantified. C: RNA from tumors was used for microarray analysis and expression of a proliferation signature was compared between *p53ko*;*jnk2wt* and *p53ko*;*jnk2ko* tumors. Significance between groups was determined by T-test. Results are indicated on the figure as follows: * for $0.05\geq p\geq 0.01$, ** for $0.01>p\geq 0.0001$, *** for $p<0.0001$.

5.3. JNK2 Does Not Inhibit *Notch1* in the Absence of p53

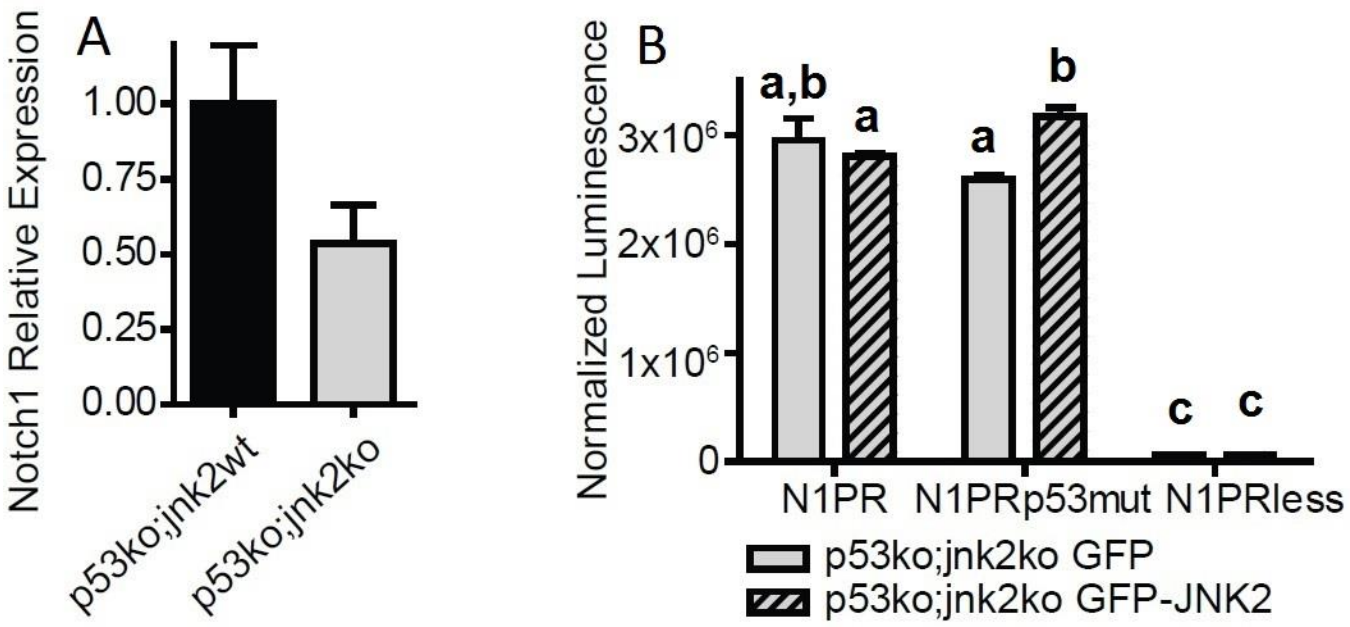

A: Expression of Notch1 was assessed in *p53ko* transplant tumors. Significance between groups was determined by T-test. Results are indicated on the figure as follows: * for $0.05 \geq p \geq 0.01$, ** for $0.01 > p \geq 0.0001$, *** for $p < 0.0001$. B: A *p53ko*;*jnk2ko* tumor cell line was generated and infected with viruses carrying either a GFP or GFP-JNK2 transgene. These cells were transfected with *notch1* promoter luciferase constructs and assessed for *notch1* promoter activity. 2way ANOVA with Bonferroni Post-test was performed and significant differences ($p < 0.05$) are indicated between columns with different letters.

5.4. JNK2 Inhibits Luminal Marker Expression in *Trp53*-null Tumors

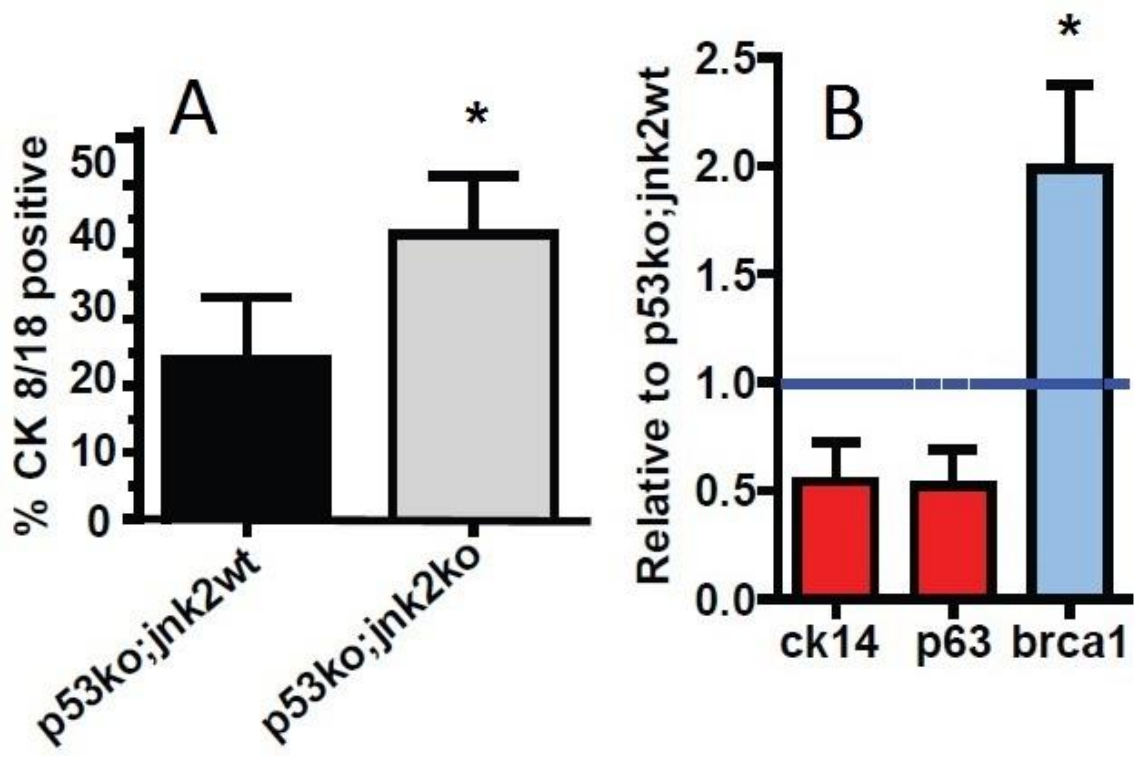

A: Transplant tumor sections were immunostained for Cytokeratin 8/18 (CK 8/18) expression to assess luminal cell populations. B: Transplant tumor RNAs were assessed for expression of basal genes (Cytokeratin14-*ck14* and *p63*) and the luminal gene, *brca1*, by qPCR. Significance between groups was determined by T-test. Results are indicated on the figure as follows: * for $0.05 \geq p \geq 0.01$, ** for $0.01 > p \geq 0.0001$, *** for $p < 0.0001$.

5.5. JNK2 Inhibits BRCA1 Pathway Expression in *Trp53*-Null Tumors

Probe ID	Gene	Fold Change	%FDR
A_52_P117090	Chek2	1.93	4.38
A_52_P18267	Brca1	2.16	4.38
A_52_P556462	Fancd2	1.76	4.38
A_51_P357182	Mapk8	2.36	2.40
A_52_P574881	Hus1	1.42	4.38
A_52_P369581	Atm	1.83	2.06

Expression of genes associated with the BRCA1 pathway were assessed in *p53ko* transplant tumors using microarray analysis.

5.6. JNK2 Inhibits Luminal Marker Expression in *Trp53*-null Cells

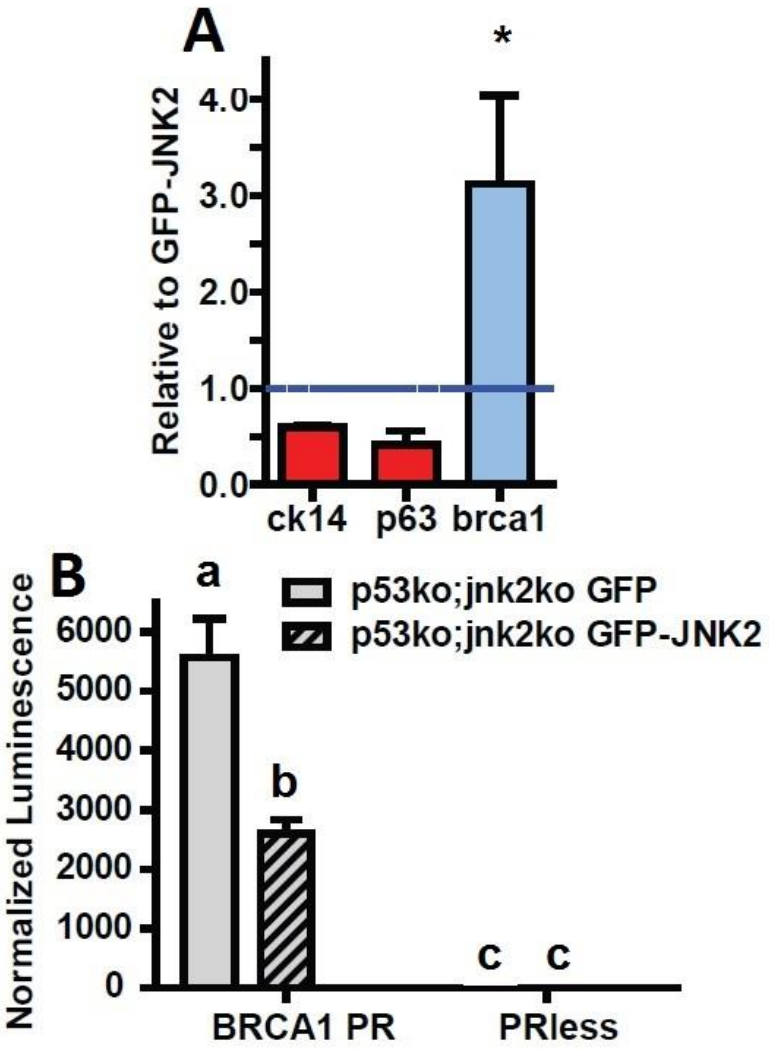

A: Tumor cell lines generated from a *p53ko*; *jnk2ko* cell line were lysed to examine expression of basal markers (*ck14* and *p63*) and the luminal marker, *brca1*, by qPCR. Significance between groups was determined by T-test. Results are indicated on the figure as follows: * for $0.05 \geq p \geq 0.01$, ** for $0.01 > p \geq 0.0001$, *** for $p < 0.0001$. B: *brca1* promoter activity was assessed in *p53ko*;*jnk2ko* cell lines. 2way ANOVA with Bonferroni Post-test was performed and significant differences ($p < 0.05$) are indicated between columns with different letters.

5.7. JNK2 Does Not Affect *Brca1* Expression in MT Tumors

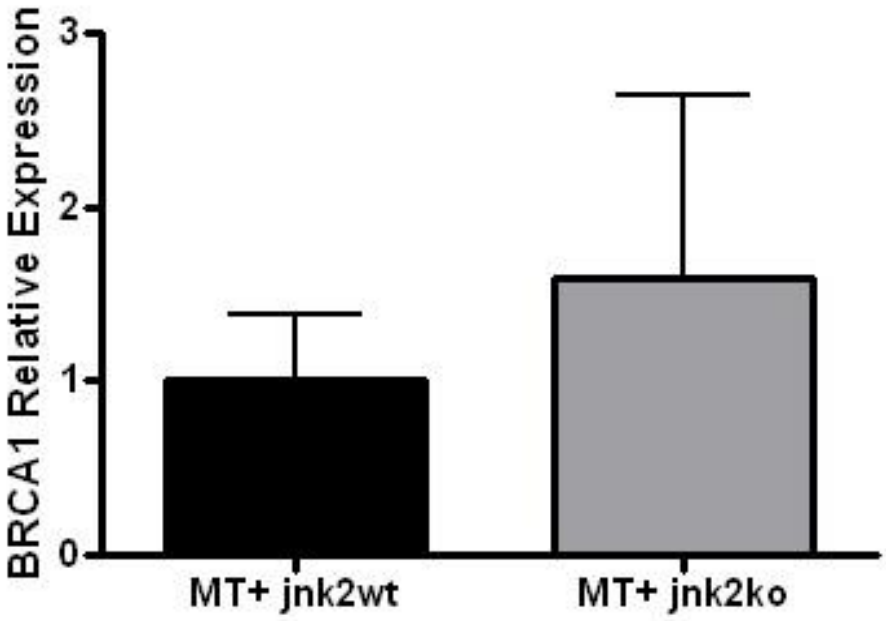

MT tumor RNA was amplified by qPCR using primers for *Brca1*. Significance between groups was determined by T-test. Results are indicated on the figure as follows: * for $0.05 \geq p \geq 0.01$, ** for $0.01 > p \geq 0.0001$, *** for $p < 0.0001$. No significant difference was found.

5.8. *Brca1* and EMT are Anti-correlated in Breast Tumors

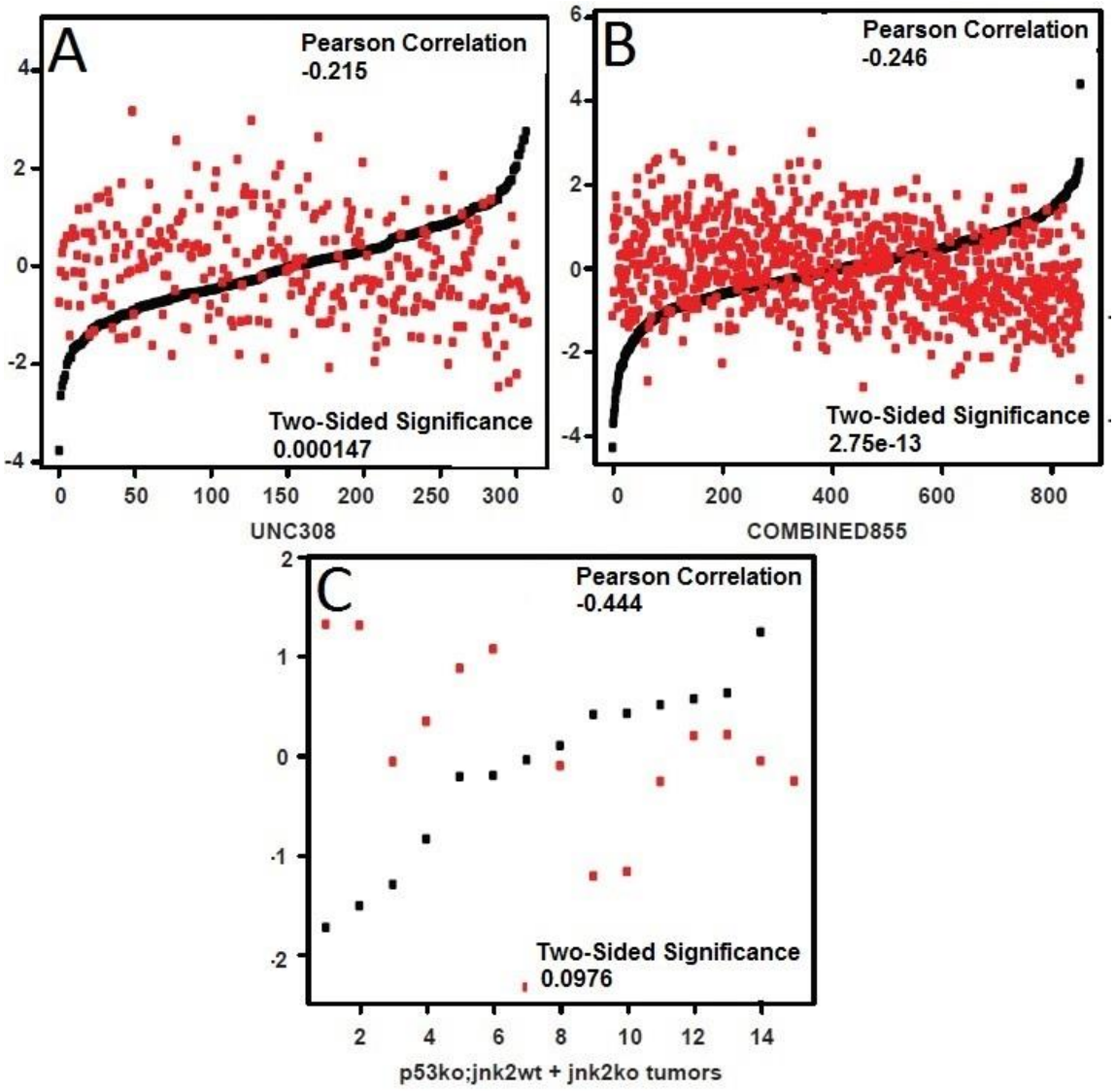

Human tumors from UNC308 (A) and COMBINED855 (B) as well as our own *p53ko* tumor microarrays (C) were ranked by level of *Brca1* expression. The level of expression of a set of genes correlated with epithelial to mesenchymal transition (EMT) was then plotted against these data points to reveal correlation.

5.9. JNK2 Promotes Epithelial to Mesenchymal Transition

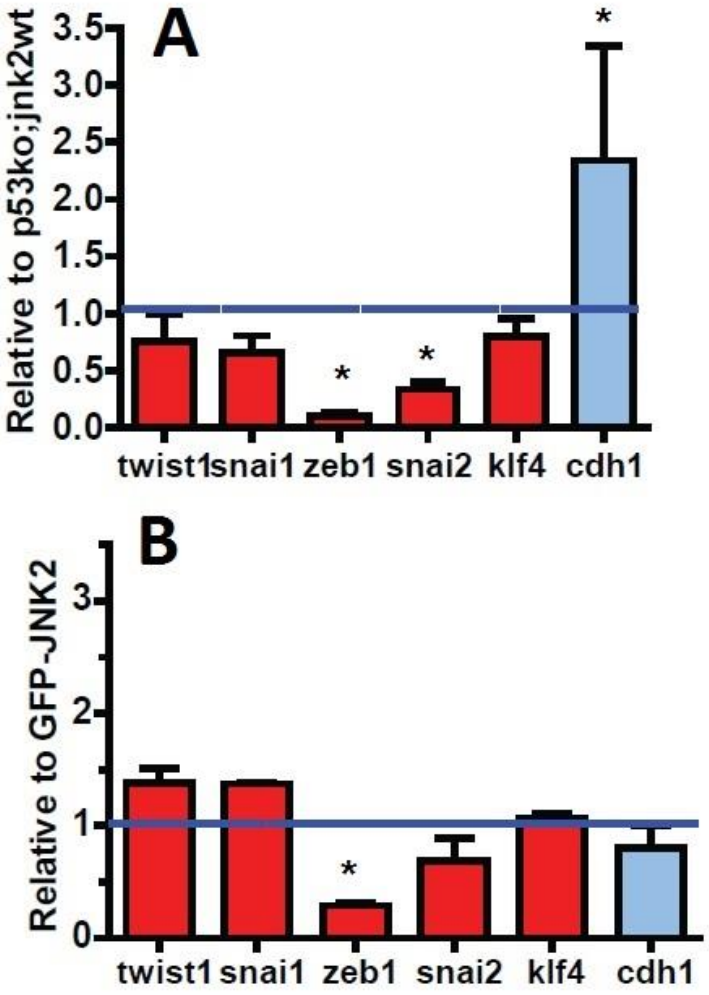

Expression of mesenchymal/stem genes in red (*twist1, snai1, zeb1, snai2,* and *klf4*) and the epithelial gene, e-cadherin in blue, were assessed by qPCR in *p53ko* tumors (A) and *p53ko;jnk2ko* tumor cell lines (B). Significance between groups was determined by T-test. Results are indicated on the figure as follows: * for $0.05 \geq p \geq 0.01$, ** for $0.01 > p \geq 0.0001$, *** for $p < 0.0001$.

5.10. Microarray Confirms JNK2 Regulation of EMT

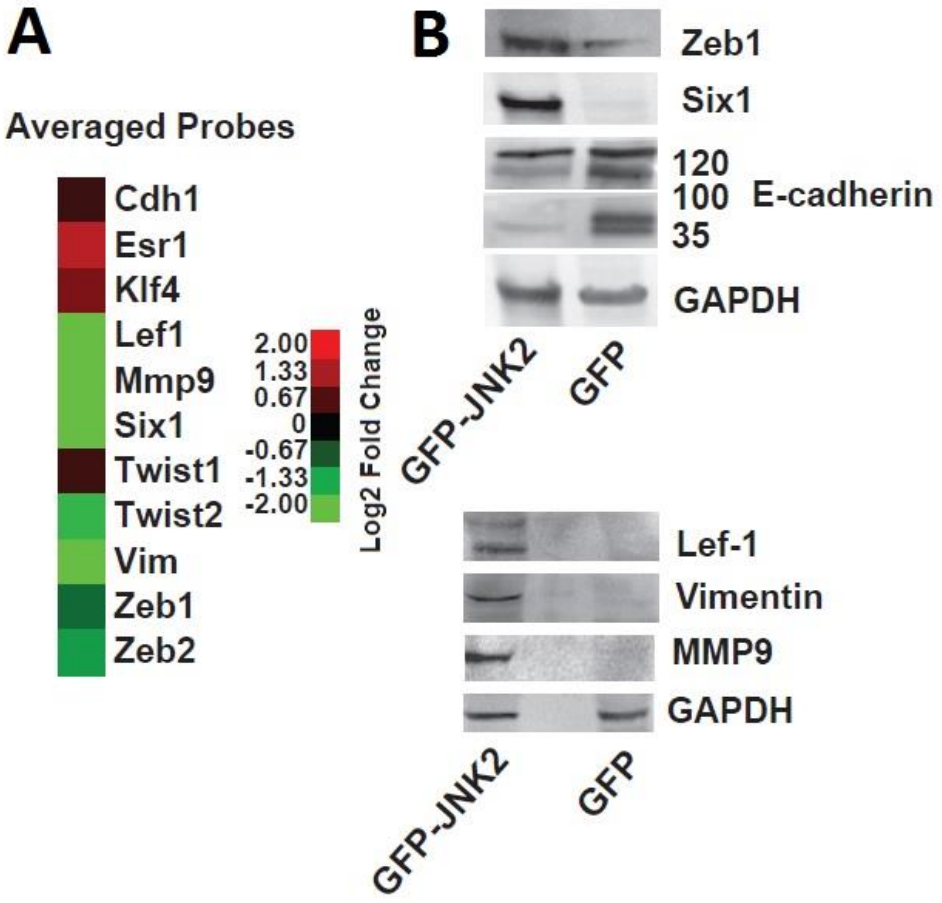

Expression of mesenchymal/stem (*Klf4, Lef1, Mmp9, Six1,Ttwist1,Ttwist2, Vim, Zeb1,* and *Zeb2*), E-cadherin (*Cdh1*), and the luminal marker, ER (*Esr1*) in *p53ko;jnk2ko* cell lines were assessed by microarray (A) and confirmed by western blot (B).

5.11. JNK2 Promotes EMT Marker Expression *in vitro*

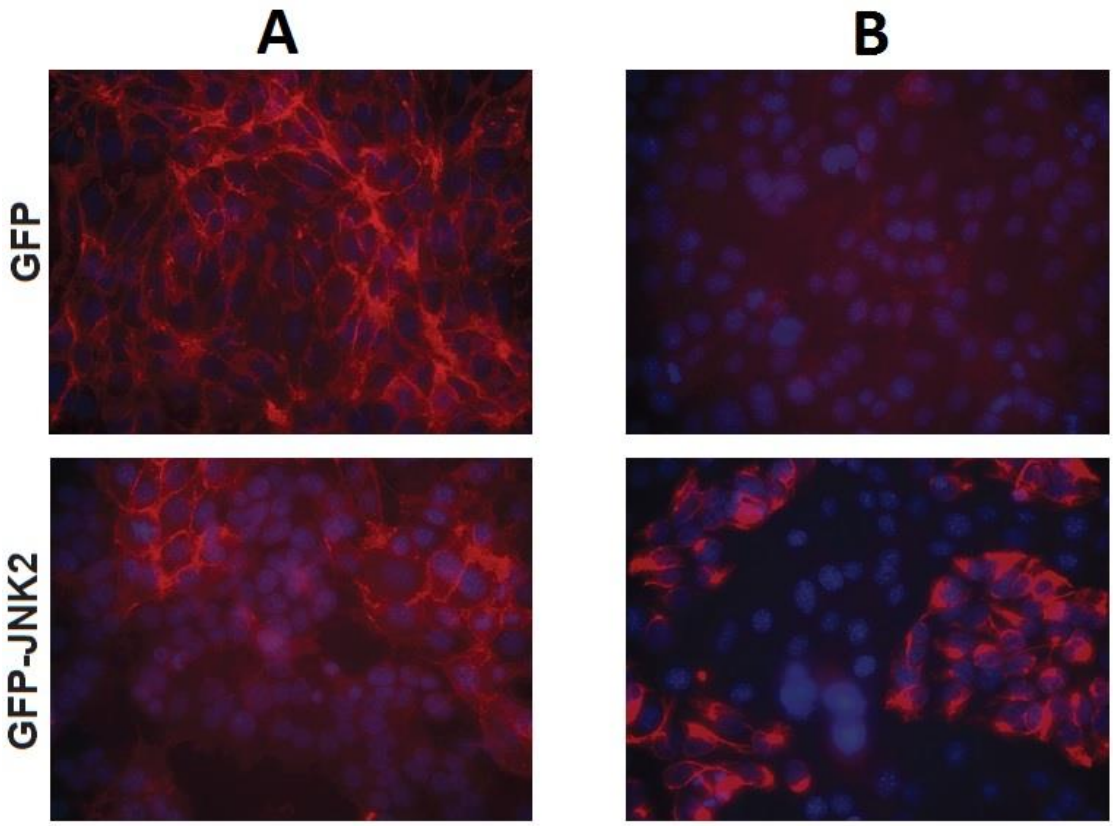

Immunocytochemistry was performed on *p53ko*;*jnk2ko* cell lines using e-cadherin (A) or vimentin (B) antibodies.

5.12. JNK2 Promotes Focal Growth of Cells in Culture

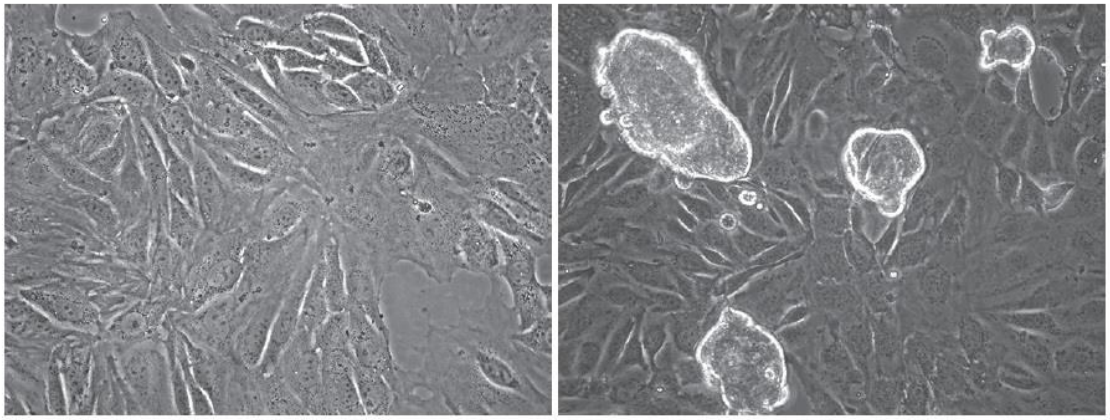

Light microscopy was used to assess morphology of *p53ko*;*jnk2ko* cell lines.

5.13. GFP-JNK2 Promotes CD24^{-} Cell Populations

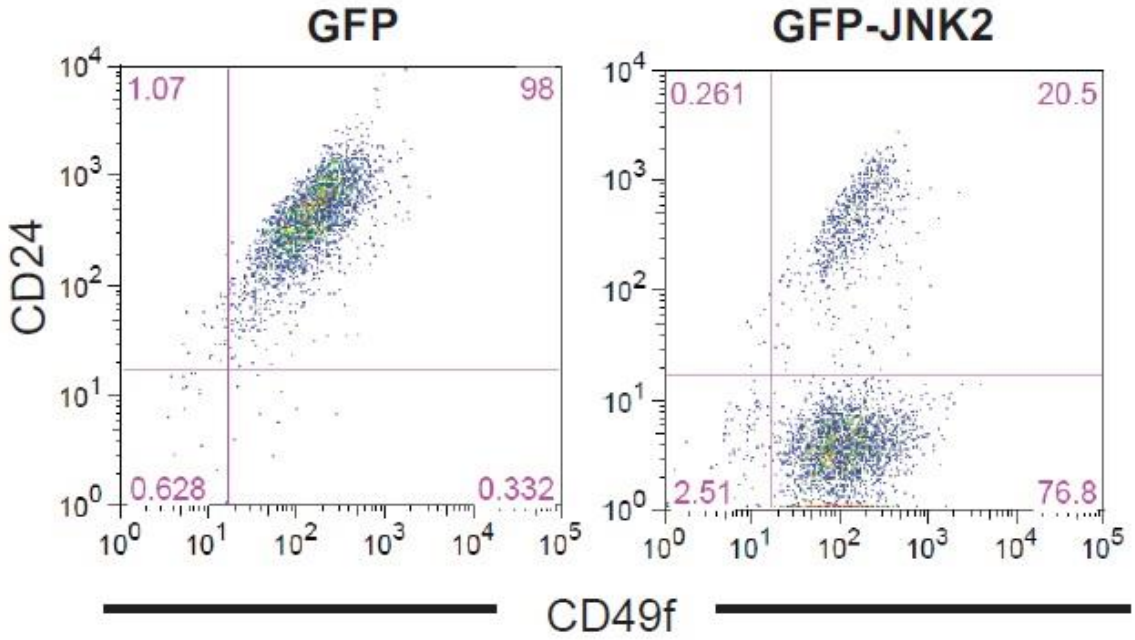

Flow cytometry was used to analyze CD24 and CD49f expression in *p53ko;jnk2ko* cell lines.

5.14. High Expression of GFP-JNK2 Correlates with CD24 Negativity

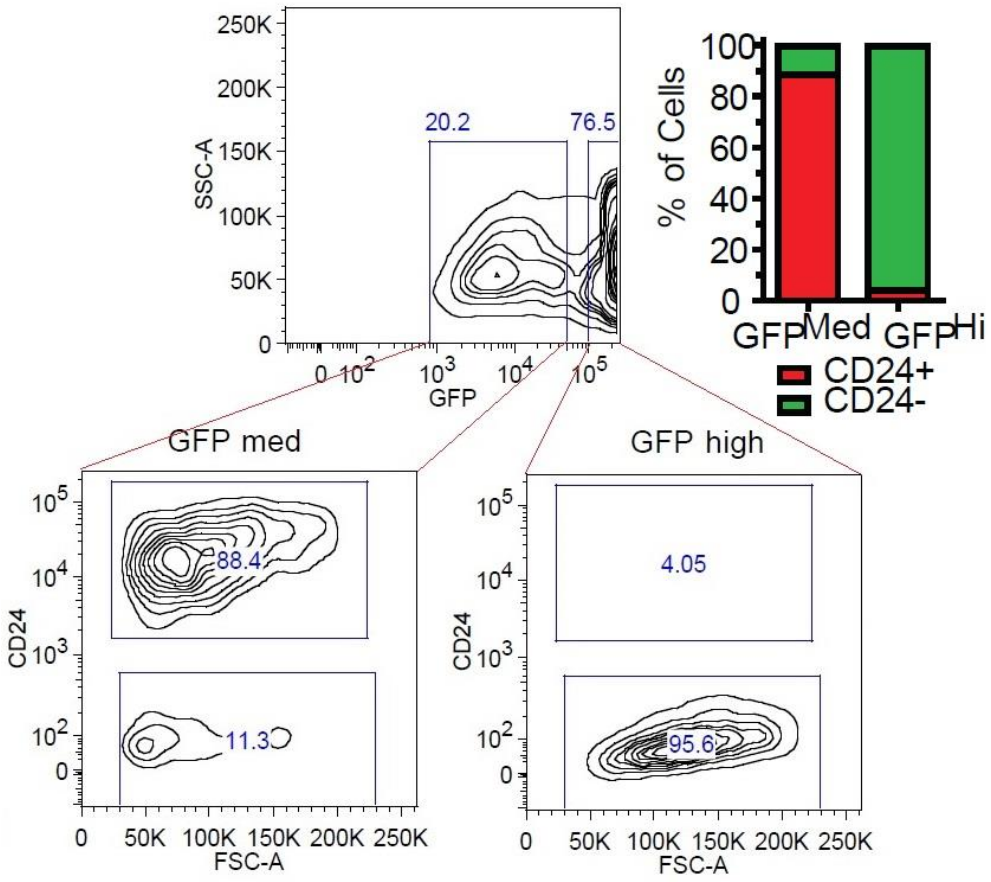

Flow cytometry was used to examine the correlation of GFP-JNK2 and CD24 expression in *p53ko*;*jnk2ko* cell lines. Cells were gated by GFP intensity (medium or high) and then assessed for CD24.

5.15. CD24^{-} Populations are Undifferentiated EMT Cells

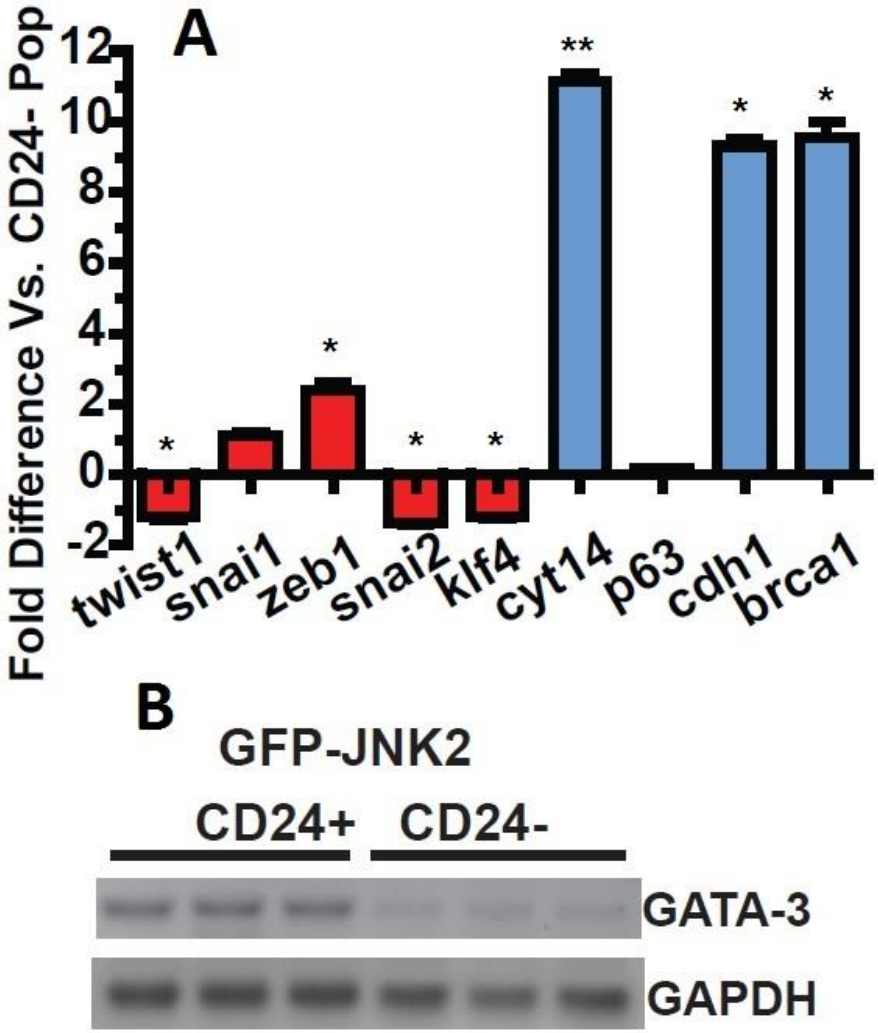

A: CD24+ and CD24- populations in *p53ko;jnk2ko* GFP-JNK2 cells were separated by flow cytometry and expression of mesenchymal/stem genes (*twist1, snai1, zeb1, snai2,* and *klf4*), and markers of differentiation (*cyt14, p63, cdh1,* and *brca1*) were assessed by qPCR. B: *gata-3*, a marker of luminal cells, was assessed by RT-PCR in these same populations. Significant fold differences as determined by T test from basal expression is indicated on figure as follows: * for $0.05 \geq p \geq 0.01$, ** for $0.01 > p \geq 0.0001$, *** for $p < 0.0001$.

5.16. *Brca1* is Sufficient to Suppress CD24$^-$ Populations

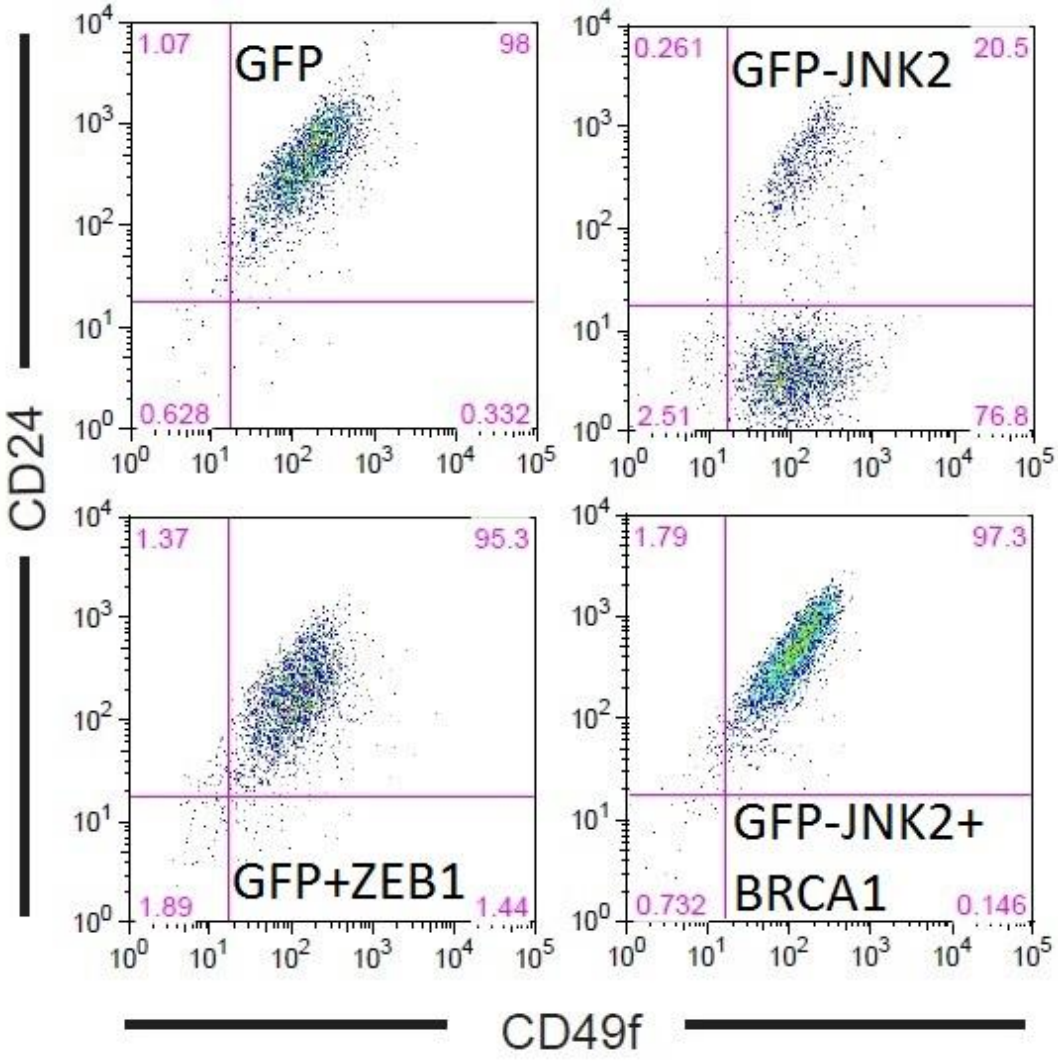

GFP and GFP-JNK2 expressing *p53ko*;*jnk2ko* cells were transfected with plasmid constructs encoding *Zeb1* and *Brca1*, respectively, and CD24/CD49f populations were assessed by flow cytometry.

5.17. JNK2 Does Not Alter EMT in MT Tumors

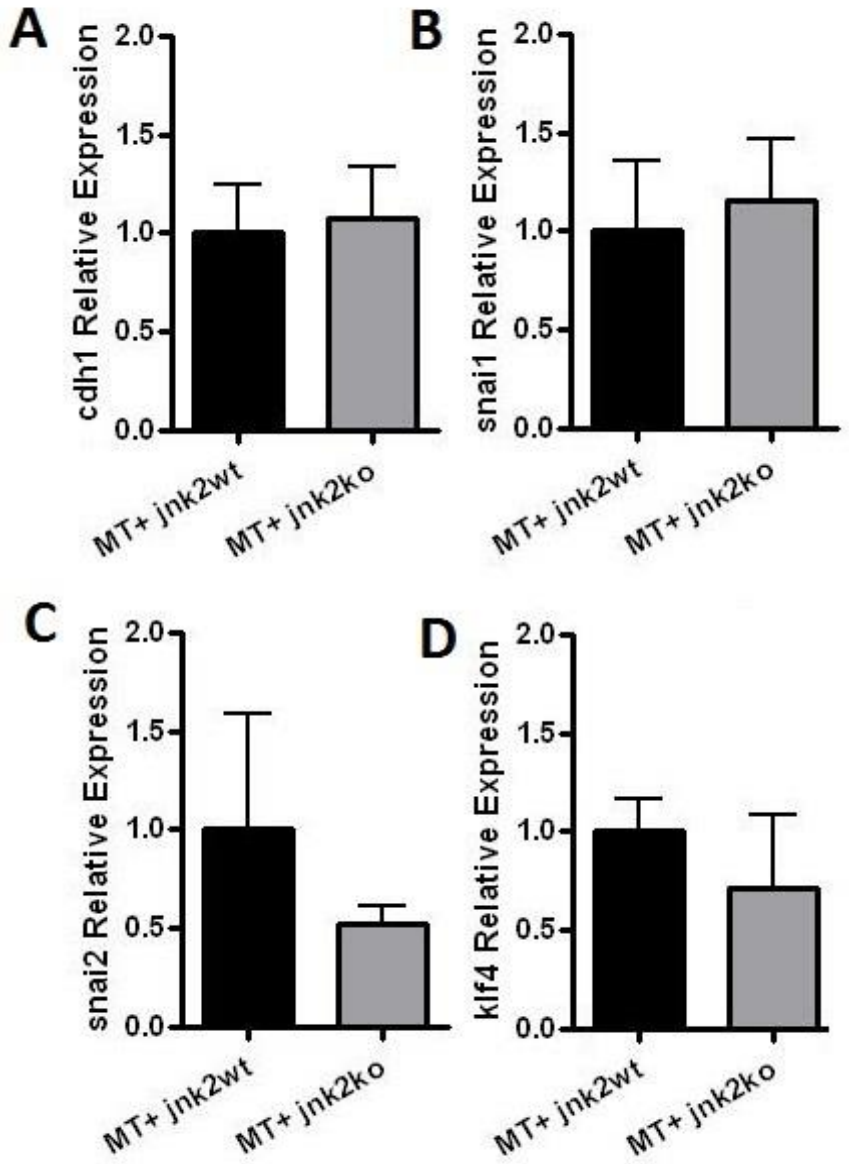

RNA from MT tumors was analyzed by qPCR for expression of *cdh1* (A), *snai1* (B), *snai2* (C), and *klf4* (D). Significance between groups was determined by T-test. Results are indicated on the figure as follows: * for $0.05 \geq p \geq 0.01$, ** for $0.01 > p \geq 0.0001$, *** for $p < 0.0001$. No significant differences were found.

5.18. JNK2 Expression Retards Cell Proliferation

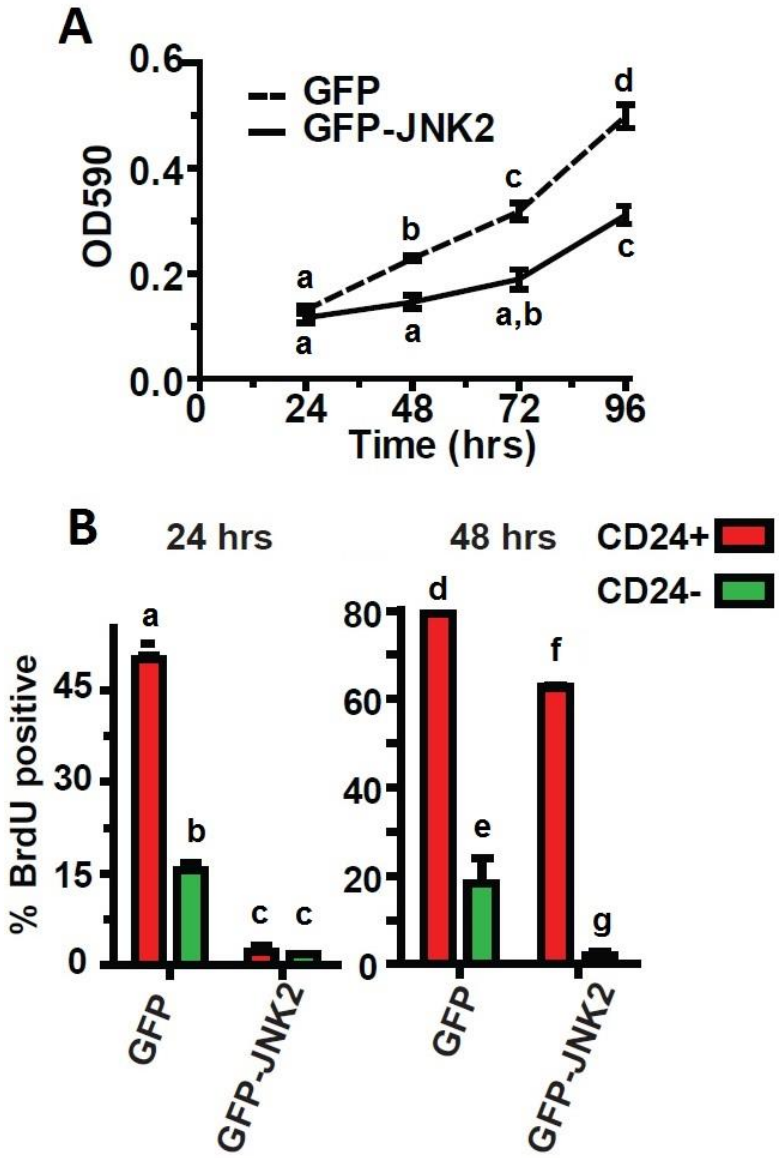

A: Proliferation rates of *p53ko;jnk2ko* cell lines were measured using MTT assay. B: Flow cytometry was used to analyze BrdU incorporation of $CD24^+$ and $CD24^-$ populaitions in *p53ko;jnk2ko* GFP-JNK2 cells. 2way ANOVA with Bonferroni Post-test was performed and significant differences ($p<0.05$) are indicated between columns with different letters.

5.19. JNK2 Inhibits ER Expression and Sensitivity

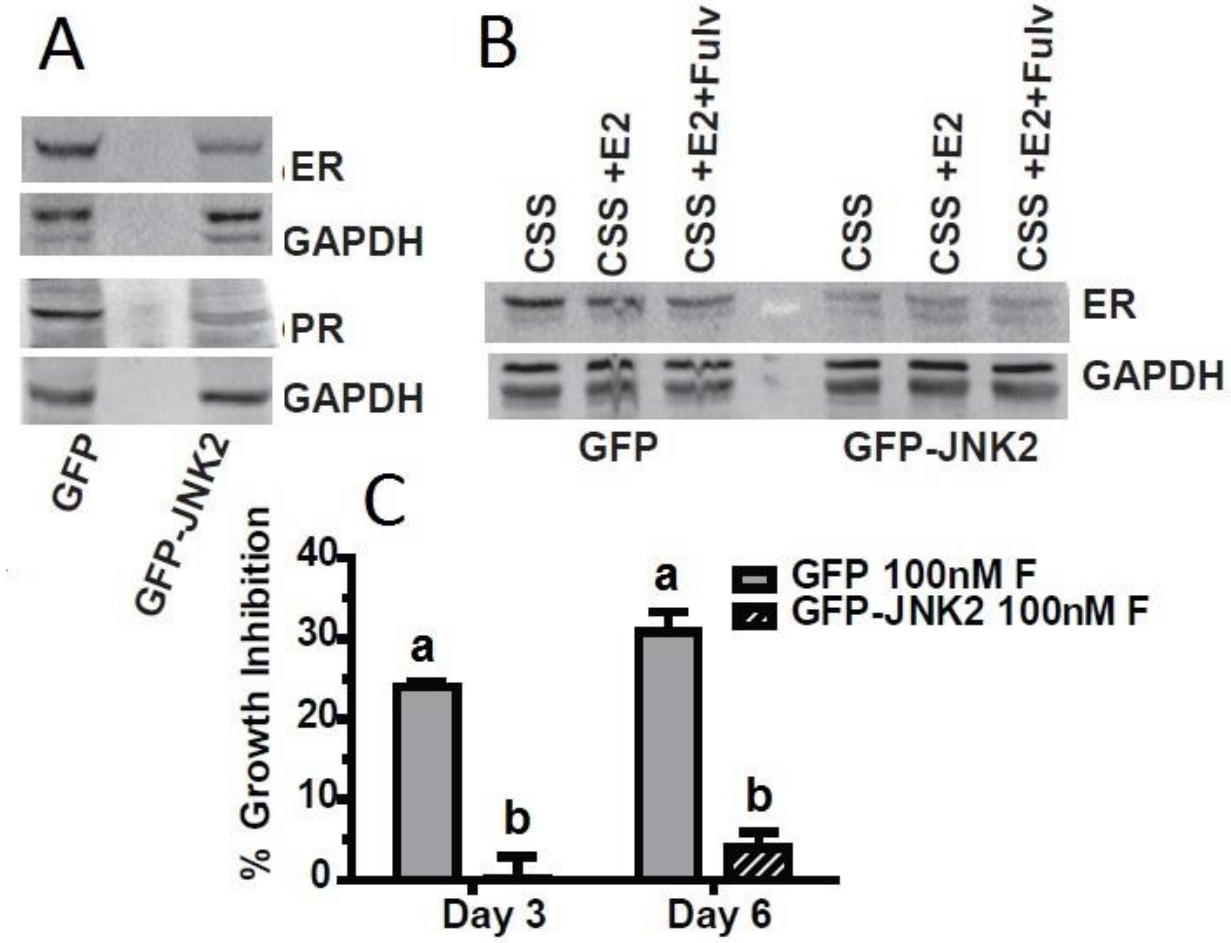

A: Expression of ER and PR were assessed in *p53ko*;*jnk2ko* cell lines by western blot. B: *p53ko*;*jnk2ko* cell lines were incubated in growth factor-free charcoal stripped serum (CSS), CSS+ estradiol (E2), or CSS+ E2+ fulvestrant (Fulv/F) and ER expression was assessed by western blot. C: MTT assay was performed on *p53ko*;*jnk2ko* cell lines in full serum with or without fulvestrant and growth inhibition was calculated. 2way ANOVA with Bonferroni Post-test was performed and significant differences ($p<0.05$) are indicated between columns with different letters.

Appendix C – Primers

qPCR primers:

hes1 (5’-CACAGAAAGTCATCAAAGCC and 5’-TGCTTGACAGTCATTTCCAG),

notch1 (5’-CTACAGAAGGTTACACAG and 5’-CAGAGGTAGGAGTTGTCACG),

p53 (5’-TGAACCGCCGACCTATCCTTA and GGCACAAACACGAACCTCAAA),

twist1 (5’-AATTCACAAGAATCAGGGCGTGGG and 5’-TCTATCAGAATGCAGAGGTGTGGG),

snai1 (5’-TCCAAACCCACTCGGATGTGAAGA and 5’-TTGGTGCTTGTGGAGCAAGGACAT),

snai2 (5’-CACATTCGAACCCACACATTGGCT and 5’-TGTGCCCTCAGGTTTGATCTGTCT),

zeb1 (5’-CAGTGTTCCATGTTTAAGAGCA and 5’-GTCTTTCATCCTGGTTTCCG),

klf4 (5’-CATTATCAAGAGTCTATGCCA and 5’-CACAGTGGTAAGGTTTCTCG),

cdh1 (5’-GCCAAGTACATCCTCTATTCTC and 5’-GCAACGAATCCCTCAAAGAC),

gapdh (5’-CGTGGAGTCTACTGGCGTCTTCAC and 5’-CGGGGATGATGAGCCTTTTGGC),

brca1 (5’-CCAAAGAAGTAATGACCGTG and 5’-GCTAACTATCCACTTTCCTCC),

gata-3 (5’-ACGAATCCAGCACAGAAGG and 5’-ATGTCCCTGCTCTCCTTG),

cyt14 (5’-TCTTCAGCAAGACAGAGGAG and 5’-CTCCAGGTTATTCTCCAGGG),

p63 (5’-GTTCAATGAGGGACAGATTGC and 5’-GAATTCAGTGCCAACCTGTG).

ChIP primers

p21 (5’-GATTTCCTTTCTATCAGCCC and GTCACAAGATACATACCACCT),

gapdh (5’-GCCAAAGACAGAAGCCAGGA and 5’-

CAGGATAGGACTCAGGGAATACAG),

notch1 (5’-GTGACCGTGGAACGTCTA 5’-CTGTCCTAGGGCTCCAC)

Works Cited

1. Stephens PJ, Tarpey PS, Davies H, Van Loo P, Greenman C, Wedge DC, et al. The landscape of cancer genes and mutational processes in breast cancer. Nature. 2012;486:400-4.
2. Ellis MJ, Ding L, Shen D, Luo J, Suman VJ, Wallis JW, et al. Whole-genome analysis informs breast cancer response to aromatase inhibition. Nature. 2012;486:353-60.
3. Chen P, O'Neal JF, Ebelt ND, Cantrell MA, Mitra S, Nasrazadani A, et al. Jnk2 effects on tumor development, genetic instability and replicative stress in an oncogene-driven mouse mammary tumor model. PloS one. 2010;5:e10443.
4. Cellurale C, Girnius N, Jiang F, Cavanagh-Kyros J, Lu S, Garlick DS, et al. Role of JNK in mammary gland development and breast cancer. Cancer research. 2012;72:472-81.
5. Cellurale C, Weston CR, Reilly J, Garlick DS, Jerry DJ, Sluss HK, et al. Role of JNK in a Trp53-dependent mouse model of breast cancer. PloS one. 2010;5:e12469.
6. Mitra S, Lee JS, Cantrell M, Van den Berg CL. c-Jun N-terminal kinase 2 (JNK2) enhances cell migration through epidermal growth factor substrate 8 (EPS8). The Journal of biological chemistry. 2011;286:15287-97.
7. Kaoud TS, Mitra S, Lee S, Taliaferro J, Cantrell M, Linse KD, et al. Development of JNK2-selective peptide inhibitors that inhibit breast cancer cell migration. ACS chemical biology. 2011;6:658-66.
8. Nasrazadani A, Van Den Berg CL. c-Jun N-terminal Kinase 2 Regulates Multiple Receptor Tyrosine Kinase Pathways in Mouse Mammary Tumor Growth and Metastasis. Genes & cancer. 2011;2:31-45.
9. Smith GH, Medina D. A morphologically distinct candidate for an epithelial stem cell in mouse mammary gland. Journal of cell science. 1988;90 (Pt 1):173-83.
10. Shackleton M, Vaillant F, Simpson KJ, Stingl J, Smyth GK, Asselin-Labat ML, et al. Generation of a functional mammary gland from a single stem cell. Nature. 2006;439:84-8.
11. Stingl J, Eirew P, Ricketson I, Shackleton M, Vaillant F, Choi D, et al. Purification and unique properties of mammary epithelial stem cells. Nature. 2006;439:993-7.
12. Stingl J, Raouf A, Emerman JT, Eaves CJ. Epithelial progenitors in the normal human mammary gland. Journal of mammary gland biology and neoplasia. 2005;10:49-59.
13. Smalley MJ, Titley J, O'Hare MJ. Clonal characterization of mouse mammary luminal epithelial and myoepithelial cells separated by fluorescence-activated cell sorting. In vitro cellular & developmental biology Animal. 1998;34:711-21.

14. Stingl J, Eaves CJ, Zandieh I, Emerman JT. Characterization of bipotent mammary epithelial progenitor cells in normal adult human breast tissue. Breast cancer research and treatment. 2001;67:93-109.
15. Sleeman KE, Kendrick H, Ashworth A, Isacke CM, Smalley MJ. CD24 staining of mouse mammary gland cells defines luminal epithelial, myoepithelial/basal and non-epithelial cells. Breast cancer research : BCR. 2006;8:R7.
16. Stingl J, Raouf A, Eirew P, Eaves CJ. Deciphering the mammary epithelial cell hierarchy. Cell cycle (Georgetown, Tex). 2006;5:1519-22.
17. Pietersen AM, Evers B, Prasad AA, Tanger E, Cornelissen-Steijger P, Jonkers J, et al. Bmi1 regulates stem cells and proliferation and differentiation of committed cells in mammary epithelium. Current biology : CB. 2008;18:1094-9.
18. Yang MH, Hsu DS, Wang HW, Wang HJ, Lan HY, Yang WH, et al. Bmi1 is essential in Twist1-induced epithelial-mesenchymal transition. Nature cell biology. 2010;12:982-92.
19. Siemens H, Jackstadt R, Hunten S, Kaller M, Menssen A, Gotz U, et al. miR-34 and SNAIL form a double-negative feedback loop to regulate epithelial-mesenchymal transitions. Cell cycle (Georgetown, Tex). 2011;10:4256-71.
20. Polyak K, Weinberg RA. Transitions between epithelial and mesenchymal states: acquisition of malignant and stem cell traits. Nature reviews Cancer. 2009;9:265-73.
21. Cicalese A, Bonizzi G, Pasi CE, Faretta M, Ronzoni S, Giulini B, et al. The tumor suppressor p53 regulates polarity of self-renewing divisions in mammary stem cells. Cell. 2009;138:1083-95.
22. Chang CJ, Chao CH, Xia W, Yang JY, Xiong Y, Li CW, et al. p53 regulates epithelial-mesenchymal transition and stem cell properties through modulating miRNAs. Nature cell biology. 2011;13:317-23.
23. Stingl J. Detection and analysis of mammary gland stem cells. The Journal of pathology. 2009;217:229-41.
24. Buono KD, Robinson GW, Martin C, Shi S, Stanley P, Tanigaki K, et al. The canonical Notch/RBP-J signaling pathway controls the balance of cell lineages in mammary epithelium during pregnancy. Developmental biology. 2006;293:565-80.
25. Bouras T, Pal B, Vaillant F, Harburg G, Asselin-Labat ML, Oakes SR, et al. Notch signaling regulates mammary stem cell function and luminal cell-fate commitment. Cell stem cell. 2008;3:429-41.
26. Raouf A, Zhao Y, To K, Stingl J, Delaney A, Barbara M, et al. Transcriptome analysis of the normal human mammary cell commitment and differentiation process. Cell stem cell. 2008;3:109-18.
27. Lee CW, Simin K, Liu Q, Plescia J, Guha M, Khan A, et al. A functional Notch-survivin gene signature in basal breast cancer. Breast cancer research : BCR. 2008;10:R97.

28. Morrison SJ, Perez SE, Qiao Z, Verdi JM, Hicks C, Weinmaster G, et al. Transient Notch activation initiates an irreversible switch from neurogenesis to gliogenesis by neural crest stem cells. Cell. 2000;101:499-510.
29. Nguyen BC, Lefort K, Mandinova A, Antonini D, Devgan V, Della Gatta G, et al. Cross-regulation between Notch and p63 in keratinocyte commitment to differentiation. Genes Dev. 2006;20:1028-42.
30. Yalcin-Ozuysal O, Fiche M, Guitierrez M, Wagner KU, Raffoul W, Brisken C. Antagonistic roles of Notch and p63 in controlling mammary epithelial cell fates. Cell death and differentiation. 2010;17:1600-12.
31. Oakes SR, Naylor MJ, Asselin-Labat ML, Blazek KD, Gardiner-Garden M, Hilton HN, et al. The Ets transcription factor Elf5 specifies mammary alveolar cell fate. Genes Dev. 2008;22:581-6.
32. Liu S, Ginestier C, Charafe-Jauffret E, Foco H, Kleer CG, Merajver SD, et al. BRCA1 regulates human mammary stem/progenitor cell fate. Proceedings of the National Academy of Sciences of the United States of America. 2008;105:1680-5.
33. Lim E, Vaillant F, Wu D, Forrest NC, Pal B, Hart AH, et al. Aberrant luminal progenitors as the candidate target population for basal tumor development in BRCA1 mutation carriers. Nature medicine. 2009;15:907-13.
34. Kouros-Mehr H, Slorach EM, Sternlicht MD, Werb Z. GATA-3 maintains the differentiation of the luminal cell fate in the mammary gland. Cell. 2006;127:1041-55.
35. Asselin-Labat ML, Sutherland KD, Barker H, Thomas R, Shackleton M, Forrest NC, et al. Gata-3 is an essential regulator of mammary-gland morphogenesis and luminal-cell differentiation. Nature cell biology. 2007;9:201-9.
36. van de Ven S, Smit VT, Dekker TJ, Nortier JW, Kroep JR. Discordances in ER, PR and HER2 receptors after neoadjuvant chemotherapy in breast cancer. Cancer treatment reviews. 2011;37:422-30.
37. Society AC. Breast Cancer Facts & Figures 2011-2012. 2011.
38. Perou CM, Sorlie T, Eisen MB, van de Rijn M, Jeffrey SS, Rees CA, et al. Molecular portraits of human breast tumours. Nature. 2000;406:747-52.
39. Sorlie T, Perou CM, Tibshirani R, Aas T, Geisler S, Johnsen H, et al. Gene expression patterns of breast carcinomas distinguish tumor subclasses with clinical implications. Proceedings of the National Academy of Sciences of the United States of America. 2001;98:10869-74.
40. Kao KJ, Chang KM, Hsu HC, Huang AT. Correlation of microarray-based breast cancer molecular subtypes and clinical outcomes: implications for treatment optimization. BMC cancer. 2011;11:143.
41. Prat A, Parker JS, Karginova O, Fan C, Livasy C, Herschkowitz JI, et al. Phenotypic and molecular characterization of the claudin-low intrinsic subtype of breast cancer. Breast cancer research : BCR. 2010;12:R68.
42. Cheang MC, Chia SK, Voduc D, Gao D, Leung S, Snider J, et al. Ki67 index, HER2 status, and prognosis of patients with luminal B breast cancer. Journal of the National Cancer Institute. 2009;101:736-50.

43. Tran B, Bedard PL. Luminal-B breast cancer and novel therapeutic targets. Breast cancer research : BCR. 2011;13:221.
44. Proia TA, Keller PJ, Gupta PB, Klebba I, Jones AD, Sedic M, et al. Genetic predisposition directs breast cancer phenotype by dictating progenitor cell fate. Cell stem cell. 2011;8:149-63.
45. Rakha EA, El-Sayed ME, Green AR, Lee AH, Robertson JF, Ellis IO. Prognostic markers in triple-negative breast cancer. Cancer. 2007;109:25-32.
46. Nielsen TO, Hsu FD, Jensen K, Cheang M, Karaca G, Hu Z, et al. Immunohistochemical and clinical characterization of the basal-like subtype of invasive breast carcinoma. Clinical cancer research : an official journal of the American Association for Cancer Research. 2004;10:5367-74.
47. Colomer R, Montero S, Lluch A, Ojeda B, Barnadas A, Casado A, et al. Circulating HER2 extracellular domain and resistance to chemotherapy in advanced breast cancer. Clin Cancer Res 2000 Jun;6(6):2356-62.
48. Carter P, Presta L, Gorman CM, Ridgway JB, Henner D, Wong WL, et al. Humanization of an anti-p185HER2 antibody for human cancer therapy. Proceedings of the National Academy of Sciences of the United States of America. 1992;89:4285-9.
49. Tokuda Y, Ohnishi Y, Shimamura K, Iwasawa M, Yoshimura M, Ueyama Y, et al. In vitro and in vivo anti-tumour effects of a humanised monoclonal antibody against c-erbB-2 product. British journal of cancer. 1996;73:1362-5.
50. Baselga J, Norton L, Albanell J, Kim YM, Mendelsohn J. Recombinant humanized anti-HER2 antibody (Herceptin) enhances the antitumor activity of paclitaxel and doxorubicin against HER2/neu overexpressing human breast cancer xenografts. Cancer research. 1998;58:2825-31.
51. Pegram M, Hsu S, Lewis G, Pietras R, Beryt M, Sliwkowski M, et al. Inhibitory effects of combinations of HER-2/neu antibody and chemotherapeutic agents used for treatment of human breast cancers. Oncogene. 1999;18:2241-51.
52. Vogel CL, Cobleigh MA, Tripathy D, Gutheil JC, Harris LN, Fehrenbacher L, et al. Efficacy and safety of trastuzumab as a single agent in first-line treatment of HER2-overexpressing metastatic breast cancer. Journal of clinical oncology : official journal of the American Society of Clinical Oncology. 2002;20:719-26.
53. Herschkowitz JI, Zhao W, Zhang M, Usary J, Murrow G, Edwards D, et al. Comparative oncogenomics identifies breast tumors enriched in functional tumor-initiating cells. Proceedings of the National Academy of Sciences of the United States of America. 2012;109:2778-83.
54. Slamon DJ, Clark GM, Wong SG, Levin WJ, Ullrich A, McGuire WL. Human Breast Cancer: Correlation of Relapse and Survival with Amplification of the HER-2/neu Oncogene. Science (New York, NY). 1987;235:177-82.
55. Sørlie T, Tibshirani R, Parker J, Hastie T, Marron JS, Nobel A, et al. Repeated observation of breast tumor subtypes in independent gene expression data sets. Proceedings of the National Academy of Sciences. 2003;100:8418-23.

56. Arnes JB, Brunet JS, Stefansson I, Begin LR, Wong N, Chappuis PO, et al. Placental cadherin and the basal epithelial phenotype of BRCA1-related breast cancer. Clinical cancer research : an official journal of the American Association for Cancer Research. 2005;11:4003-11.
57. Foulkes WD, Brunet JS, Stefansson IM, Straume O, Chappuis PO, Begin LR, et al. The prognostic implication of the basal-like (cyclin E high/p27 low/p53+/glomeruloid-microvascular-proliferation+) phenotype of BRCA1-related breast cancer. Cancer research. 2004;64:830-5.
58. Teulière J, Faraldo MM, Deugnier M-A, Shtutman M, Ben-Ze'ev A, Thiery JP, et al. Targeted activation of β-catenin signaling in basal mammary epithelial cells affects mammary development and leads to hyperplasia. Development (Cambridge, England). 2005;132:267-77.
59. Liu BY, McDermott SP, Khwaja SS, Alexander CM. The transforming activity of Wnt effectors correlates with their ability to induce the accumulation of mammary progenitor cells. Proceedings of the National Academy of Sciences. 2004;101:4158-63.
60. Asselin-Labat ML, Shackleton M, Stingl J, Vaillant F, Forrest NC, Eaves CJ, et al. Steroid hormone receptor status of mouse mammary stem cells. Journal of the National Cancer Institute. 2006;98:1011-4.
61. Lan T, Chen Y, Sang J, Wu Y, Wang Y, Jiang L, et al. Type II cGMP-dependent protein kinase inhibits EGF-induced MAPK/JNK signal transduction in breast cancer cells. Oncology reports. 2012;27:2039-44.
62. Farias GG, Alfaro IE, Cerpa W, Grabowski CP, Godoy JA, Bonansco C, et al. Wnt-5a/JNK signaling promotes the clustering of PSD-95 in hippocampal neurons. The Journal of biological chemistry. 2009;284:15857-66.
63. Killick R, Ribe EM, Al-Shawi R, Malik B, Hooper C, Fernandes C, et al. Clusterin regulates beta-amyloid toxicity via Dickkopf-1-driven induction of the wnt-PCP-JNK pathway. Molecular psychiatry. 2012.
64. Qiu W, Chen L, Kassem M. Activation of non-canonical Wnt/JNK pathway by Wnt3a is associated with differentiation fate determination of human bone marrow stromal (mesenchymal) stem cells. Biochemical and biophysical research communications. 2011;413:98-104.
65. Kesavan K, Lobel-Rice K, Sun W, Lapadat R, Webb S, Johnson GL, et al. MEKK2 regulates the coordinate activation of ERK5 and JNK in response to FGF-2 in fibroblasts. Journal of cellular physiology. 2004;199:140-8.
66. Cha Y, Kim DK, Hyun J, Kim SJ, Park KS. TCEA3 binds to TGF-beta receptor I and induces Smad-independent, JNK-dependent apoptosis in ovarian cancer cells. Cellular signalling. 2013.
67. Wang W, Zhou G, Hu MC, Yao Z, Tan TH. Activation of the hematopoietic progenitor kinase-1 (HPK1)-dependent, stress-activated c-Jun N-terminal kinase (JNK) pathway by transforming growth factor beta (TGF-beta)-activated kinase (TAK1), a kinase mediator of TGF beta signal transduction. The Journal of biological chemistry. 1997;272:22771-5.

68. Zhang Y, Neo SY, Wang X, Han J, Lin S-C. Axin Forms a Complex with MEKK1 and Activates c-Jun NH2-terminal Kinase/Stress-activated Protein Kinase through Domains Distinct from Wnt Signaling. Journal of Biological Chemistry. 1999;274:35247-54.
69. Tang F, Tang G, Xiang J, Dai Q, Rosner MR, Lin A. The absence of NF-kappaB-mediated inhibition of c-Jun N-terminal kinase activation contributes to tumor necrosis factor alpha-induced apoptosis. Molecular and cellular biology. 2002;22:8571-9.
70. Nishitoh H, Saitoh M, Mochida Y, Takeda K, Nakano H, Rothe M, et al. ASK1 is essential for JNK/SAPK activation by TRAF2. Molecular cell. 1998;2:389-95.
71. Alter J, Rozentzweig D, Bengal E. Inhibition of myoblast differentiation by tumor necrosis factor alpha is mediated by c-Jun N-terminal kinase 1 and leukemia inhibitory factor. The Journal of biological chemistry. 2008;283:23224-34.
72. Van Slambrouck S, Grijelmo C, De Wever O, Bruyneel E, Emami S, Gespach C, et al. Activation of the FAK-src molecular scaffolds and p130Cas-JNK signaling cascades by alpha1-integrins during colon cancer cell invasion. International journal of oncology. 2007;31:1501-8.
73. Wilson DJ, Fortner KA, Lynch DH, Mattingly RR, Macara IG, Posada JA, et al. JNK, but not MAPK, activation is associated with Fas-mediated apoptosis in human T cells. European journal of immunology. 1996;26:989-94.
74. Zanke BW, Boudreau K, Rubie E, Winnett E, Tibbles LA, Zon L, et al. The stress-activated protein kinase pathway mediates cell death following injury induced by cis-platinum, UV irradiation or heat. Current biology : CB. 1996;6:606-13.
75. Robitaille K, Daviau A, Lachance G, Couture JP, Blouin R. Calphostin C-induced apoptosis is mediated by a tissue transglutaminase-dependent mechanism involving the DLK/JNK signaling pathway. Cell death and differentiation. 2008;15:1522-31.
76. Yang DD, Kuan CY, Whitmarsh AJ, Rincon M, Zheng TS, Davis RJ, et al. Absence of excitotoxicity-induced apoptosis in the hippocampus of mice lacking the Jnk3 gene. Nature. 1997;389:865-70.
77. Harkin DP, Bean JM, Miklos D, Song YH, Truong VB, Englert C, et al. Induction of GADD45 and JNK/SAPK-dependent apoptosis following inducible expression of BRCA1. Cell. 1999;97:575-86.
78. Xu Z, Maroney AC, Dobrzanski P, Kukekov NV, Greene LA. The MLK family mediates c-Jun N-terminal kinase activation in neuronal apoptosis. Molecular and cellular biology. 2001;21:4713-24.
79. Deng Y, Ren X, Yang L, Lin Y, Wu X. A JNK-dependent pathway is required for TNFalpha-induced apoptosis. Cell. 2003;115:61-70.
80. Schreiber M, Kolbus A, Piu F, Szabowski A, Mohle-Steinlein U, Tian J, et al. Control of cell cycle progression by c-Jun is p53 dependent. Genes Dev. 1999;13:607-19.

81. Tournier C, Hess P, Yang DD, Xu J, Turner TK, Nimnual A, et al. Requirement of JNK for stress-induced activation of the cytochrome c-mediated death pathway. Science (New York, NY). 2000;288:870-4.
82. Nuntharatanapong N, Chen K, Sinhaseni P, Keaney JF, Jr. EGF receptor-dependent JNK activation is involved in arsenite-induced p21Cip1/Waf1 upregulation and endothelial apoptosis. American journal of physiology Heart and circulatory physiology. 2005;289:H99-H107.
83. Buschmann T, Potapova O, Bar-Shira A, Ivanov VN, Fuchs SY, Henderson S, et al. Jun NH2-terminal kinase phosphorylation of p53 on Thr-81 is important for p53 stabilization and transcriptional activities in response to stress. Molecular and cellular biology. 2001;21:2743-54.
84. Fuchs SY, Adler V, Pincus MR, Ronai Z. MEKK1/JNK signaling stabilizes and activates p53. Proceedings of the National Academy of Sciences of the United States of America. 1998;95:10541-6.
85. Bost F, McKay R, Bost M, Potapova O, Dean NM, Mercola D. The Jun kinase 2 isoform is preferentially required for epidermal growth factor-induced transformation of human A549 lung carcinoma cells. Molecular and cellular biology. 1999;19:1938-49.
86. Potapova O, Gorospe M, Dougherty RH, Dean NM, Gaarde WA, Holbrook NJ. Inhibition of c-Jun N-terminal kinase 2 expression suppresses growth and induces apoptosis of human tumor cells in a p53-dependent manner. Molecular and cellular biology. 2000;20:1713-22.
87. Chen N, Nomura M, She QB, Ma WY, Bode AM, Wang L, et al. Suppression of skin tumorigenesis in c-Jun NH(2)-terminal kinase-2-deficient mice. Cancer research. 2001;61:3908-12.
88. She QB, Chen N, Bode AM, Flavell RA, Dong Z. Deficiency of c-Jun-NH(2)-terminal kinase-1 in mice enhances skin tumor development by 12-O-tetradecanoylphorbol-13-acetate. Cancer research. 2002;62:1343-8.
89. Kim CG, Lee JJ, Jung DY, Jeon J, Heo HS, Kang HC, et al. Profiling of differentially expressed genes in human stem cells by cDNA microarray. Molecules and cells. 2006;21:343-55.
90. Mandal A, Bhowmik S, Patki A, Viswanathan C, Majumdar AS. Derivation, characterization, and gene expression profile of two new human ES cell lines from India. Stem cell research. 2010;5:173-87.
91. Brill LM, Xiong W, Lee KB, Ficarro SB, Crain A, Xu Y, et al. Phosphoproteomic analysis of human embryonic stem cells. Cell stem cell. 2009;5:204-13.
92. Ryu JM, Han HJ. L-threonine regulates G1/S phase transition of mouse embryonic stem cells via PI3K/Akt, MAPKs, and mTORC pathways. The Journal of biological chemistry. 2011;286:23667-78.
93. Cellurale C, Sabio G, Kennedy NJ, Das M, Barlow M, Sandy P, et al. Requirement of c-Jun NH(2)-terminal kinase for Ras-initiated tumor formation. Molecular and cellular biology. 2011;31:1565-76.

94. Liu Q, Zhang Y, Mao H, Chen W, Luo N, Zhou Q, et al. A crosstalk between the Smad and JNK signaling in the TGF-beta-induced epithelial-mesenchymal transition in rat peritoneal mesothelial cells. PloS one. 2012;7:e32009.
95. Matsuda K, Sato A, Okada M, Shibuya K, Seino S, Suzuki K, et al. Targeting JNK for therapeutic depletion of stem-like glioblastoma cells. Scientific reports. 2012;2:516.
96. Cui J, Han SY, Wang C, Su W, Harshyne L, Holgado-Madruga M, et al. c-Jun NH(2)-terminal kinase 2alpha2 promotes the tumorigenicity of human glioblastoma cells. Cancer research. 2006;66:10024-31.
97. Kyriakis JM, Banerjee P, Nikolakaki E, Dai T, Rubie EA, Ahmad MF, et al. The stress-activated protein kinase subfamily of c-Jun kinases. Nature. 1994;369:156-60.
98. Kallunki T, Deng T, Hibi M, Karin M. c-Jun can recruit JNK to phosphorylate dimerization partners via specific docking interactions. Cell. 1996;87:929-39.
99. Gonzalez FA, Raden DL, Davis RJ. Identification of substrate recognition determinants for human ERK1 and ERK2 protein kinases. The Journal of biological chemistry. 1991;266:22159-63.
100. Xie X, Gu Y, Fox T, Coll JT, Fleming MA, Markland W, et al. Crystal structure of JNK3: a kinase implicated in neuronal apoptosis. Structure (London, England : 1993). 1998;6:983-91.
101. Heo YS, Kim SK, Seo CI, Kim YK, Sung BJ, Lee HS, et al. Structural basis for the selective inhibition of JNK1 by the scaffolding protein JIP1 and SP600125. The EMBO journal. 2004;23:2185-95.
102. Shaw D, Wang SM, Villasenor AG, Tsing S, Walter D, Browner MF, et al. The crystal structure of JNK2 reveals conformational flexibility in the MAP kinase insert and indicates its involvement in the regulation of catalytic activity. Journal of molecular biology. 2008;383:885-93.
103. Lawler S, Fleming Y, Goedert M, Cohen P. Synergistic activation of SAPK1/JNK1 by two MAP kinase kinases in vitro. Current biology : CB. 1998;8:1387-90.
104. Kallunki T, Su B, Tsigelny I, Sluss HK, Derijard B, Moore G, et al. JNK2 contains a specificity-determining region responsible for efficient c-Jun binding and phosphorylation. Genes Dev. 1994;8:2996-3007.
105. Sluss HK, Barrett T, Derijard B, Davis RJ. Signal transduction by tumor necrosis factor mediated by JNK protein kinases. Molecular and cellular biology. 1994;14:8376-84.
106. Gupta S, Barrett T, Whitmarsh AJ, Cavanagh J, Sluss HK, Derijard B, et al. Selective interaction of JNK protein kinase isoforms with transcription factors. The EMBO journal. 1996;15:2760-70.
107. Kuan CY, Whitmarsh AJ, Yang DD, Liao G, Schloemer AJ, Dong C, et al. A critical role of neural-specific JNK3 for ischemic apoptosis. Proceedings of the National Academy of Sciences of the United States of America. 2003;100:15184-9.

108. Zhan L, Rosenberg A, Bergami KC, Yu M, Xuan Z, Jaffe AB, et al. Deregulation of scribble promotes mammary tumorigenesis and reveals a role for cell polarity in carcinoma. Cell. 2008;135:865-78.
109. Society AC. Cancer Treatment and Survivorship Facts & Figures 2012-2013. 2012.
110. Jacks T, Remington L, Williams BO, Schmitt EM, Halachmi S, Bronson RT, et al. Tumor spectrum analysis in p53-mutant mice. Current biology : CB. 1994;4:1-7.
111. Kuan CY, Yang DD, Samanta Roy DR, Davis RJ, Rakic P, Flavell RA. The Jnk1 and Jnk2 protein kinases are required for regional specific apoptosis during early brain development. Neuron. 1999;22:667-76.
112. Lefort K, Mandinova A, Ostano P, Kolev V, Calpini V, Kolfschoten I, et al. Notch1 is a p53 target gene involved in human keratinocyte tumor suppression through negative regulation of ROCK1/2 and MRCKalpha kinases. Genes Dev. 2007;21:562-77.
113. Yugawa T, Handa K, Narisawa-Saito M, Ohno S, Fujita M, Kiyono T. Regulation of Notch1 gene expression by p53 in epithelial cells. Molecular and cellular biology. 2007;27:3732-42.
114. DiNardo DN, Butcher DT, Robinson DP, Archer TK, Rodenhiser DI. Functional analysis of CpG methylation in the BRCA1 promoter region. Oncogene. 2001;20:5331-40.
115. Welm BE, Dijkgraaf GJ, Bledau AS, Welm AL, Werb Z. Lentiviral transduction of mammary stem cells for analysis of gene function during development and cancer. Cell stem cell. 2008;2:90-102.
116. Debnath J, Muthuswamy SK, Brugge JS. Morphogenesis and oncogenesis of MCF-10A mammary epithelial acini grown in three-dimensional basement membrane cultures. Methods (San Diego, Calif). 2003;30:256-68.
117. Jerry DJ, Kittrell FS, Kuperwasser C, Laucirica R, Dickinson ES, Bonilla PJ, et al. A mammary-specific model demonstrates the role of the p53 tumor suppressor gene in tumor development. Oncogene. 2000;19:1052-8.
118. Herschkowitz JI, Simin K, Weigman VJ, Mikaelian I, Usary J, Hu Z, et al. Identification of conserved gene expression features between murine mammary carcinoma models and human breast tumors. Genome biology. 2007;8:R76.
119. de Hoon MJ, Imoto S, Nolan J, Miyano S. Open source clustering software. Bioinformatics (Oxford, England). 2004;20:1453-4.
120. Saldanha AJ. Java Treeview--extensible visualization of microarray data. Bioinformatics (Oxford, England). 2004;20:3246-8.
121. Kopan R, Ilagan MX. The canonical Notch signaling pathway: unfolding the activation mechanism. Cell. 2009;137:216-33.
122. Wu L, Sun T, Kobayashi K, Gao P, Griffin JD. Identification of a family of mastermind-like transcriptional coactivators for mammalian notch receptors. Molecular and cellular biology. 2002;22:7688-700.

123. Hu C, Dievart A, Lupien M, Calvo E, Tremblay G, Jolicoeur P. Overexpression of activated murine Notch1 and Notch3 in transgenic mice blocks mammary gland development and induces mammary tumors. Am J Pathol. 2006;168:973-90.
124. Gallahan D, Jhappan C, Robinson G, Hennighausen L, Sharp R, Kordon E, et al. Expression of a truncated Int3 gene in developing secretory mammary epithelium specifically retards lobular differentiation resulting in tumorigenesis. Cancer research. 1996;56:1775-85.
125. Mazzone M, Selfors LM, Albeck J, Overholtzer M, Sale S, Carroll DL, et al. Dose-dependent induction of distinct phenotypic responses to Notch pathway activation in mammary epithelial cells. Proceedings of the National Academy of Sciences of the United States of America. 2010;107:5012-7.
126. Rahman M, Zhang Z, Mody AA, Su DM, Das HK. Intraperitoneal injection of JNK-specific inhibitor SP600125 inhibits the expression of presenilin-1 and Notch signaling in mouse brain without induction of apoptosis. Brain research. 2012;1448:117-28.
127. Tsao PN, Wei SC, Huang MT, Lee MC, Chou HC, Chen CY, et al. Lipopolysaccharide-induced Notch signaling activation through JNK-dependent pathway regulates inflammatory response. Journal of biomedical science. 2011;18:56.
128. Liao YF, Wang BJ, Cheng HT, Kuo LH, Wolfe MS. Tumor necrosis factor-alpha, interleukin-1beta, and interferon-gamma stimulate gamma-secretase-mediated cleavage of amyloid precursor protein through a JNK-dependent MAPK pathway. The Journal of biological chemistry. 2004;279:49523-32.
129. Curry CL, Reed LL, Nickoloff BJ, Miele L, Foreman KE. Notch-independent regulation of Hes-1 expression by c-Jun N-terminal kinase signaling in human endothelial cells. Laboratory investigation; a journal of technical methods and pathology. 2006;86:842-52.
130. Kim JW, Kim MJ, Kim KJ, Yun HJ, Chae JS, Hwang SG, et al. Notch interferes with the scaffold function of JNK-interacting protein 1 to inhibit the JNK signaling pathway. Proceedings of the National Academy of Sciences of the United States of America. 2005;102:14308-13.
131. Kolev V, Mandinova A, Guinea-Viniegra J, Hu B, Lefort K, Lambertini C, et al. EGFR signalling as a negative regulator of Notch1 gene transcription and function in proliferating keratinocytes and cancer. Nature cell biology. 2008;10:902-11.
132. Ravitz MJ, Yan S, Dolce C, Kinniburgh AJ, Wenner CE. Differential regulation of p27 and cyclin D1 by TGF-beta and EGF in C3H 10T1/2 mouse fibroblasts. Journal of cellular physiology. 1996;168:510-20.
133. Schramek D, Kotsinas A, Meixner A, Wada T, Elling U, Pospisilik JA, et al. The stress kinase MKK7 couples oncogenic stress to p53 stability and tumor suppression. Nature genetics. 2011;43:212-9.

134. Donehower LA, Harvey M, Slagle BL, McArthur MJ, Montgomery CA, Jr., Butel JS, et al. Mice deficient for p53 are developmentally normal but susceptible to spontaneous tumours. Nature. 1992;356:215-21.
135. Tzeng YJ, Zimmermann C, Guhl E, Berg B, Avantaggiati ML, Graessmann A. SV40 T/t-antigen induces premature mammary gland involution by apoptosis and selects for p53 missense mutation in mammary tumors. Oncogene. 1998;16:2103-14.
136. Nielsen TO, Parker JS, Leung S, Voduc D, Ebbert M, Vickery T, et al. A comparison of PAM50 intrinsic subtyping with immunohistochemistry and clinical prognostic factors in tamoxifen-treated estrogen receptor-positive breast cancer. Clinical cancer research : an official journal of the American Association for Cancer Research. 2010;16:5222-32.
137. Taube JH, Herschkowitz JI, Komurov K, Zhou AY, Gupta S, Yang J, et al. Core epithelial-to-mesenchymal transition interactome gene-expression signature is associated with claudin-low and metaplastic breast cancer subtypes. Proceedings of the National Academy of Sciences of the United States of America. 2010;107:15449-54.
138. Vieira AF, Ricardo S, Ablett MP, Dionisio MR, Mendes N, Albergaria A, et al. P-cadherin is coexpressed with CD44 and CD49f and mediates stem cell properties in basal-like breast cancer. Stem cells (Dayton, Ohio). 2012;30:854-64.
139. Joshi PA, Jackson HW, Beristain AG, Di Grappa MA, Mote PA, Clarke CL, et al. Progesterone induces adult mammary stem cell expansion. Nature. 2010;465:803-7.
140. Mani SA, Guo W, Liao MJ, Eaton EN, Ayyanan A, Zhou AY, et al. The epithelial-mesenchymal transition generates cells with properties of stem cells. Cell. 2008;133:704-15.
141. Jiang Z, Deng T, Jones R, Li H, Herschkowitz JI, Liu JC, et al. Rb deletion in mouse mammary progenitors induces luminal-B or basal-like/EMT tumor subtypes depending on p53 status. The Journal of clinical investigation. 2010;120:3296-309.
142. Herschkowitz JI, He X, Fan C, Perou CM. The functional loss of the retinoblastoma tumour suppressor is a common event in basal-like and luminal B breast carcinomas. Breast cancer research : BCR. 2008;10:R75.
143. Valentin MD, da Silva SD, Privat M, Alaoui-Jamali M, Bignon YJ. Molecular insights on basal-like breast cancer. Breast cancer research and treatment. 2012;134:21-30.
144. Liu Y, Elf SE, Miyata Y, Sashida G, Huang G, Di Giandomenico S, et al. p53 regulates hematopoietic stem cell quiescence. Cell stem cell. 2009;4:37-48.
145. Armesilla-Diaz A, Bragado P, Del Valle I, Cuevas E, Lazaro I, Martin C, et al. p53 regulates the self-renewal and differentiation of neural precursors. Neuroscience. 2009;158:1378-89.

146. Meletis K, Wirta V, Hede SM, Nister M, Lundeberg J, Frisen J. p53 suppresses the self-renewal of adult neural stem cells. Development (Cambridge, England). 2006;133:363-9.
147. Arizti P, Fang L, Park I, Yin Y, Solomon E, Ouchi T, et al. Tumor suppressor p53 is required to modulate BRCA1 expression. Molecular and cellular biology. 2000;20:7450-9.
148. Murtagh J, McArdle E, Gilligan E, Thornton L, Furlong F, Martin F. Organization of mammary epithelial cells into 3D acinar structures requires glucocorticoid and JNK signaling. The Journal of cell biology. 2004;166:133-43.
149. Carrozzino F, Pugnale P, Feraille E, Montesano R. Inhibition of basal p38 or JNK activity enhances epithelial barrier function through differential modulation of claudin expression. American journal of physiology Cell physiology. 2009;297:C775-87.
150. Johnston SR, Lu B, Scott GK, Kushner PJ, Smith IE, Dowsett M, et al. Increased activator protein-1 DNA binding and c-Jun NH2-terminal kinase activity in human breast tumors with acquired tamoxifen resistance. Clinical cancer research : an official journal of the American Association for Cancer Research. 1999;5:251-6.
151. Buse P, Woo PL, Alexander DB, Reza A, Firestone GL. Glucocorticoid-induced functional polarity of growth factor responsiveness regulates tight junction dynamics in transformed mammary epithelial tumor cells. The Journal of biological chemistry. 1995;270:28223-7.
152. Wu ZQ, Li XY, Hu CY, Ford M, Kleer CG, Weiss SJ. Canonical Wnt signaling regulates Slug activity and links epithelial-mesenchymal transition with epigenetic Breast Cancer 1, Early Onset (BRCA1) repression. Proceedings of the National Academy of Sciences of the United States of America. 2012;109:16654-9.
153. Morrison SJ, Kimble J. Asymmetric and symmetric stem-cell divisions in development and cancer. Nature. 2006;441:1068-74.
154. Marquis ST, Rajan JV, Wynshaw-Boris A, Xu J, Yin GY, Abel KJ, et al. The developmental pattern of Brca1 expression implies a role in differentiation of the breast and other tissues. Nature genetics. 1995;11:17-26.
155. Molyneux G, Geyer FC, Magnay FA, McCarthy A, Kendrick H, Natrajan R, et al. BRCA1 basal-like breast cancers originate from luminal epithelial progenitors and not from basal stem cells. Cell stem cell. 2010;7:403-17.
156. Visvader JE, Lindeman GJ. Cancer stem cells: current status and evolving complexities. Cell stem cell. 2012;10:717-28.
157. Bennett BL, Sasaki DT, Murray BW, O'Leary EC, Sakata ST, Xu W, et al. SP600125, an anthrapyrazolone inhibitor of Jun N-terminal kinase. Proceedings of the National Academy of Sciences. 2001;98:13681-6.
158. Carboni S, Hiver A, Szyndralewiez C, Gaillard P, Gotteland J-P, Vitte P-A. AS601245 (1,3-Benzothiazol-2-yl (2-{[2-(3-pyridinyl) ethyl] amino}-4 pyrimidinyl) Acetonitrile): A c-Jun NH2-Terminal Protein Kinase Inhibitor with

Neuroprotective Properties. Journal of Pharmacology and Experimental Therapeutics. 2004;310:25-32.
159. Ferrandi C, Ballerio R, Gaillard P, Giachetti C, Carboni S, Vitte P-A, et al. Inhibition of c-Jun N-terminal kinase decreases cardiomyocyte apoptosis and infarct size after myocardial ischemia and reperfusion in anaesthetized rats. British Journal of Pharmacology. 2004;142:953-60.
160. Bain J, McLauchlan H, Elliott M, Cohen P. The specificities of protein kinase inhibitors: an update. The Biochemical journal. 2003;371:199-204.
161. Zhang T, Inesta-Vaquera F, Niepel M, Zhang J, Ficarro SB, Machleidt T, et al. Discovery of potent and selective covalent inhibitors of JNK. Chemistry & biology. 2012;19:140-54.

Vita

Michael was born in St. Louis County, Missouri and attended Pattonville Senior High School in Maryland Heights before moving on to Omaha, Nebraska to pursue his Bachelor of Science degree in Biology at Creighton University. While in Omaha, Michael performed biochemical research at Boys' Town National Research Hospital, under the supervision of Dr. Dominic Cosgrove. Michael received the Phi Sigma Outstanding Research Award for this work. Michael graduated in 2006 and began post-graduate studies in Cellular and Molecular Biology at the University of Texas at Austin under the supervision of Dr. Carla L. Van Den Berg. During his graduate studies, Michael received a fellowship from the Institute of Cellular and Molecular Biology as well as two nominations for Outstanding Teaching Assistant of the Year from the College of Natural Sciences, winning the award once.

This dissertation was typed by the author, Michael Andrew Cantrell.

Permanent Address: 3087 Post Port Lane
Maryland Heights, MO 63043